CLASSIFICATION CHANGED TO CONFIDENTIAL
SECRET

COPY NO. 204

N-35480

NATIONAL ADVISORY COMMITTEE FOR AERONAUTICS

NACA CONFERENCE ON ENGINE STALL AND SURGE

CLASSIFICATION CHANGED
UNCLASSIFIED
To ...
By authority of ... Date ...

Lewis Flight Propulsion Laboratory
Cleveland, Ohio

February 3, 1955

(NASA-TM-X-67600) NACA CONFERENCE ON ENGINE STALL AND SURGE (NASA) 111 p
N74-77114 THRU N74-77120 Unclas 00/99 52158

NACA

(NACA-TM-X-67600) NACA CONFERENCE ON ENGINE STABLE AND SURGE (NASA) 3 Feb. 1955 111 p
X72-70636 thru X72-70672 Unclas 00/99 13880

(ACCESSION NUMBER) 111 (PAGES)
(THRU) None (CODE)
TMX-67600 (NASA CR OR TMX OR AD NUMBER)
(CATEGORY)
FF No. 602(A)
AVAILABLE TO NASA OFFICES AND NASA RESEARCH CENTERS ONLY

CONFIDENTIAL
ANNOUNCEMENTS NO. ... DATE ... BY ...

[redacted]

3665

NACA CONFERENCE ON ENGINE STALL AND SURGE

Lewis Flight Propulsion Laboratory
Cleveland, Ohio

February 3, 1955

[redacted]

DECLASSIFIED

[redacted]

3665

INTRODUCTION

This volume contains copies of the technical papers presented at the NACA conference on Engine Stall and Surge on February 3, 1955 at the Lewis Flight Propulsion Laboratory. A list of the conferees, who are members of the military services, is included.

NATIONAL ADVISORY COMMITTEE
FOR AERONAUTICS

[redacted]

DECLASSIFIED

[redacted]

TABLE OF CONTENTS

I - STALL AND SURGE IN TURBOJET ENGINES
D. S. Gabriel, Chairman
E. W. Conrad
H. B. Finger
R. W. Graham

II - EFFECT OF ROTATING STALL ON COMPRESSOR BLADE VIBRATION
S. S. Manson, Chairman
A. J. Meyer, Jr.
A. A. Medeiros
M. P. Hanson

III - INLET FLOW DISTORTION
D. D. Wyatt, Chairman
L. J. Obery
T. G. Piercy
M. J. Saari

IV - EFFECT OF DISTORTION ON PERFORMANCE
W. A. Fleming, Chairman
R. P. Geye
E. T. Jansen, Jr.
R. R. Miller

V - REMEDIES FOR COMPRESSOR STALL AND BLADE VIBRATION
W. A. Benser, Chairman
M. C. Huppert
L. E. Wallner
H. F. Calvert

VI - STALL AND FLAME-OUT RESULTING FROM FIRING OF ARMAMENT
J. H. Childs, Chairman
F. D. Kochendorfer
R. J. Lubick
R. Friedman

[redacted]

Page intentionally left blank

DECLASSIFIED

NATIONAL ADVISORY COMMITTEE FOR AERONAUTICS
LEWIS FLIGHT PROPULSION LABORATORY
Cleveland, Ohio

LIST OF CONFEREES

The following conferees were registered at the NACA Conference on Engine Stall and Surge, February 3, 1955.

Name	Affiliation
Anderson, James	WADC, Dayton, Ohio
Appold, Col. N. C.	WADC, Dayton, Ohio
Atkinson, A. S.	Bureau of Aeronautics - Wash. D. C.
Ayres, Lt. Col. L. F.	ARDC, Baltimore, Md.
Bakemeyer, Lt. W. F.	WADC, Dayton, Ohio
Becketl, Lt. Col. Walter R.	ARDC, Baltimore, Md.
Blom, Trygve	WADC, Dayton, Ohio
Brenholtz, Major G.	ARDC, Baltimore, Md.
Brown, Col. W. G.	WADC, Dayton, Ohio
Chell, Capt. Paul L.	WADC, Dayton, Ohio
Dailey, Lt. William	WADC, Dayton, Ohio
DeGutis, A.	WADC, Dayton, Ohio
Dubois, Maj. J. M.	ARDC, Cleveland, Ohio
Ellis, F. E.	Bureau of Aeronautics, Wash. D. C.
Feldmeier, Lt. Col. A. L.	Bureau of Aeronautics, Wash. D. C.
Francis, R.	Bureau of Aeronautics, Wash. D. C.
Gangl, Alfred	WADC, Dayton, Ohio
Gates, C. R.	Headquarters, USAF, Wash. D. C.
Gershon, Isak	WADC, Dayton, Ohio
Gray, Major B.	ARDC, Baltimore, Md.
Haugen, Brig. Gen. Victor	WADC, Dayton, Ohio
Hayward, Lt. T. B.	NATS, Patuxent, Md.
Hensley, Lt. Col. R.	ARDC, Baltimore, Md.
Hertz, Major R. J.	WADC, Dayton, Ohio
Hesse, Dr. W. S.	NATS, Patuxent, Md.
Holm, Col. F.	WADC, Dayton, Ohio
Holmquist, Lt. Cdr. C. O.	NATS, Patuxent, Md.
Horan, J. E.	Bureau of Aeronautics, Wash. D. C.
Jones, Major K. L.	WADC, Dayton, Ohio
Koch, Cdr. L. C.	Bureau of Aeronautics, Wash. D. C.
Kotcher, Ezra	WADC, Dayton, Ohio

[redacted]

Lawson, Maurice	WADC, Dayton, Ohio
Lingard, Col. A. I.	WADC, Dayton, Ohio
Litton, Richard	WADC, Dayton, Ohio
Miller, R. T.	Bureau of Aeronautics, Wash. D. C.
Mortel, Donald	WADC, Dayton, Ohio
Newman, Major. J. C.	ARDC, Baltimore, Md.
Ours, S. R.	Bureau of Aeronautics, Wash. D. C.
Parsons, Lt. Col. F. T.	WADC, Dayton, Ohio
Patella, Frank	WADC, Dayton, Ohio
Pinnes, R. W.	Bureau of Aeronautics, Wash. D. C.
Powell, Cdr. L.	Bureau of Aeronautics, Wash. D. C.
Rall, Lt. F. T.	WADC, Dayton, Ohio
Robbins, Major H. W.	ARDC, Baltimore, Md.
Rostkowski, Capt. F. J.	ARDC, Cleveland, Ohio
Roy, Robert	WADC, Dayton, Ohio
Saunders, Lt. D. M.	Bureau of Aeronautics, Wash. D. C.
Seaberg, Major J. D.	WADC, Dayton, Ohio
Scherberg, Max	WADC, Dayton, Ohio
Shoemacher, P. E.	WADC, Dayton, Ohio
Sliuka, W. R.	NATTS, Trenton, N. J.
Smith, E. A.	NATTS, Trenton, N. J.
Smith, Cdr. J. H.	Bureau of Aeronautics, Wash. D. C.
Stephens, Major W. R.	WADC, Dayton, Ohio
Sumner, Capt. T. M.	WADC, Dayton, Ohio
von O'Hain, Hans	WADC, Dayton, Ohio
Watton, Alan, Jr.	WADC, Dayton, Ohio
Weitzen, W.	Headquarters, USAF, Wash. D. C.
Woodhull, Cdr. R. B.	Bureau of Aeronautics, Wash. D. C.
Wynne, Lt. Col. E. P.	ARDC, Baltimore, Md.

DECLASSIFIED

3665

I - STALL AND SURGE IN TURBOJET ENGINES

D. S. Gabriel, Chairman

E. W. Conrad

H. B. Finger

R. W. Graham

CD-4213

DECLASSIFIED

I - STALL AND SURGE IN TURBOJET ENGINES

Compressor stall limits the useful operating range of turbojet engines. In order to achieve maximum performance, modern engines must operate very close to the stall limits at some operating conditions. Consequently, avoiding compressor stall has become one of the the most pressing operational problems. The purpose of this paper is to explain the basic reasons for the existence of stall and to describe some of the effects of stall limits on the operation of modern engines.

TYPES OF STALL

Stall originates in the compressor and is associated with the well-known flow breakaway or separation in the compressor blades. The compressor blades are, of course, very similar to wings, and the stall phenomenon in compressor blades is similar to that in wings.

Wing Stall

The occurrence of stall in a wing is illustrated in figure 1. In the upper part of the figure, a wing or isolated airfoil is shown oriented in an airstream at a small angle of attack. At this small angle of attack the flow around the wing is smooth, and lift is developed because of the difference in pressure on the upper and lower surfaces of the wing. As the angle of attack is increased, the lift increases; but at some high angle of attack breakaway of the flow or separation begins on the wing upper surface. If the angle of attack is increased sufficiently, a large area of separated flow develops as indicated by the sketch at the bottom of figure 1, and the flow over the airfoil is no longer smooth and continuous. As a consequence of this separation, the lift no longer increases as the angle of attack is increased, and the wing is said to be stalled.

Propagating Stall

In a compressor the airfoils are arranged in rows or cascades as indicated in figure 2. At low angles of attack the flow over the blades is smooth and lift is developed. If angle of attack is sufficiently increased, stall will occur in the cascade. The stall in a cascade at high angle of attack is illustrated in figure 3.

In general, in a cascade, because of some transient perturbation of flow or slight geometrical differences between blades, stall starts in only a portion of the cascade rather than over the whole cascade at once. In figure 3, the stalled portion of the cascade is represented

by the passage between blades 2 and 3, although in actual practice several adjacent blades may be stalled simultaneously. Separation of the flow in the stalled blade passage restricts the flow area and dams up the flow between the blades (as indicated by the heavily shaded area). This blockage diverts the flow around the inlet to the blade passage, which, as indicated by the arrows, causes the blades above the stalled region (blades 3 and 4) to experience increased angles of attack and the blades below the stalled passage to experience decreased angles of attack. The increased angles of attack on blades 3 and 4 cause stall of these blades, whereas the decreased angles of attack on the lower blades cause these blades to unstall. As a result, the stalled region is effectively propagated across the cascade and the low-pressure or stalled region moves across the cascade.

Rotating Stall

As shown in figure 4, the compressor cascade (sketch on the left) when wrapped around a disk becomes the compressor blade row or single-stage compressor. Propagation of the stalled region across the cascade is therefore analogous to rotation around the compressor rotor. Propagating stall in the compressor rotor is therefore called rotating stall. It has been observed in many compressors that the stall zones rotate around the compressor annulus at about half rotational speed. If a hot-wire anemometer at rest with respect to the compressor case is inserted in the airstream behind the blade row, it will show a decrease in local air flow each time a stall zone passes the anemometer. A diagram of a typical flow-time trace from such a probe is shown on the right side of figure 4. A depression in flow occurs each time a stall zone passes the probe, and the depressions are in general evenly spaced.

Rotating stall occurs in the single-stage compressor only at high angles of attack. At lower angles of attack, lift or pressure ratio may be developed without stall. An example of the effects of angle of attack on the performance of a single-stage compressor is shown in figure 5.

Single-stage performance. - In figure 5 pressure ratio is plotted against weight flow for lines of constant compressor rotational speed. The pressure ratio is produced by the lift of the blades, and the weight flow is inversely proportional to the angle of attack. The lower the flow through the compressor at any constant engine speed, the higher the angle of attack.

At each speed, if the outlet flow is throttled (flow through the compressor decreased), the lift and hence the pressure ratio increases. Just as in the case of the isolated wing, if the flow is decreased or the angle of attack increased sufficiently, stall occurs and further decreases in flow result in a reduction in pressure ratio. At flows somewhat lower than the values for complete stall, the rotating-stall zones, previously discussed, are found.

DECLASSIFIED

The data of figure 5 are replotted in a more convenient form in figure 6. Weight flow is replaced by the ratio of volume flow to speed, and pressure ratio is replaced by an equivalent pressure ratio corrected for engine speed. This substitution of coordinates brings the three curves of figure 5 together into one curve. In other words, the single curve of figure 6 is valid for all speeds. All subsequent single-stage performance curves are presented in this form.

Types of rotating stall. - During operation of single-stage compressors in the rotating-stall region, many types of stalled flow occur. Two of the most common types of flow are illustrated in figure 7. In the upper part of the figure are the stage performance and a diagram of the stall zones for the type of rotating stall that has been called "progressive," and in the lower part of the figure are the characteristics of the type of rotating stall called "abrupt."

Progressive stall, which usually occurs in stages with long blades, originates at the end of the blades. Various numbers of these stalled zones may exist; in this case, three are shown. As the angle of attack is increased, the stalled area becomes gradually larger, and the continuous pressure-ratio characteristic develops as shown on the left. The rotating-stall zones may actually become large enough or numerous enough to join together and create a complete ring of stalled flow around the compressor annulus; this is called "tip stall." A gradual decrease in pressure ratio occurs as the ratio of flow to speed is decreased (angle of attack increased) beyond the stalled condition.

The abrupt stall usually occurs in stages with short blade lengths, in which case the angle of attack becomes critical along the entire blade at nearly the same time. In abrupt stall, the blades stall suddenly over their entire radial length at the same time and the rotating-stall zone may extend over a large portion of the circumference. This sudden stall results in discontinuous drop in pressure ratio at the stall condition, as indicated by compressor characteristic in the lower left part of figure 7.

As indicated by the dashed lines and arrows on the compressor performance curves for the abrupt stall, a hysteresis exists in the stall region. If the ratio of flow to speed is decreased until the compressor stalls, a sudden drop in pressure ratio occurs. If the ratio of flow to speed is then increased to reduce the angle of attack and unstall the compressor, the rotating stall and associated low pressure ratio persist to a higher value of flow to speed ratio than was required to force the compressor to stall originally. If the ratio of flow to speed is increased sufficiently, the rotating stall suddenly ceases and the pressure ratio jumps up to the unstalled branch of the performance curves. Thus, the hysteresis loop indicated by the arrows exists.

[redacted]

MULTISTAGE-COMPRESSOR STALL

As shown in the sketch at the top of figure 8, the multistage compressor is, of course, a series of single-stage compressors combined. Each stage in the compressor is designed to accept the flow from the previous stage and to produce a certain pressure rise. As the flow progresses through the compressor, the pressure and the density of the compressed air increase. Because of this increase in density and the constant mass flow, it is necessary to reduce the annular flow area through the compressor. The annular area and the blades in the various stages are matched so that all the stages will operate at good efficiency and the flow will pass smoothly through the compressor without stall at the design conditions. The design conditions are indicated by circled points on the typical performance curves for an inlet and an exit stage in the lower part of figure 8.

If the compressor is a part of an engine, it must operate at speeds both higher and lower than design in order to permit regulation of engine thrust. At these off-design speeds, the flow areas and blade settings become mismatched and lead to stall problems.

If speed is reduced below design, the rise in pressure and density across each stage is less than at the design condition. Of course, pumping capacity and hence mass flow through the compressor also decrease. The decrease in density, however, outweighs the decrease in mass flow in the rear stages of the compressor, with a resulting increase in volume flow or velocity in the annular compressor passage in the rear of the compressor. The reduction in mass flow causes the inlet stages of the compressor to operate at reduced velocities. Therefore, the flow area in the rear of the compressor must be increased from its design value or the flow area in the front of the compressor must be decreased to keep each stage operating at the design value of the ratio of flow to speed. Methods of effectively altering this area are discussed in paper V. This paper is confined to fixed-geometry compressors.

The high velocities in the rear of the compressor at low compressor speeds force the operating point of the exit stages to move toward lower angles of attack in the direction of the arrow in the lower right part of figure 8. The rear stages therefore operate at reduced angle of attack as speed is reduced, and the high velocities in the rear stages lead to choking of the flow. This choking of the air flow in the exit stages blocks the flow and forces the inlet stages of the compressor to operate at even lower velocity and higher angle of attack than would be required at low compressor speed if the rear stages were not choked, as indicated by the arrow on the lower left figure. If speed is reduced appreciably, the inlet stages stall and rotating stall occurs in the compressor. The rotating-stall zones may actually extend through the compressor, interfere with the operation of some of the later compressor stages, and cause premature stall of these stages.

[redacted]

If speed is increased above design, the density in the rear stages of the compressor is higher than design. Therefore, the velocities are decreased below the design value, and the angle of attack of the rear stages is increased above the design value. At speeds higher than design, the rear stages tend to stall. The higher density in the rear stages reduces the restriction to flow, more flow enters the compressor, and the front stages experience an increase in flow and move toward their choke limit and toward reduced angles of attack.

Thus, operation of the multistage compressor appreciably off the design speed results in stall in some stage of the compressor. At low speeds, choking in the rear of the compressor causes the inlet stages to stall. When the inlet stages stall, rotating stall occurs. At high speeds, the back stages tend to stall.

The higher the compressor design pressure ratio, the greater the differences required in flow area and density between the inlet and exit of the compressor at the design point. Accordingly, the higher the over-all pressure ratio, the more severe are the off-design stall problems.

Over-All Compressor Performance

In the previous discussion the performance curves shown were for individual stages operating as a part of a multistage compressor. The over-all or composite performance of a multistage compressor is illustrated in figure 9, where over-all compressor pressure ratio is plotted against weight flow through the compressor for a constant engine speed. As in the case of the single-stage compressor, throttling the outlet of the multistage compressor increases the over-all pressure ratio up to the compressor stall limit. As the weight flow is reduced, the pressure ratio across each stage increases and approaches the stall point. Finally, a condition is reached at which stall becomes so severe that a sudden drop in pressure ratio occurs. This point, as indicated in figure 9, is called the compressor stall limit. The stall limit is the limit of useful operation of the multistage compressor.

Two distinctly different flow phenomena are possible for operation beyond the stall limit. Either the compressor may operate on the stalled branch of the performance curve, denoted in figure 9 by the shaded area, or surge may occur. If the compressor is a part of an engine, operation along the stalled branch of the performance curves is actually not practical. Compressor performance falls off so radically that over-temperature of the turbine results.

If the combination of the compressor characteristics in stall and the size and arrangement of the rest of the engine are such as to form a basically unstable system, the engine may surge when the compressor

[redacted]

drops into stall. During surge, violent low-frequency pressure oscillations occur throughout the engine. These pressure oscillations are associated with cyclic operation around the hysteresis loop indicated by the arrows in figure 9. Regardless of whether surge or operation in stall occurs, the stall limit is the limit of useful compressor and engine operation.

Compressor performance map. - As has been discussed in connection with figures 8 and 9, over-all compressor performance is affected by two independent operating variables, engine or compressor rotating speed and weight flow through the compressor. Therefore, the complete compressor performance map (fig. 10) comprises a series of constant-speed operating lines similar to the one shown in figure 9 on a plot of over-all compressor pressure ratio against weight flow through the compressor. The line labeled first-stage stall denotes the boundary of operation without rotating stall. As previously discussed, if speed is reduced below the values indicated by the boundary line, stall of the early stages results and rotating stall occurs in the compressor. Even with this rotating stall present, sufficient damping of the pressure oscillation occurs, so that the engine may operate within the shaded region without large-amplitude pressure oscillations in the engine. If the compressor pressure ratio is increased sufficiently along any of the constant-speed lines, the stall limit or limit of useful engine operation discussed in connection with figure 9 is encountered. The broken line drawn through these stall-limit points is labeled the compressor stall limit. It is evident, therefore, that the stall limit and the boundary of rotating stall are not the same. The rotating-stall boundary simply denotes the separation between a region of operation in which rotating stall occurs and another region of operation in which rotating stall is absent. The stall limit, on the other hand, denotes the limit of useful engine operation.

At low engine speeds (in this case below about 65 percent), if the stall limit is encountered, the engine may operate stably along the stalled branch of the performance curve (fig. 9) or the engine may surge. Whether or not surge occurs at low engine speeds depends on the characteristics of the individual compressor and the rest of the engine or, in other words, on whether or not sufficient damping is present to inhibit surge oscillations. If the stall limit is encountered at higher speeds, the engine invariably surges. As a general rule, sufficient damping is not present to prevent surge at high speeds. It is evident that the stall-limit line definitely limits engine operation at all engine speeds.

Characteristics of stall and surge. - The distinction between stall and surge is evident from figure 11, where the variation in flow with time measured by a hot-wire anemometer installed in the compressor is shown for operation during rotating stall (upper trace) and for operation

[redacted]

DECLASSIFIED

during surge. During operation with rotating stall, the amplitude of the pressure oscillations is small and the frequency is high. To all outward appearances, the engine operates stably with these small disturbances. As shown by the lower trace, large-amplitude oscillations exist during surge. Just before surge, the engine goes into rotating stall, as indicated by the small pressure pulses, and these small disturbances build up into the large surge pulses shown at A and B. During surge, loud pounding noises are audible, and flames periodically shoot out the engine exhaust nozzle. One some occasions, smoke and vapors have been observed periodically issuing from the engine inlet. The whole engine system is unstable during surge, and flight with a surging engine is not practical.

Steady-state operating line. - The importance of the stall and surge limits in the operation of modern engines depends on the proximity of the stall limits to the normal engine operating conditions, which are usually defined with the aid of the steady-state operating line. A compressor map similar to that of figure 10 is shown in figure 12. When a compressor is operating as a part of a turbojet engine, the weight flow through the compressor and the pressure ratio it develops are controlled by the flow area of the turbine and the engine exhaust nozzle. That is, the turbine and exhaust nozzle are analogous to a throttle after the compressor in a compressor test rig. If the geometry of the engine (flow area) is fixed, the compressor will operate in steady state at only one pressure ratio at any given speed. In figure 12, a line connecting these steady-state operating points is shown. All along the steady-state operating line, the compressor, turbine, and exhaust nozzle are matched, so that the compressor will operate at points on this curve with a fixed throttle setting or fuel flow. Increasing the exhaust-nozzle area causes a decrease in compressor pressure ratio from this line at a constant speed; decreasing exhaust-nozzle area causes an increase in compressor pressure ratio.

It is evident, therefore, that the position of the steady-state operating line relative to the stall limit indicates the importance of the stall limit to engine operation. The steady-state operating line is usually very close to the stall limit at low speeds and extends down into the region of rotating stall. This proximity of the stall limit and the operating line introduces engine acceleration problems.

Acceleration

Typical engine acceleration data for a single spool engine are shown in figures 13 and 14. The steady-state operating line and the stall-limit line are shown in figure 13 along with an acceleration path that denotes compressor operating conditions during acceleration. The fuel flow is rapidly increased to accelerate the engine. This increase in fuel flow

causes an increase in gas temperature at the turbine, which increases the volume of the gases passing through the turbine. More pressure is therefore required to force the gases through the turbine; and, consequently, the compressor pressure ratio rises above the steady-state operating line, as indicated in figure 13. For this particular acceleration, the operating point during acceleration just skirts the stall limit; and, as indicated by the time marks, the acceleration is completed in about 5 or 6 seconds.

If it is desirable to accelerate in less time, more fuel must be introduced. The sequence of events with a larger increase in fuel flow is shown in figure 14. For the acceleration in figure 14, a 5 percent larger increase in fuel flow was used than for the acceleration shown in figure 13. The operating pressure ratio during acceleration increased, therefore, to a higher level and encountered the stall limit. The engine then entered surge; and, after a few pulses, the fuel flow was reduced to avoid damage to the engine. Acceleration was impossible in this case.

These examples show that the margin between the steady-state operating line and the stall limit is a measure of the maximum possible rate of acceleration. This margin is therefore referred to as the acceleration margin.

Compressor surge does not always result when the stall limit is reached during an acceleration. As previously discussed, the compressor may in some cases fall into abrupt rotating stall, and overtemperature of the turbine may limit acceleration. In other cases, the compressor may enter abrupt stall or surge and actually accelerate through it. In any event these stall phenomena are sufficiently severe and unreliable to make the stall limit the real limit of acceleration.

Part-Speed Stall

In some engines the steady-state operating line intersects the stall-limit line at low or intermediate speeds even without acceleration. In these cases it is not only impossible to accelerate but also impossible to operate the engine in steady-state at these part-speed conditions.

An example of this part-speed stall problem is provided by the performance of the compressor shown in figure 15. The problem results from the sharp knee or discontinuity in the stall-limit line at speeds from about 70 to 85 percent of rated speed. This discontinuity is caused by the simultaneous abrupt stall of several stages of this high-pressure-ratio (about 9:1) compressor. It is evident that the steady-state operating line

DECLASSIFIED

(dashed line, fig. 15) passes through the compressor stall limit and makes operation of the engine in steady state impossible at these part-speed conditions without variable-geometry devices.

High-Speed Stall

The part-speed stall occurs because the front stages of the compressor are stalled. As previously discussed, at high speeds the back stages tend to stall. This high-speed stall is illustrated by the performance shown in figure 16. The stall limit bends over and approaches the steady-state operating line at speeds above design. The stall limit and the operating line intersect at an engine speed about 8 percent higher than the design, making operation at higher speeds impossible.

3665

The steady-state operating line and the stall-limit line are actually functions of the equivalent engine speed, as shown in figure 16. The equivalent speed is simply the ratio of the actual rotating speed to the square root of the compressor-inlet temperature. At high altitutes, where the compressor-inlet temperature is low, the equivalent speed is high. The high-speed stall limit is therefore usually encountered primarily at high altitudes. The high-speed stall limit is a general limit existing in most engines.

STALL OF TWO-SPOOL ENGINES

The discussion so far has dealt with the single-spool engine. The two-spool engine is also subject to stall. A sketch of a hypothetical two-spool engine and a plot of the relation between inner- and outer-spool speeds are shown in figure 17. The outer compressor is driven by the outer turbine, and the inner compressor by the inner turbine. Since there is no mechanical connection between the two spools, the operation of the two spools is determined entirely by the aerodynamic and thermodynamic relations involved in the design; that is, the speeds, pressure ratios, and air flow of the two spools are determined by the flow areas and power production or absorption characteristics of the components. For this reason there can be a very wide variety of types of operation of two-spool engines, but some of the operational characteristics are fairly general. These more general characteristics are discussed in the following paragraphs.

[redacted]

The speed of the inner compressor is plotted against the speed of the outer compressor for a hypothetical engine at the bottom of figure 17. In this case the inner compressor is designed for a speed of 10,000 rpm, and the outer compressor for 6000 rpm. The pressure rise across a compressor stage increases as speed increases. It is evident, therefore, that the inner compressor may develop a higher pressure ratio than the outer compressor for the same number of stages; and in actual practice the two-spool engines do operate at higher pressure ratios than the single-spool engines.

In the two-spool engine, however, there are two compressors and therefore two stall limits. These stall limits and the over-all steady-state performance of the hypothetical two-spool compressor are shown in figure 18, where over-all compressor pressure ratio is plotted against weight flow through the compressor. The broken line is the steady-state operating line, which is very similar to the operating line for a single-spool compressor. In the two-spool compressor, however, the pressure ratio obtained is the product of the pressure ratio being developed by the the outer and inner spools. As a consequence of the aerodynamic coupling of the outer and inner spools during steady-state operation, when the over-all pressure ratio of the two-spool compressor is slowly increased above the steady-state operating line, the pressure ratio of the outer compressor actually decreases slightly. This decrease is, of course, more than made up by the increase in inner-compressor pressure ratio. The important thing is that, when over-all pressure ratio is increased slowly, the pressure ratio of the outer spool actually moves away from its stall limit. Because of the difference in the aerodynamic coupling of the two spools during transients, the preceding discussion and figure 18 are not applicable to transient operation. As indicated in figure 18, the inner-compressor stall limit is the only limit to a gradual increase in over-all pressure ratio. Conversely, the outer-compressor stall limit is a limit to a gradual decrease in over-all pressure ratio. The steady-state operating line must be oriented between these two stall limits.

Although it may seem from casual examination that the stall limits are more restrictive in the two-spool than in the single-spool design, higher over-all compressor pressure ratios may be achieved by proper design in the two-spool than in the single-spool engine with no more severe stall problems. Similar stall problems at part speed and at high speed do exist, however.

An example of the stall limits for the two-spool J57 engine are shown in figure 19, where over-all compressor pressure ratio is plotted against inner-compressor speed. As shown in the figure, the steady-state operating line runs into the outer-compressor stall limit at about 84 percent of rated speed, and this speed becomes a lower limit unless variable-geometry devices are used. The bleed valve which is installed between the outer and inner spools of the J-57 provides this variable-geometry and so removes this limitation. The operating line and the inner-compressor stall limit intersect at a speed 9 percent

[redacted]

DECLASSIFIED

higher than the rated speed, and thus speed becomes the upper limit of operation. Thus, it is evident that the same stall-limit problems that exist in the single-spool engine are also present in the two-spool engine.

CONCLUSIONS

Stall or flow breakaway, which occurs in wings at high angles of attack, also occurs in compressors. In compressors, stall limits the pressure ratio that can be developed by the compressor. If the single-stage compressor is operated in stall, local regions of stalled flow appear that propagate around the compressor annulus. This propagating stall is called rotating stall.

In the multistage compressor, operation at speeds lower than design forces the front stages of the compressor to stall and causes rotating stall to appear. At speeds higher than design, the rear stages of the compressor tend to stall.

If the pressure ratio of the multistage compressor is increased sufficiently at any speed, a limit of useful compressor operation is encountered. This limit of operation is called the compressor stall limit and is the point at which stall becomes sufficiently widespread in the compressor, or sufficiently severe, to cause a large discontinuous drop in compressor pressure ratio and efficiency.

If the compressor as a part of an engine is operated beyond the stall limit, either excessive turbine-inlet temperatures will result, which make operation impractical, or the engine will surge. Which thing happens depends upon the characteristics of the individual compressor and the amount of damping present in the rest of the engine. Experience has shown that, although either type of limit may occur at low compressor rotative speeds, surge invariably occurs at high speeds. In any case, the stall limit is the real limit of engine operation.

In order to achieve maximum performance with minimum size, modern engines are designed so that the stall limits occur close to the steady-state operating lines of the engine. This proximity of the stall and operating lines introduces two major problems in modern engines: (1) The acceleration margin, and hence the acceleration rate, is limited, or the steady-state operating line and the stall-limit line may actually intersect at part speed, necessitating the use of some remedial device; (2) the stall-limit and steady-state operating lines may intersect at speeds higher than design, which may make the engine inoperative at the lower compressor inlet temperatures accompanying high-altitude flight conditions. All of the modern engines are subject to these limitations.

FLOW ACROSS A WING SECTION

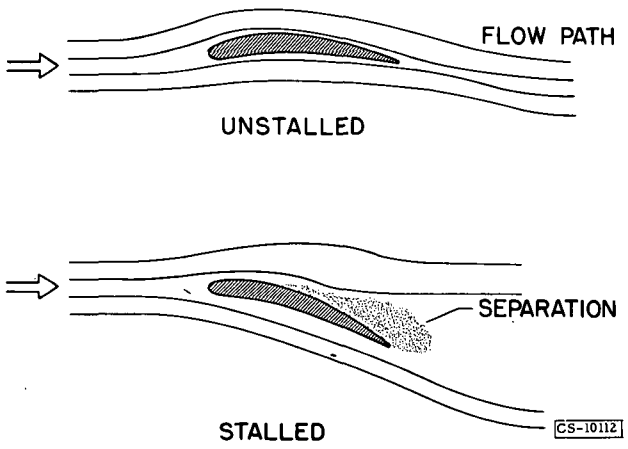

Figure 1.

UNSTALLED CASCADE

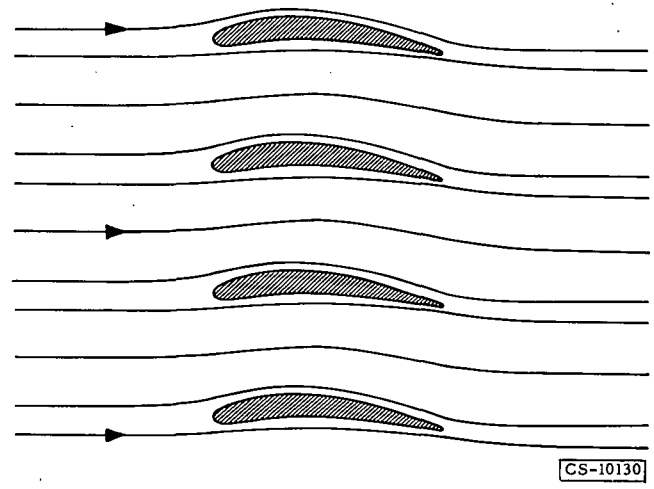

Figure 2.

STALL PROPAGATION IN CASCADE

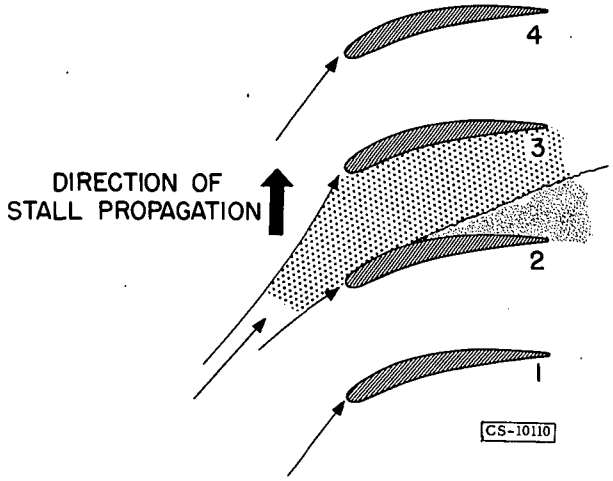

Figure 3.

STALL PROPAGATION IN ROTOR OR STATOR
ROTATING STALL

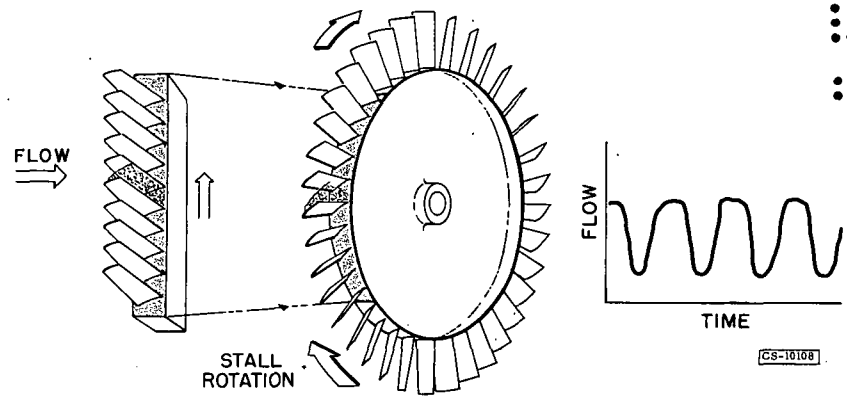

Figure 4.

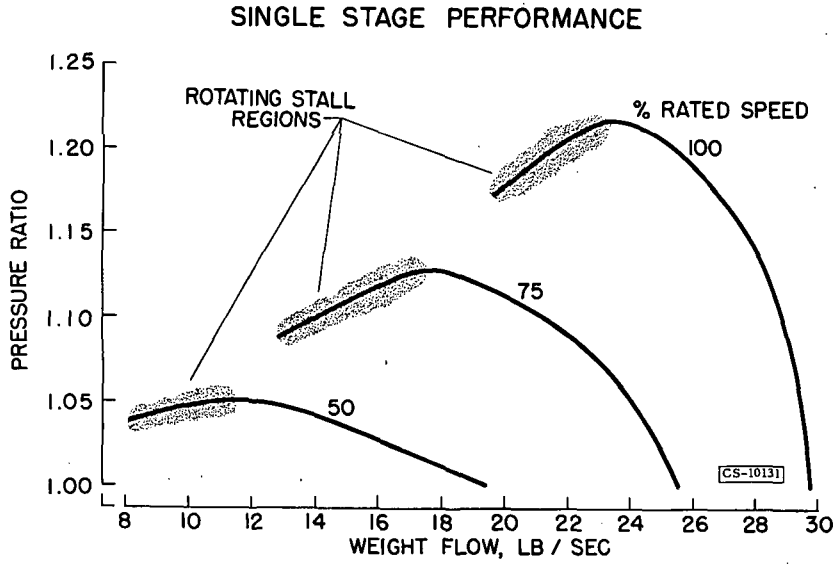

Figure 5.

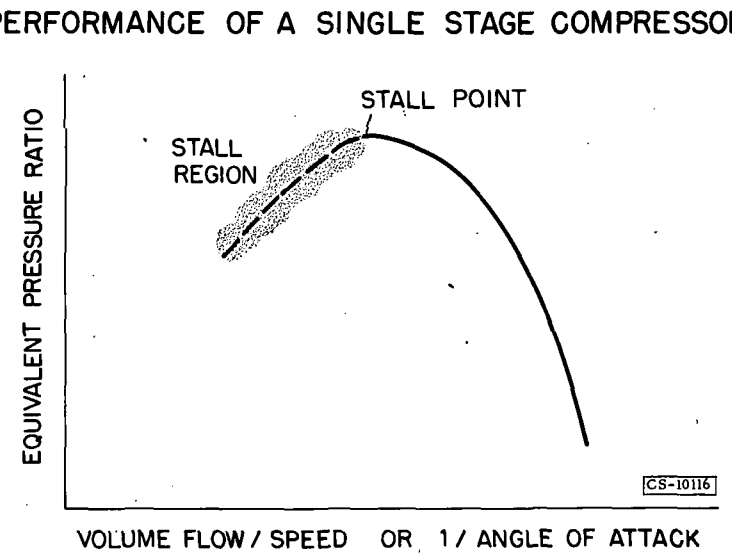
PERFORMANCE OF A SINGLE STAGE COMPRESSOR
STALL POINT
STALL REGION
EQUIVALENT PRESSURE RATIO
CS-10116
VOLUME FLOW / SPEED OR 1 / ANGLE OF ATTACK

Figure 6.

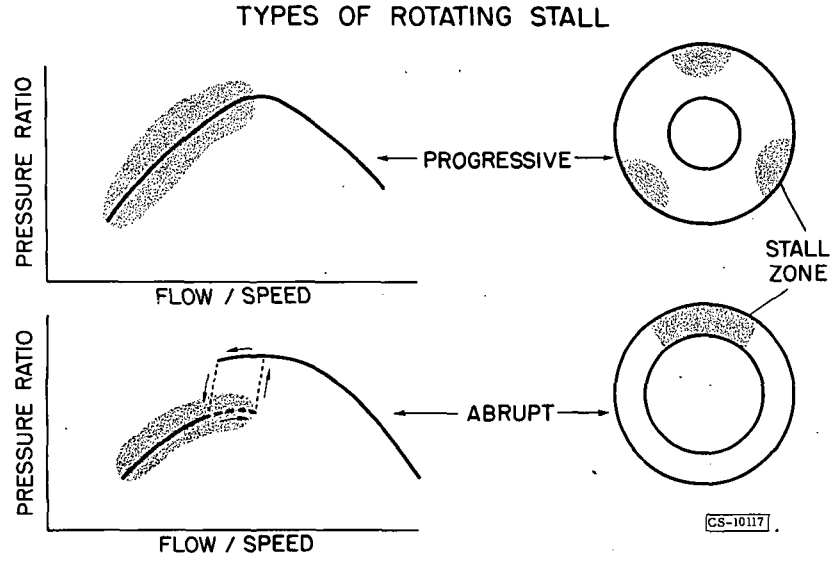

Figure 7.

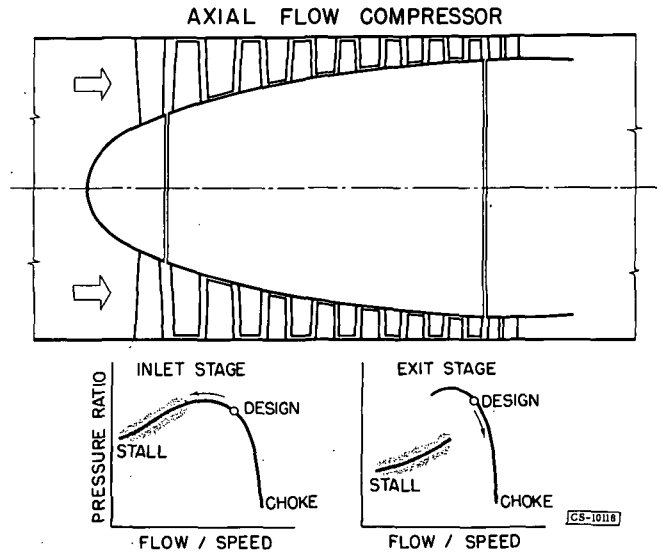

Figure 8.

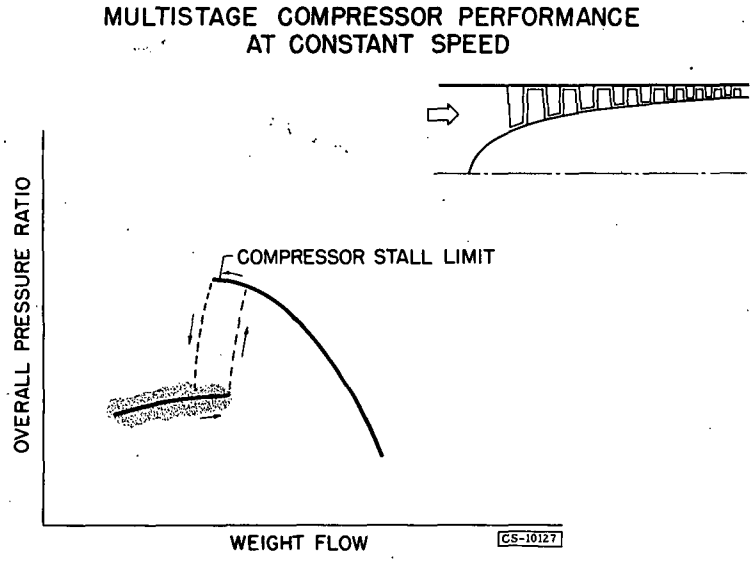

Figure 9.

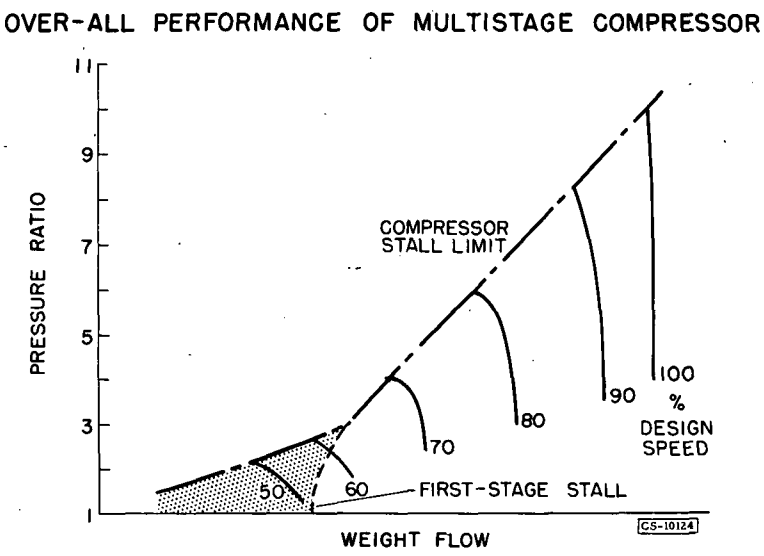

Figure 10.

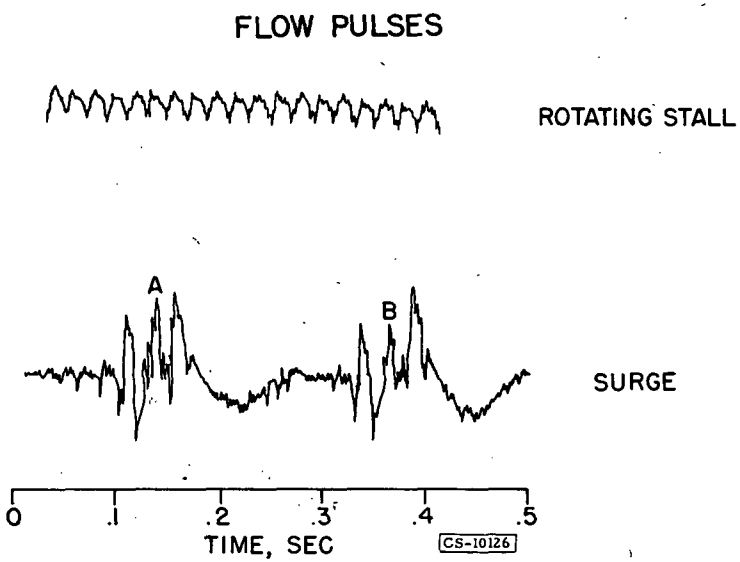

Figure 11.

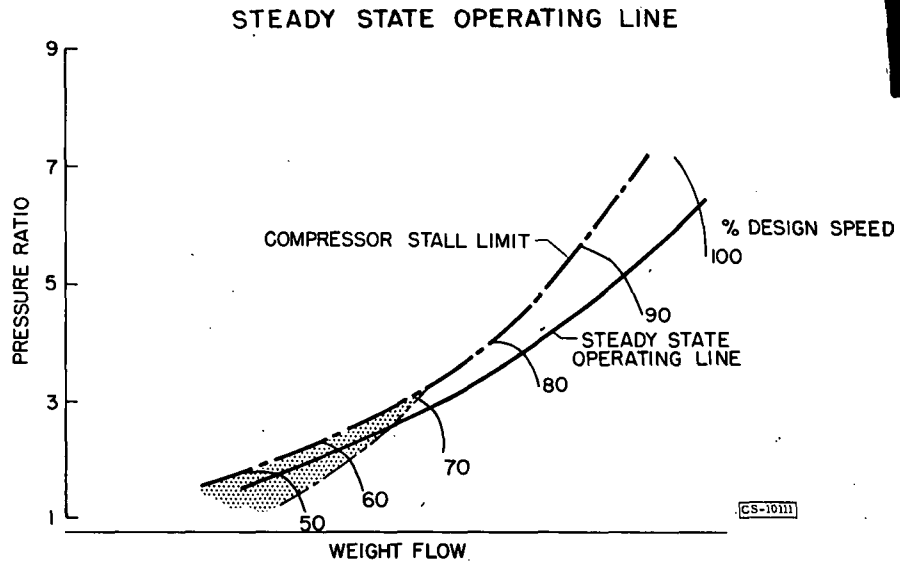

Figure 12.

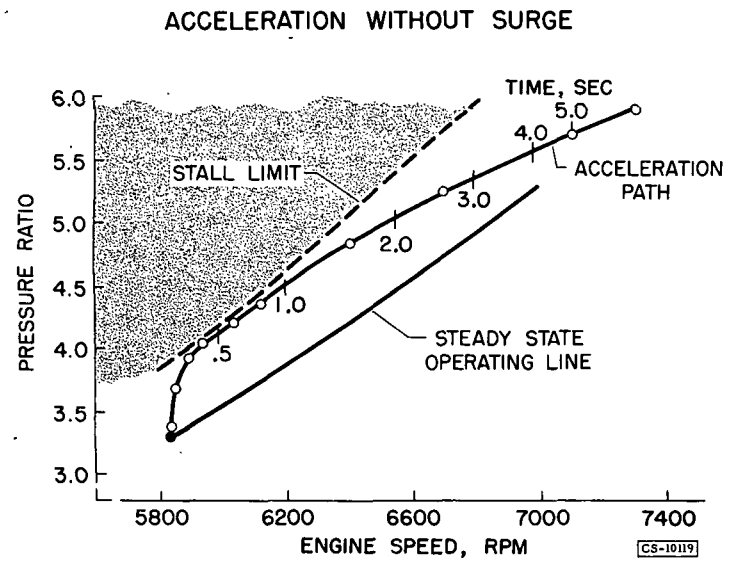

Figure 13.

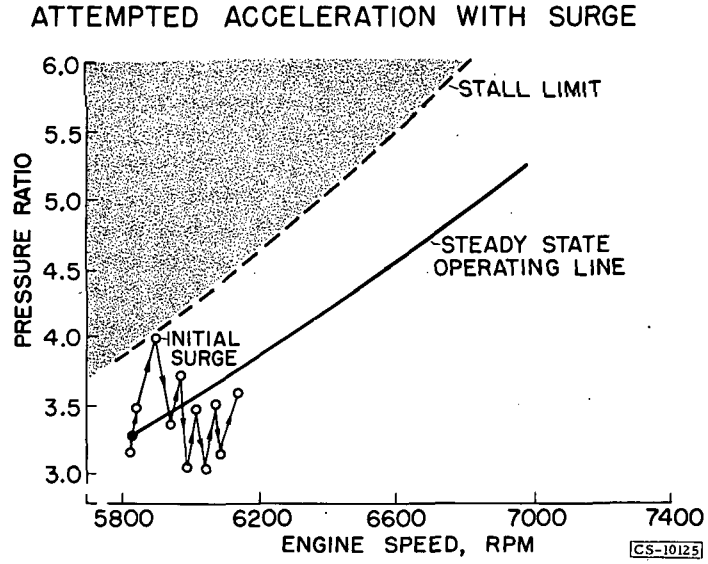

Figure 14.

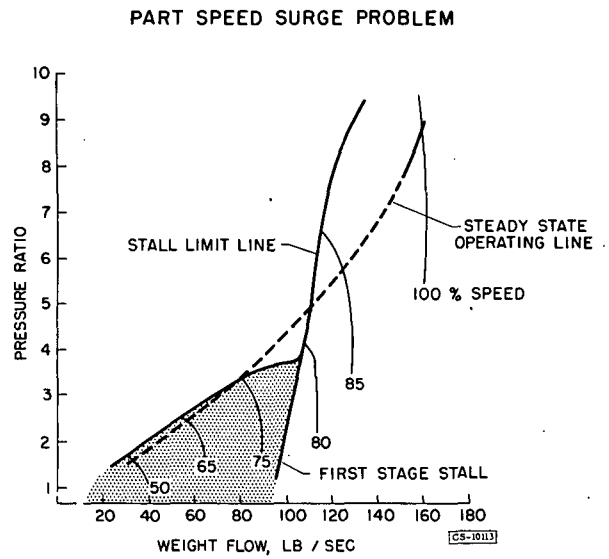

Figure 15.

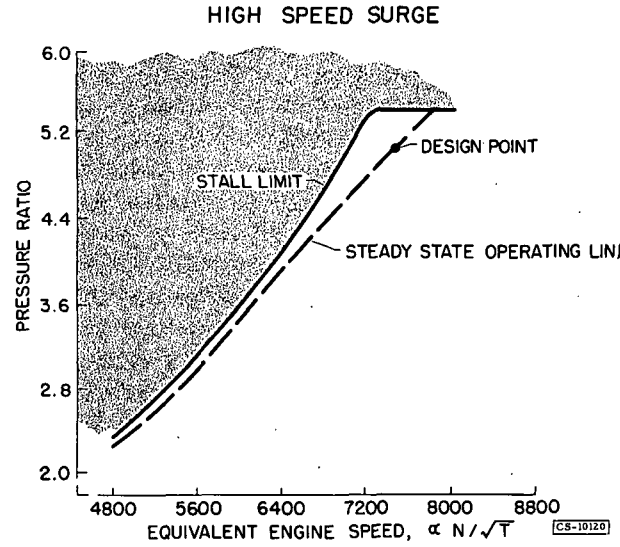

Figure 16.

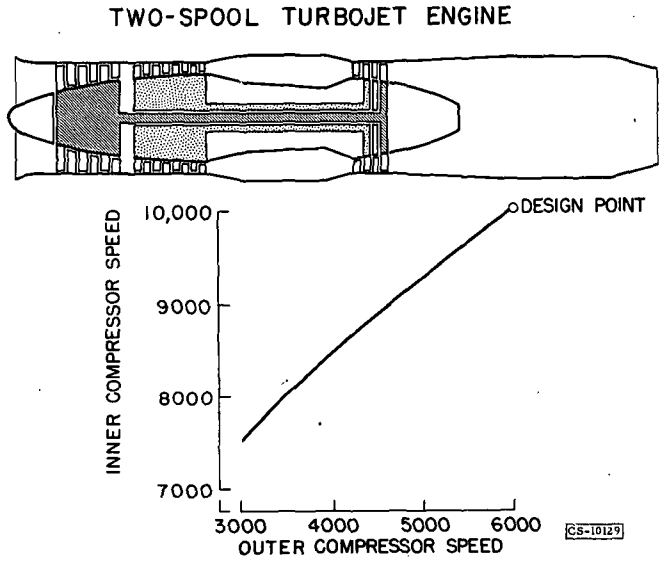

Figure 17.

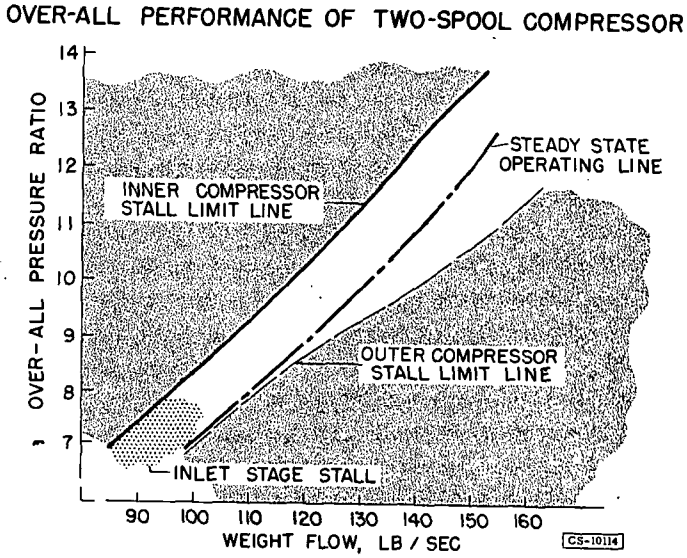

Figure 18.

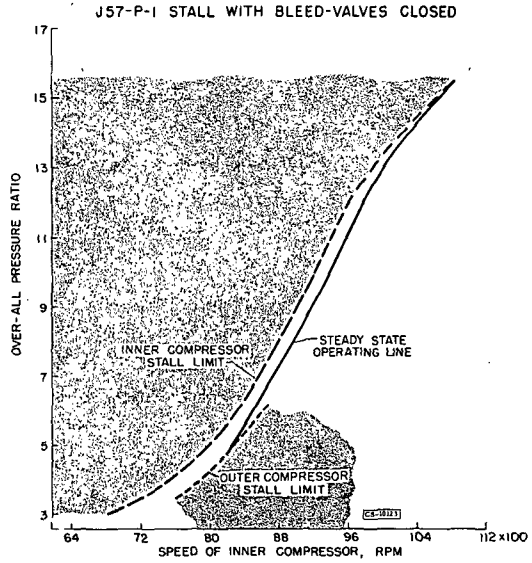

Figure 19.

DECLASSIFIED

[redacted]

3665

II - EFFECT OF ROTATING STALL ON COMPRESSOR BLADE VIBRATION

S. S. Manson, Chairman

A. J. Meyer, Jr.

A. A. Medeiros

M. P. Hanson

[redacted]

CD-4216

DECLASSIFIED

[redacted]

II - EFFECT OF ROTATING STALL ON COMPRESSOR BLADE VIBRATION

INTRODUCTION

Rotating stall has two important effects: (1) It affects the aerodynamic performance of the compressor, and (2) it may produce compressor blade vibrations. A number of compressor blade failures, both in experimental rigs and in production compressors, have been traced to vibration induced by rotating stall. The present discussion indicates the reason that rotating stall induces vibration, presents some vibration data obtained in operating compressors, and outlines several remedies that might be used in overcoming this problem.

3665

MECHANISM OF VIBRATION EXCITATION

Relative Velocity between Rotating Stall and Compressor Blades

To demonstrate the reason for vibration excitation by rotating stall, it is necessary first to determine the relative velocity between the stall zones and the compressor blading. For the stator blades the relative velocity is obviously the absolute velocity of the rotating stall. For the rotor blades the relative velocity is determined as in figure 1. In this figure, a row of stator blades is shown, followed by a row of rotating blades. It is assumed that rotating stall has been established. The velocity of the rotating stall in the stators is equal to vector A, and the velocity of the rotor blades is designated by vector B. If a given stall pattern exists within one stage of compressors, in most cases its effect is felt throughout the unit (ref. 1). Thus, the velocity of the rotating stall in the rotor blades, vector A', is equal to vector A. The velocity of the rotating stall relative to the rotor blades is then equal to vector B minus vector A', or vector C.

Because of the relative motion between the stall and the blades, each blade experiences alternate regions of high and low pressure. By use of hot-wire anemometers, various patterns of rotating stall and consequent pressure fluctuations have been determined. Typical configurations are shown in figure 2. The circles represent the annulus of the compressor, and the shaded areas the stalled regions. Figure A represents a hub stall configuration; figure B, a combination of hub stall and a tip stall. In figure C the stall exists over the entire blade span; and in figures D, E, and F are shown tip stalls, both evenly and unevenly spaced. As the pressure variations due to the stall zones pass by the blades, they produce periodic forces that may excite the blades into vibration if they are of the proper frequency.

[redacted]

[redacted]

Condition of Resonance

To determine under what conditions rotating-stall frequencies will produce blade vibrations, a typical response curve of a blade is shown in figure 3 (ref. 2, pp. 61-70). When a blade is excited by a sinusoidal force, the amplitude of vibration depends on the ratio of the frequency of the exciting force to the natural frequency of the blade. For low ratio of excitation to blade natural frequency, the amplitude is relatively low. However, as the exciting frequency approaches the natural frequency of the blade, the amplitude increases rapidly. Were there no damping, the amplitude would become infinitely great when the exciting frequency is equal to the natural frequency. Because friction is always present, the amplitude does not become infinite, but does achieve a high value at this condition of equality between exciting frequency and blade natural frequency. Vibration under such a condition is known as resonant vibration. For exciting frequencies above the natural frequency of the blade, the amplitude again falls off and rapidly approaches zero as the exciting frequency is increased. Thus, to obtain high vibration amplitudes, it is necessary for the exciting frequency to be at or near the natural frequency of the blade.

3665

Exciting Frequencies Contained in Rotating-Stall Signals

The meaning of the exciting frequency of the rotating stall must be clarified. Actually, a given rotating-stall pattern contains a large number of exciting frequencies, as can be seen in figure 4. In the upper part of the figure is shown a typical signal obtained from a hot-wire anemometer. Rather than being sinusoidal, the wave is complex. Since the natural motion of the blade during vibration is, however, sinusoidal, it turns out that, to analyze blade vibrations, the complex wave must be replaced by a combination of sine and cosine waves.

With the use of a Fourier analysis (ref. 2, pp. 19-30), it is found that the upper signal can be replaced by the combination of the signals of the sine and cosine signals in the lower part of the figure. There exists first a uniform component, indicated by the horizontal line H, as well as a number of sine and cosine waves. At any point such as P, the sum of OA, OB, OC, OD, and the steady-state component (the distance between the axis and horizontal line H) is equal to the amplitude of the original signal. The effect of the original stall signal is therefore exactly the same as the effect of the combined signals as far as blade vibration is concerned.

The steady-state component does not produce any vibrations, but each of the sine waves can produce a vibration if it is at or near the natural frequency of the blade. For example, if the frequency of the stall signal is 100 cps, then there will exist a wave as shown on the figure for a

[redacted]

frequency of 100 cps, which is called the fundamental. In addition, there will exist a wave having a frequency 200 cps called the second harmonic, and other waves for 300 and 400 cps, and so forth, as the third and fourth harmonics, and so forth. Thus, because of the complexity of the stall signal, it becomes possible to encounter a large number of resonances within the operating range of the engine.

3665

Critical-Speed Diagram

After the stall signal has been resolved into its harmonic components, it becomes possible to predict the speeds at which resonant vibrations occur by use of a critical-speed diagram such as shown in figure 5. On the horizontal axis is shown engine speed, and on the vertical the frequency of excitation. The frequency of rotating stall is approximately linear with rotative speed, and the lowest inclined line represents the variation of exciting frequency of the fundamental of a given stall pattern. Excitation is also produced at any engine speed by the second harmonic at a frequency exactly twice the fundamental frequency, and by the third harmonic at a frequency three times the fundamental, and so forth. Therefore, a number of exciting lines exist, as shown by the solid lines in figure 5. Also shown in the figure by the dotted line is the natural frequency of the blade, which increases slightly with rotative speed as a result of centrifugal stiffening. Each time the natural-frequency line intersects one of the lines of excitation, resonance occurs.

Figure 6 shows a more realistic critical-speed diagram, in which the natural-frequency lines for the first five stages are shown. Lines of excitation are shown for a single-stall-zone pattern, two-stall-zone patterns, and three-, four-, and five-zone stall patterns. Also shown are the second harmonics of the three- and four-zone stall configurations. The dotted and solid lines intersect at many points, indicating that blade vibrations are possible at many engine speeds. In practice, it is practically impossible to avoid resonance with one or another of the stages and the various exciting lines possible whenever rotating stall occurs. However, not all resonances cause serious vibrations. As indicated in figure 4, the amplitudes of the various harmonics are not all high. The energy available for vibration excitation depends on the amplitude of the particular harmonic which is in resonance with the blade natural frequency. Thus, although resonance occurs in some cases, the amplitude developed may be low if the available excitation energy is low.

TYPICAL VIBRATIONS IN OPERATING COMPRESSORS

The vibration measurement as obtained in a number of operating compressors will now be presented by use of critical-speed diagrams as previously described.

[redacted]

J65 Engine

The J65 engine was the first engine in which a serious problem of blade vibration induced by rotating stall was clearly recognized. The results of this investigation are summarized in figures 7 and 8 (ref. 3). The critical-speed diagram (fig. 7) indicates the exciting lines due to the fundamentals of one- to five-stall-zone excitations. The heavier sections of the lines represent the speed ranges in which the stall zones were encountered for the inlet conditions used in the test. None of the fundamentals of the stall configurations was capable of producing blade vibrations because of their low frequency. However, the second harmonic of the three-zone rotating-stall configuration intersected the natural-frequency line of the first-stage blades at a speed of approximately 5200 rpm. The stress as measured by means of strain gages mounted on these blades is shown in the first of the curves of figure 8. At resonance, a stress amplitude of $\pm$26,000 psi was obtained.

In the second-stage rotor blades, the important exciting force was the second harmonic of the three-zone stall configuration, intersecting the natural-frequency line at a speed of 5800 rpm (fig. 7) and likewise producing a resonance stress amplitude of $\pm$26,000 psi (fig. 8).

In the third stage, the significant excitation occurred as a result of the second harmonic of the four-zone stall configuration intersecting the natural-frequency line at a speed, again, of 5200 rpm, but inducing stress of only $\pm$16,000 psi, as shown in figure 8.

Effect of exhaust-nozzle area. - Examination of figures 7 and 8 indicates that two critical vibrations both occur at 5200 rpm, one excited by the three-stall-zone pattern and the other by the four-stall-zone pattern. Actually, the two vibrations do not occur simultaneously at 5200 rpm; the particular configuration that is induced at this speed depends on other engine conditions, as is demonstrated in figure 9. The compressor total-pressure ratio is plotted against equivalent weight flow for lines of constant equivalent speed. This map is plotted for the low-speed range, where the inlet stages are operating at stall conditions. The various stall patterns are indicated by the regions labeled 2, 3, 4, and 5. Any point of operation bounded by lines OA and OB resulted in a rotating stall with two zones; any region bounded by lines OB and OC resulted in rotating stall with three zones, and so forth. Although the regions are shown as distinct from each other, there is in practice some overlap between these regions, and the boundaries separating the regions are not as clear as indicated in the figure. In general, along the stall-limit line, only one stall zone was experienced, not only at the speeds shown in the figure, but at all speeds.

Steady-state operating lines for two nozzle areas are shown as the broken lines. At sea-level inlet temperatures, the equivalent speed line of 5200 rpm will also correspond to an actual engine speed of 5200 rpm.

[redacted]

Therefore, with a large exhaust-nozzle area, four stall zones would occur at 5200 rpm, thereby resulting in high vibration amplitudes in the third stage. If, however, the nozzle area is decreased, the number of stall zones at 5200 rpm changes to three, and vibrations now are induced in the first stage rather than the third. Thus, although vibration can occur because of the three- and four-stall-zone excitation, shown in figures 7 and 8, each occurs at a different engine operating condition, but at a speed of 5200 rpm.

Effect of inlet temperature. - Even with constant exhaust-nozzle area, it is also possible to obtain a change in stall pattern depending on the inlet temperature, as shown in figure 10 (ref. 4). Again, the total-pressure ratio is plotted against equivalent weight flow, and the regions of the various stall configurations are delineated by lines OA, OB, OC, and so forth. At an actual engine speed of 5200 rpm, a temperature of 59° F, and with operation along the steady-state operating line, three stall zones exist as indicated by the circled point. If the mechanical speed is held constant at 5200 rpm but the inlet temperature is changed to 20° F, equivalent speed is changed to approximately 5400 rpm and a four-zone stall predominates, as indicated by the diamond in figure 10. The change in stall configuration shifts vibration from the first to the third stage as before.

If the inlet temperature is decreased to -67° F, corresponding to the temperature at high altitudes, and the engine speed is still maintained at 5200 rpm, the equivalent speed becomes 6000 rpm. As indicated by the square, operation now occurs at a condition outside the region of rotating stall, and no high-amplitude blade vibrations are encountered. Thus, blade vibration depends not only upon the actual engine speed, but upon other engine parameters. An engine may not have a vibration problem at one inlet temperature or nozzle setting, but may have a serious vibration problem when either of these variables is changed.

J47 Engine

Critical-speed diagram. - The critical-speed diagram for the J47-23 engine is shown in figure 11 (ref. 5). Stall patterns from one to seven were observed in a limited speed range from 4500 to somewhat less than 6000 rpm. The fundamental frequencies of the first five stall patterns were not sufficiently high to induce vibration. The sixth- and seventh-zone stalls did, however, induce vibrations in the first rotor, and the seventh stall configuration also induced vibrations in the second stage, as indicated in figure 11. The second harmonic of the four- and five-stall zones induced vibrations in the third and fourth stages, respectively. No vibrations of practical significance were measured in the other stages. The vibration that was encountered was greatly influenced by the exhaust-nozzle setting. Figure 12 shows that, with the nozzle in the rated position, the maximum stress amplitude was ±26,500 psi; whereas, with the nozzle closed, the stress amplitude was ±60,000 psi.

[redacted]

Effect of acceleration. - The nozzle in this engine was closed in order to obtain a complete performance map of the rotating-stall areas, so that the stall patterns encountered during various acceleration paths could be predicted. Figure 13 shows that, in the region bounded by OA and OB, seven stall zones predominated. Along the stall-limit line, one stall zone predominated. When the acceleration path is the dotted line PQ, the seven-zone rotating stall is encountered, and high stress amplitudes in the vicinity of ±60,000 psi are developed. By following acceleration path PR, however, the seven-stall-zone pattern is avoided. The single stall zone is encountered, but it is not sufficiently strong to induce high-amplitude vibrations. By bypassing the fuel-control system, acceleration path PR was actually followed, and the maximum stresses developed were only ±30,000 psi; whereas, in following path PQ, stresses of ±60,000 psi were obtained.

J73 Engine

Vibrations due to rotating stall have also been encountered under accelerating conditions in the J73-GE-3 engine (ref. 6). This engine is provided with adjustable inlet guide vanes in order to permit rapid engine acceleration. At high speeds the inlet guide vanes are in the open, or low-turning, position; and at low speeds they are in the closed, or high-turning, position. For test purposes, the two guide-vane positions were run over the entire speed range. The critical-speed diagrams and stress-speed curve for the first-stage rotor blade are shown in figure 14. With the inlet guide vanes open, a single stall zone was found in the speed range from 5500 to 7000 rpm. The fourth harmonic of this single stall frequency produced a maximum stress of ±27,500 psi. Of course, in this speed range the guide vanes would normally be closed. With the guide vanes closed, no rotating stall was encountered in the intermediate-speed range even with the minimum nozzle area used in the test. However, during rapid engine accelerations, a single-stall-zone pattern was encountered at speeds between 5000 to 5600 rpm. The fourth harmonic of this stall frequency excited the first-stage rotor blades to a stress of ±24,000 psi.

J57 Engine

The J57 engine has a two-spool compressor. Under certain constant-speed and acceleration operation vibratory stresses have been encountered due to rotating stall in the standard engine. As shown in figure 15, the J57-P1 engine, unlike the single-spool units discussed earlier, had a three-stall-zone pattern during acceleration. The second harmonic of this pattern intersected the natural-frequency line of the first stage at a speed of 4100 rpm and produced a vibratory stress of ±30,000 psi.

RELATION BETWEEN VIBRATORY STRESS AND FATIGUE FAILURE

The fact that every engine that has been examined has shown manifestations of rotating stall and associated blade vibration does not necessarily mean that all engines are expected to fail. In some cases the stress levels are below the endurance limit of the material. Even when the vibratory stresses are above the endurance limit, immediate failure is not always to be expected. Figure 16 shows a modified S-N curve for fatigue of compressor blade materials that indicates why some engines fail after a very short period of operation while others can be operated for many hours before failure. In this figure vibratory stress required to produce failure is plotted against the number of cycles. The lowest horizontal dotted line is known as the endurance limit. Any vibratory stress lower than this value can be withstood indefinitely without failure. This stress level has been adjusted to take into account the steady-state centrifugal stress to which the engine is subjected. Blades in engines with vibratory stresses in the neighborhood of 44,000 psi can withstand approximately one million cycles. A blade with a natural frequency of 200 cps can withstand 83 minutes of vibration before failing. At very high stress levels, such as 75,000 psi, which are occasionally experienced as a result of rotating stall, failure can be expected in the very short time of 1000 cycles, or 5 seconds.

Experience indicates that rotating stall is a very common cause of blade failure. Obviously, in some cases, the stresses induced are above tolerable levels. It is thus desirable to indicate several remedies that can be applied in coping with this problem. The most obvious of these is, of course, minimizing the rotating stall itself, as is discussed in paper V. The present discussion is limited to mechanical approaches.

POTENTIAL METHODS OF REDUCING STRESS AMPLITUDES

Design Modifications

One way of minimizing the problem of failure due to vibration is to provide a structure that will withstand the vibratory stresses. Where these failures are in the blade root region, the use of heavy sections and large radii of curvature can be beneficial. Figure 17 shows roots intended for operation in the same compressor (ref. 7). In design A, four serrations were used and the fillet radii were small. The result was cracking in the root across the second pair of serrations. In design B, the section is heavier and the number of fillets is reduced to three, thereby permitting the use of larger radii in the fillets. Preliminary tests indicate that design B can withstand the stress levels encountered in the J65 engine that caused the failure of blade root A.

[redacted]

Mechanical Friction

Another method of limiting vibration amplitude is the use of loose blades. A blade that is loose in its mount produces considerable friction, thereby inducing damping. Studies have been made on root damping, and some of the results are shown in figure 18 (ref. 8). Here root damping is plotted as a function of rotor speed for several designs investigated. Generally, there is a decreasing trend in the damping with increased speed, because the centrifugal force tightens the blade in its mount, thereby overcoming to some extent the original looseness provided by the designer. At the rated speed of the engine, the root damping is very low; however, at part speed, considerable damping may still be present.

The amount of damping depends on the root design. The fir-tree type of design produced considerably more damping, for example, than the ball-root design. Also shown at the upper right in this figure is a design in which the friction is produced by the side pressure between the tangs of the blade and the disk. At low speeds, the friction was so high that the vibration induced was not sufficient to measure the damping. At the high speeds, the available damping was maintained because the side pressure which caused the friction was not affected by centrifugal force. Thus, new designs conducive to looseness and to the introduction of friction in the mounting should prove beneficial in the solution of vibration problems. In current production engines, the trend has been toward the use of loose blades.

Materials with High Internal Damping

Damping can also be achieved by the use of materials having high internal damping capacity. For example, attention should be directed toward the use of plastic compressor blades (ref. 9). Figure 19 shows a comparison of the damping characteristics of a Bakelite-impregnated fiberglass plastic and several other materials that have been used as compressor blading. Damping capacity depends on stress level, and the figure shows the damping capacity at both 5000 and 25,000 psi, the latter being of greater interest in connection with operation near the point of failure. At a stress level of around 25,000 psi, the damping of the plastic is approximately 20 percent, compared with 4 percent for the type 403 stainless steel used in most of the current engines. Titanium and aluminum have very low internal damping.

Some experience has already been obtained with the use of the Bakelite-impregnated fiberglass plastics (ref. 9). The tests were run on a J47 engine under normal steady-state operating conditions. As previously indicated, no severe vibration due to rotating stall is obtained under these conditions; and, therefore, the evaluation was not made to

[redacted]

DECLASSIFIED

determine the applicability in the solution of vibration problems. The preliminary tests were made largely to determine whether the blades were sufficiently durable to withstand normal conditions of operation. A third stage of a J47 compressor was completely fitted with plastic blades and operated at rated take-off conditions for approximately 100 hours. No detectable deterioration was observed.

CONCLUDING REMARKS

Rotating stall induces vibration because the relative motion of the stall and blading results in pressure fluctuations on the blades. Since the wave form of the rotating stall is complex, the number of harmonics available to induce vibration is large. When any of these harmonics is in resonance with the natural frequency of the blade, high vibrations may be induced. In multistage compressors, it is almost impossible to avoid resonant vibration with one or another of the stages whenever rotating stall exists.

The rotating stall and associated vibrations are critically affected by engine operating conditions such as inlet temperature, exhaust-nozzle area, and conditions of acceleration. The sensitivity of the rotating stall to these conditions in some cases results in apparently erratic behavior of the rotating-stall characteristics. Thus, on some occasions, rotating stall will be present during one run but vanish in the next run in which the only difference is a small change in inlet-temperature conditions.

Rotating stall and associated vibrations have been observed in every compressor investigated. However, the stress amplitudes are not always high enough to cause failure. For cases involving high vibration amplitudes, several remedial measures are potentially possible. Among those that have been mentioned are redesign to minimize stress concentration and increased rigidity, incorporation of high root damping, and use of materials with high internal damping. Any conventional approach that would tend to minimize vibration amplitude should prove beneficial. The most valuable approaches involve measures that reduce the tendency for rotating stall to initiate and propagate. These measures are discussed in paper V.

REFERENCES

1. Huppert, Merle C., and Benser, William A.: Some Stall and Surge Phenomena in Axial-Flow Compressors. Jour. Aero. Sci., vol. 20, no. 12, Dec. 1953, pp. 835-845.

2. Den Hartog, J. P.: Mechanical Vibrations. Second ed., McGraw-Hill Book Co., Inc., 1940, pp. 19-30.

3. Calvert, Howard F., Braithwaite, Willis M., and Medeiros, Arthur A.: Rotating-Stall and Rotor-Blade-Vibration Survey of a 13-Stage Axial-Flow Compressor in a Turbojet Engine. NACA RM E54J18, 1954.

4. Medeiros, Arthur A., Calvert, Howard F., and Fenn, David B.: Effect of Inlet Pressure and Temperature on Rotating Stall and Blade Vibration in a Multistage Axial-Flow Compressor. (To be published.)

5. Hanson, Morgan P., Johnson, Donald F., and Meyer, André J., Jr.: Compressor-Blade Vibration and Performance in a J47-23 Turbojet Engine under Conditions of Rotating Stall. NACA RM E54L20a, 1954.

6. Conrad, E. William, Hanson, Morgan P., and McAulay, John E.: Effect of Inlet Air-Flow Distortion on the Steady-State Altitude Performance of an Axial-Flow Turbojet Engine. (To be published.)

7. Meyer, André J., Jr., and Kaufman, Albert: Correlation of Vibratory Root Failures and Stress Distribution in J65 Compressor Blades. NACA RM E54L24, 1955.

8. Hanson, M. P., Meyer, A. J., Jr., and Manson, S. S.: A Method of Evaluating Loose-Blade Mounting as a Means of Suppressing Turbine and Compressor Blade Vibration. Proc. Soc. Exp. Stress Analysis, vol. 10, no. 2, Nov. 1952, pp. 103-116.

9. Johnson, Donald F., and Meyer, André J., Jr.; Preliminary Investigation of the Strength and Endurance of Plastic-Impregnated Fiberglass Compressor Blades. NACA RM E54I27a, 1955.

3665

RELATIVE MOTION OF STALLED ZONES

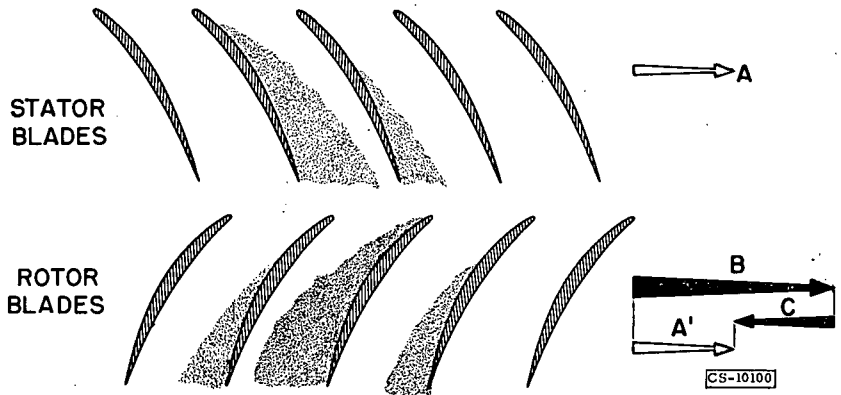

Figure 1.

TYPES OF ROTATING STALL PATTERNS OBSERVED

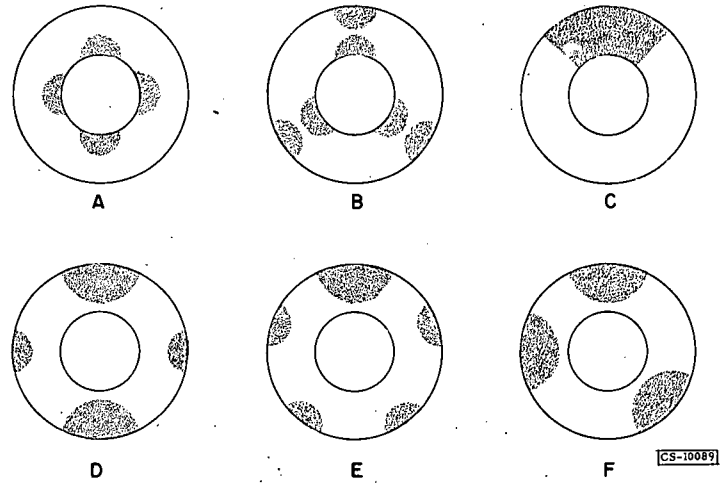

Figure 2.

TYPICAL RESONANCE CURVE

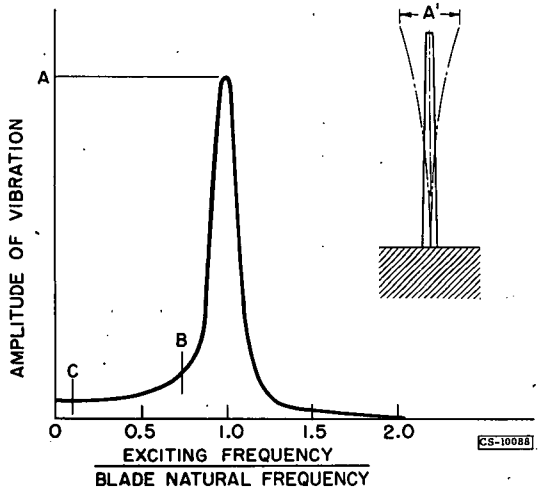

Figure 3.

ROTATING-STALL WAVE FORM AND HARMONIC CONTENT

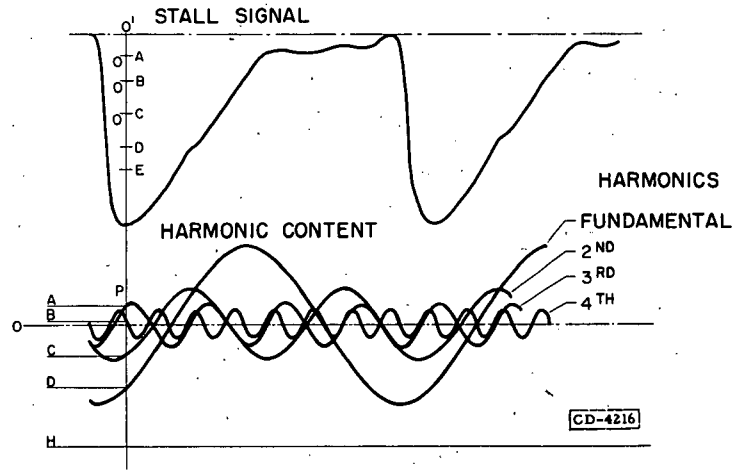

Figure 4.

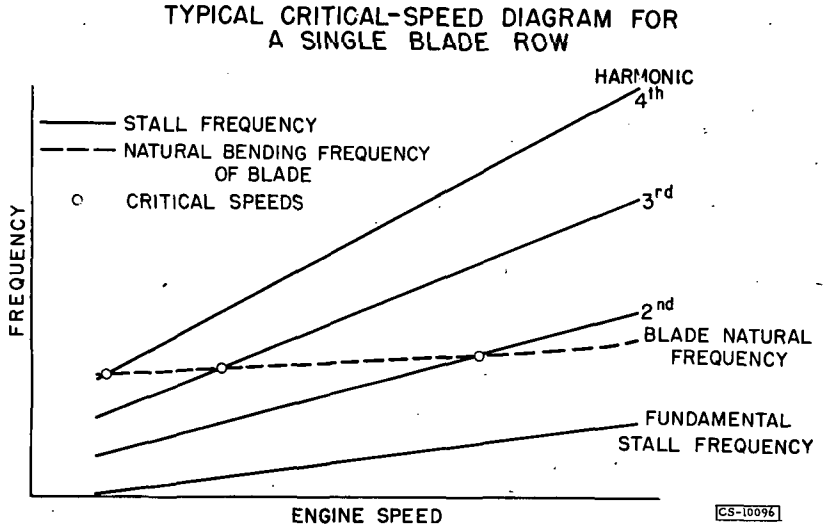

Figure 5.

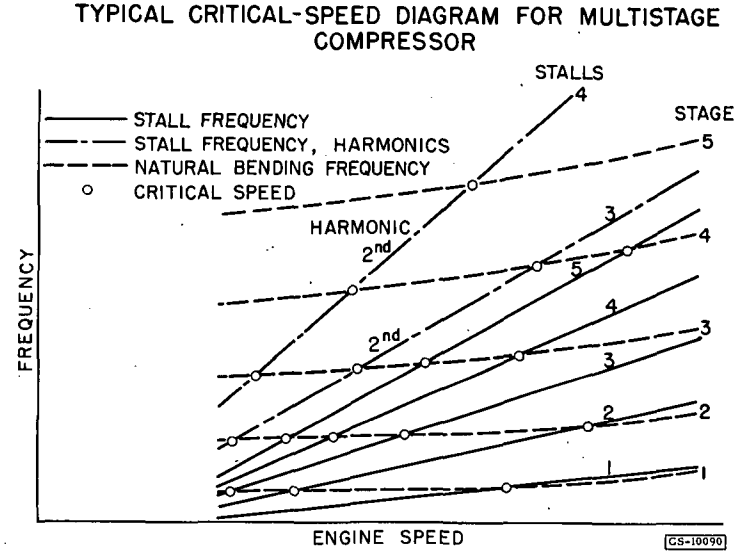

Figure 6.

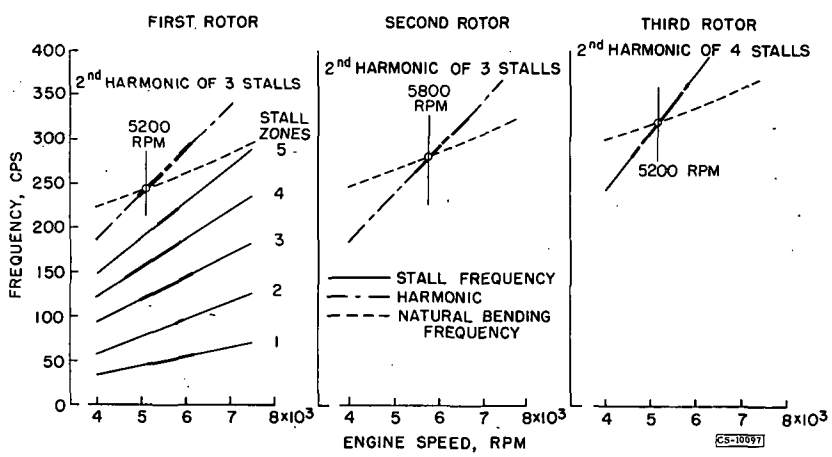

Figure 7.

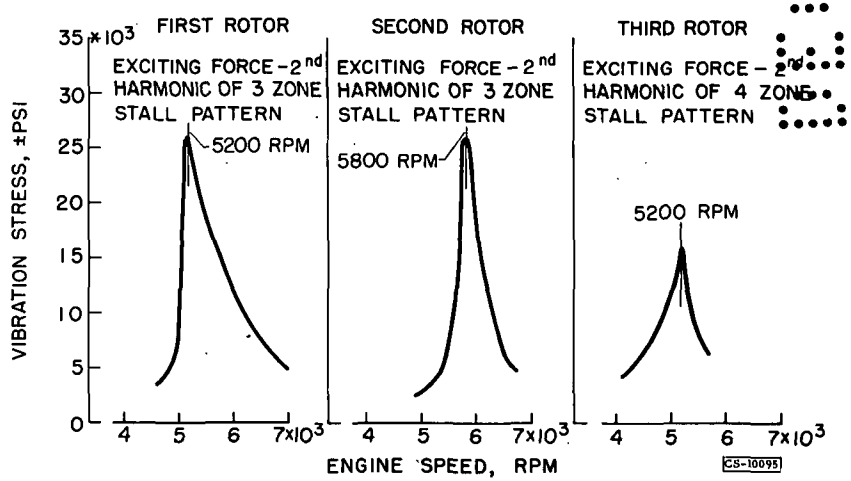

Figure 8.

NOZZLE AREA AND STALL

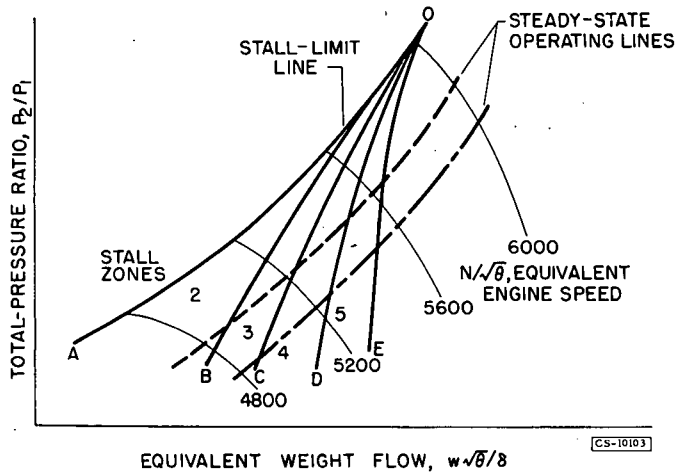

Figure 9.

INLET TEMPERATURE AND STALL

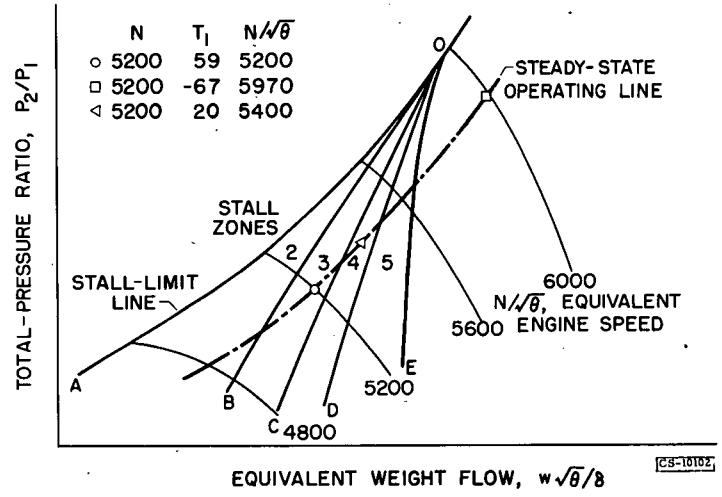

Figure 10.

VIBRATION EXCITATION DUE TO ROTATING STALL IN A J 47-23 ENGINE

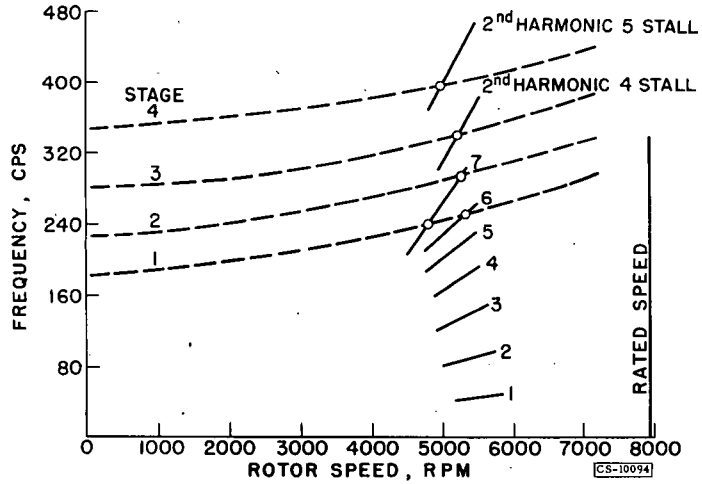

Figure 11.

2ND STAGE VIBRATION DUE TO ROTATING STALL

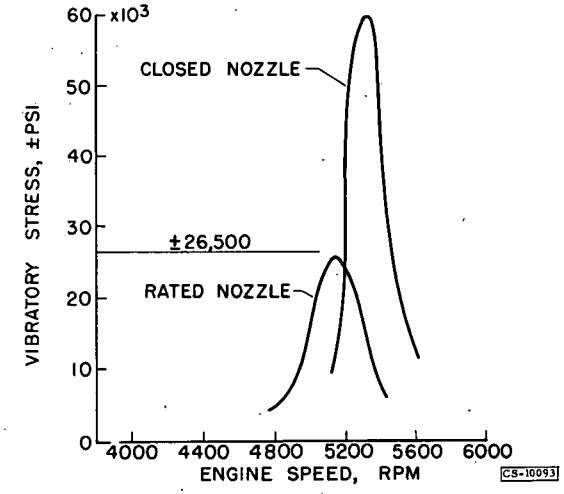

Figure 12.

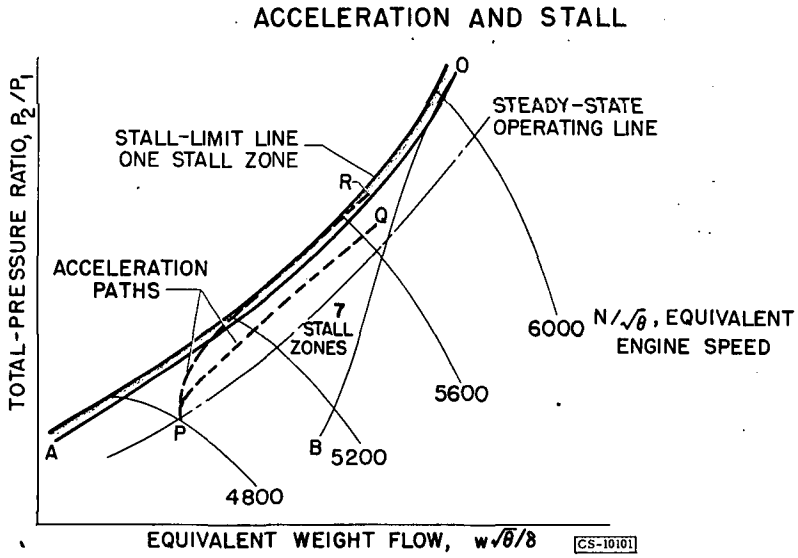

Figure 13.

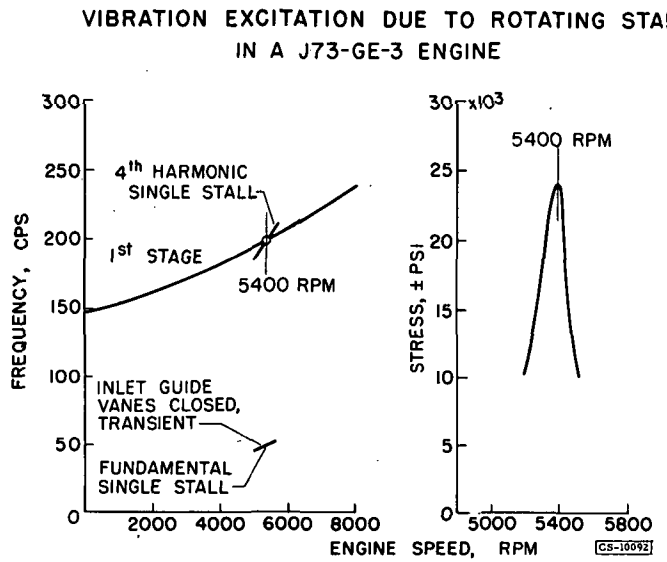

Figure 14.

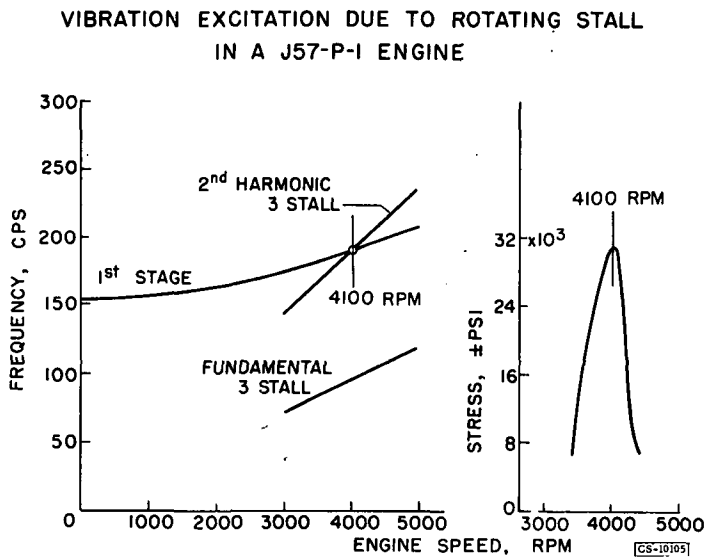

Figure 15.

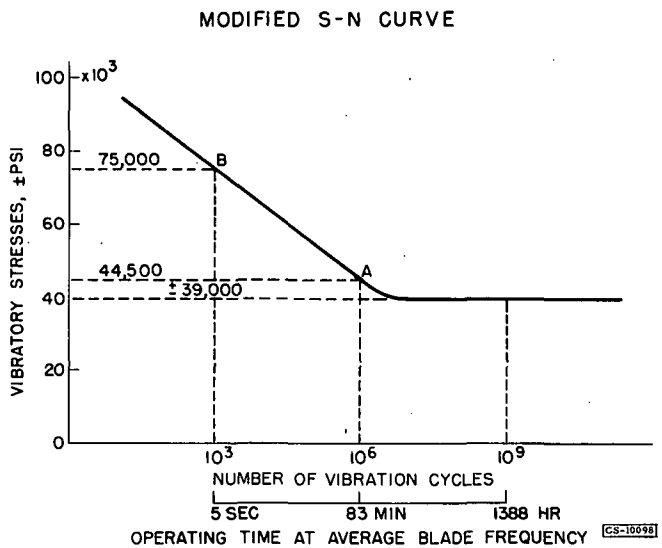

Figure 16.

ELIMINATION OF FAILURE BY ROOT REDESIGN

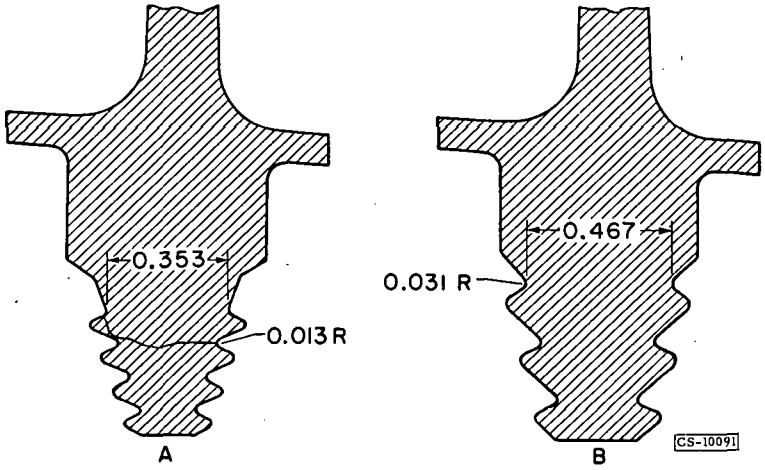

Figure 17.

ROOT DAMPING FOR SEVERAL DESIGNS

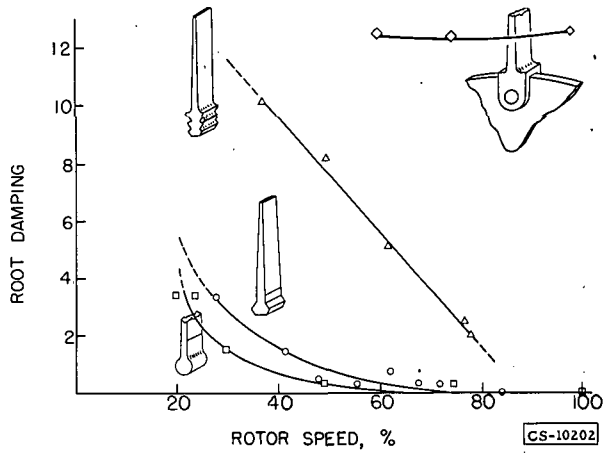

Figure 18.

MATERIAL DAMPING

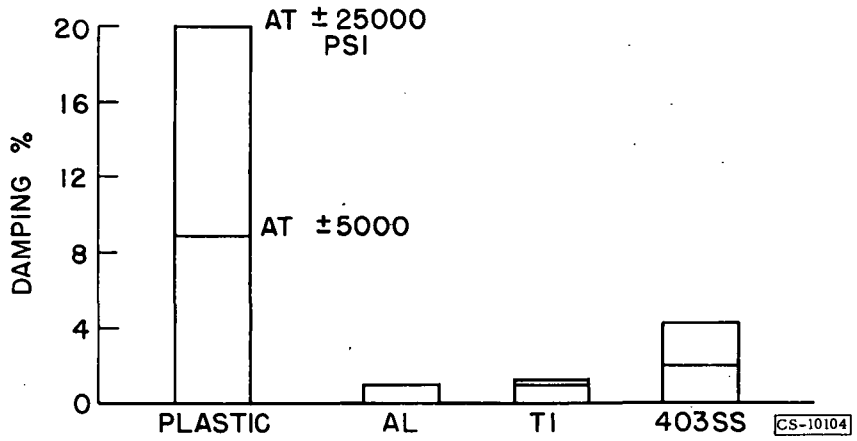

Figure 19.

DECLASSIFIED

[redacted]

III - INLET FLOW DISTORTION

D. D. Wyatt, Chairman

L. J. Obery

T. G. Piercy

M. J. Saari

[redacted]

DECLASSIFIED

III - INLET FLOW DISTORTION

INTRODUCTION

A discussion of the stall and surge phenomena of turbojet engines would be incomplete without a consideration of the effects of nonuniform velocities entering the compressor. The qualitative effect of such distortions is indicated in figure 1. In the left portion of this figure the velocity diagram entering the first compressor rotor row is shown for three axial-velocity conditions. When the axial velocity corresponds to the design value, the design angle of attack will exist on the blade. If a velocity distortion exists at the compressor face, the average axial velocity may correspond to the design value but the design velocity diagram will only exist over part of the compressor face.

3665

In those regions of the flow in which the axial velocity is lower than the average value, the angle of attack of the first stage will be increased. If the axial velocity is of a low enough value and of sufficient extent, the first stage may stall. Such stalling may manifest itself as either a partial or complete compressor stall, depending on the extent of the low-velocity region.

In those regions of the flow in which the axial velocity is higher than the design value, the angle of attack on the first rotor stage will be reduced. As a consequence of the resultant reduction in the first-stage blade loading, the rear stages of the compressor may choke and thereby cause abrupt compressor stall.

As indicated by the velocity diagrams of figure 1, it is the velocity distortions at the compressor face that may be expected to alter the distortion-free characteristics of the turbojet engine. In the experimental evaluation of inlet air-flow distortions, however, velocity distributions cannot be measured directly. Total-pressure distributions can be measured with a good degree of accuracy. The concomitant static-pressure variations cannot easily be measured with the same degree of accuracy; and, consequently, most duct distortion data are presented only in the form of total-pressure distributions. The curves on the right side of figure 1 show the correlation between total-pressure distortions in a duct and the corresponding axial-velocity distortions for uniform duct static pressures.

In this figure the total-pressure distortion is defined as the local total pressure minus the average total pressure divided by the average total pressure. Correspondingly, the velocity distortion is defined as the local velocity minus the average velocity divided by the average velocity. Positive values thus indicate regions of the flow having local total pressures and velocities higher than the average values.

[redacted]

These curves show that a given level of total-pressure distortion may not suffice to predict distortion effects on turbojet-engine performance, since the corresponding velocity distortion is also a function of the average axial Mach number. A total-pressure distortion of 5 percent, for example, may result in velocity distortions of from 3 to 100 percent or more, depending on the average axial Mach number of the flow. (At design conditions current engines have axial inlet Mach numbers from 0.5 to 0.6.)

Typical total-pressure distortions observed in current subsonic and transonic airplanes and in duct model tests of projected supersonic airplanes and missiles are discussed herein. The results of some preliminary investigations into methods of reducing the distortion level at the engine inlet are also presented. The effects of inlet-flow distortions on turbojet-engine performance are not analyzed.

DISTORTIONS IN SUBSONIC AND TRANSONIC AIRPLANES

The military services and various airframe manufacturers have furnished the NACA with total-pressure distortions measured on several current subsonic and transonic airplanes. These data are presented on figures 2 to 4.

The distortions for two current Navy airplanes are shown in figure 2. The upper portion of the figure shows the total-pressure contours measured at the engine face. The contours indicate the variation in total pressure from the average value. For example, a 0 contour represents a line of average pressure in the duct. A -3 contour is a line of pressures 3 percent below the average value. A value of $\Delta P/P_{av}$ is indicated alongside each contour plot. This value represents the maximum total-pressure variation in the duct, or maximum total pressure minus minimum total pressure divided by average total pressure.

The total-pressure distortions are frequently measured and presented as cross sections or profiles of the flow field at the engine face. Two typical profiles for each of the airplanes are presented at the bottom of figure 2. One of the profiles shows the radial variation in total pressure from the accessory housing to the outer duct wall just ahead of the engine intake. The other profile shows the circumferential variation in total pressure at some arbitrary radius.

Only profile data are available for the Air Force airplanes for which distortion data are shown in figure 3. Although the airplanes had different inlet configurations and different flight conditions, the profiles are all qualitatively similar. The total distortions for the airplanes varied from 15 to 19 percent, with maximum pressures from 3 to 5 percent above the average and minimum pressures 12 to 14 percent below the average.

[redacted]

DECLASSIFIED

The distortion data presented in figure 4 for several nacelle-type bomber engine installations indicate that the symmetrical, short inlet systems produce flow distortions of about the same magnitude as those experienced in fighter airplanes. Total distortions of from 10 to 20 percent may be noted for these configurations.

The relatively meager distortion data available for currently flying subsonic and transonic airplanes indicate that total-pressure distortions of as high as 20 percent are being encountered, and not infrequently. Although some of the configurations examined have lower distortions, it must not be automatically presumed that these have better duct configurations with respect to distortion, since the relative severity of the flight conditions represented by the various data is not known.

ORIGIN OF FLOW DISTORTIONS

It can generally be presumed that air inlet configurations designed for and operated at subsonic-flight-speed conditions should have little or no total-pressure loss from the free stream to the inlet. Consequently, the total-pressure distortion at the throat of the inlet should be zero. The pressure distortions observed in subsonic configurations, therefore, probably arise in the subsonic-diffuser passages between the inlet throat and the engine intake. Some of the potential causes of distortion are illustrated in figure 5.

As shown in the upper left sketch of figure 5, too rapid a diffusion rate in the subsonic-diffuser passage can cause the flow to separate from the diffuser wall. Although this separation generally reattaches, the phenomenon of separation causes a reduction in the local total-pressure level. Unless this low-pressure zone regains energy through mixing with the main flow, it will appear at the engine face as a region of low pressure and hence represent a distortion.

The separation can be induced by excessive local angles of attack of the entering air on the inlet lips. As illustrated by the upper right sketch, this may occur as a result of high inlet angles of attack. The same phenomenon can result from operation of the inlet at excessive values of inlet velocity ratio, as indicated by the lower left sketch.

Internal flow separation, as differentiated from separation due to high angles of attack, is not restricted to conditions in which the duct area undergoes too rapid expansion. This type of separation is a function of local wall curvature and hence may occur when any part of the duct wall has too small a radius of curvature. One example of sufficient conditions for separation is shown in the sketch on the lower right of figure 5. Local separation may occur in curving ducts, although the general area

[redacted]

[redacted]

variation along the duct may be very gradual. In a like manner, a separation may occur from local protuberances formed in the duct to fair over interfering parts or from local duct surfaces during passage shape transitions.

The foregoing analysis of the subsonic-inlet distortion problem is at least qualitatively substantiated by the experimental data of figures 2 to 4. In general, these data show that the average pressure (zero distortion) is near the maximum pressure value or, in other words, that the positive pressure distortions are of low magnitude. The negative pressure distortions are of much greater magnitude. Since the products of the positive distortions and their areas must equal the products of the negative distortions and their areas, it follows that the low-pressure regions (negative distortions) are localized. Therefore, these low-pressure regions probably have localized sources within the ducts.

3665

Although it appears probable that flow distortions are internally induced in subsonic-inlet systems, such does not seem to be the primary cause of flow distortions at supersonic speeds. Figure 6 indicates the results of theoretical calculations of the throat total-pressure distributions in a spike-type inlet at Mach number 2.0. Even at 0° angle of attack, the throat total pressure is not uniform. The conical compression surface causes a nonuniform compression in the flow field entering the inlet, and behind the theoretical terminal shocks the pressure recovery will vary about 3 percent.

If the inlet is operated in a subcritical condition (flow spillage through the terminal shock), the theoretical pressure distributions are worsened at the throat. In this condition part of the flow would pass through a two-shock system and part through a one-shock system, so that the pressure recovery at the throat would vary about 18 percent.

Operation of the inlet at angle of attack also theoretically increases the throat pressure distortion. The compression is unchanged on the side axis of the cone from the 0° condition, but the compression is weakened on the upper cone surface and strengthened on the lower surface. Consequently, circumferential total-pressure gradients are introduced into the flow downstream of the terminal shock wave.

The flow is further complicated for all the cases shown in figure 6 as a result of shock - boundary-layer interactions, which are known to promote the tendency for separation and hence worsen the flow conditions entering the subsonic-diffuser portion of the inlet system. As a result of the nonuniform compressions and the shock - boundary-layer separations in the supersonic inlets, the role of the internal diffuser passage is markedly different from that of the subsonic intake system. Instead of being required to maintain the characteristics of a good entering flow, the passage behind a supersonic inlet must correct a poor throat flow if

[redacted]

DECLASSIFIED

low distortions are to be delivered to the engine face. This correction must be obtained by a mixing process within the subsonic-diffuser passage. During this mixing process, the diffuser must not induce flow separations of the previously discussed subsonic type if low engine-inlet distortions are to be realized.

DISTORTIONS IN SUPERSONIC AIRPLANES AND MISSILES

Flow distortions measured at a Mach number of 2.0 for a symmetrical spike-type inlet system designed for the nacelles of the B-58 bomber are indicated in figure 7. The three parts to the figure show the effects of operating conditions on the inlet at 0° angle of attack. With critical inlet flow, the maximum total-pressure distortion was 10 percent. When the inlet mass flow was reduced to give a subcritical condition, the distortion increased slightly, to 13 percent. This configuration corresponds to that for which a throat distortion of 18 percent would be predicted for these operating conditions. Hence, there is evidence of some mixing taking place in the diffusion process.

When the back pressure on the inlet was reduced to give supercritical flow (shock drawn into the subsonic diffuser), the distortion increased rapidly and for the condition presented reached a value of 30 percent. This increase is partly due to increased shock - boundary-layer interaction as a result of increased terminal shock strength and partly to increased flow nonuniformities behind the terminal shock as a result of increased Mach number gradients in the internal flow passages. The high level of distortion illustrates the general advisability of avoiding supercritical operation with regard to distortion.

The flow distortions presented in figure 7 are largely radial in nature. When the inlet is operated at angle of attack, the flow distortions also assume a strong circumferential character, as illustrated by the data in figure 8. At angles of attack up to 6° the magnitude of the distortion does not increase above the value for critical flow at 0°, although the distortion pattern is greatly modified. At higher angles of attack the distortion with critical inlet flow increases rapidly and, as shown, reached a value of 27 percent at 10° angle of attack.

Nose or nacelle inlets of the type shown in figures 7 and 8 generally operate in uniform flow fields, so that the distortion-producing flow mechanisms are confined to the inlet geometry. Side inlets, on the other hand, operate in flow fields that are influenced by the fuselage, so that flow distortions may be present in the flow before it enters the inlet. The fuselage effect will vary not only with the fuselage shape, but also with the location of the inlet on the body and with the compression geometry arrangement of the inlet. Consequently, it is impossible to generalize the distortion characteristics of side inlets. This problem is illustrated by the data of figure 9.

CONFIDENTIAL

The inlet of figure 9, a research model investigated at the NACA Langley laboratory, was a half-spike configuration wrapped around a symmetrical body of revolution. The body could be rotated so that the inlet could be located at any arbitrary circumferential location on the body. Distortion data are presented for three locations around the body. When the body was operated at 0° angle of attack, the distortion pattern was independent of the circumferential inlet location. As indicated by the left data figure, the total distortion was 7 percent for this condition. When the inlet was located on the side of the body, the distortion level increased to 18 percent at 6° angle of attack. In this location the inlet is subject to twice the angle of attack of the body as a result of crossflow. Consequently, the inlet was effectively operating at 12° angle of attack for the condition presented. If the inlet is located on the bottom of the body, it is largely shielded from the angle-of-attack variations and tends to operate at 0° angle of attack for all body angles of attack. As shown by the data in the right figure, the distortion level for a body angle of attack of 12° remains at about the 0° angle-of-attack level when the inlet is in this underslung position.

These data show not only that the distortion levels of side-inlet configurations are influenced by the location of the inlet on the body, but that if freedom is available to the designer he can have a measure of control over distortion by judiciously controlling the inlet location.

The inlet for which data are presented in figure 9 did not have an offset discharge duct and, consequently, was probably less subject to distortions arising in the internal ducting than most practical side-inlet installations. Figure 10 presents data for the X-3 airplane duct arrangement, which illustrates the effect of duct curvature. The inlet had a two-dimensional compression ramp followed by a semicircular cowl. The location of the cowl relative to the discharge duct is indicated in the data figures. At 0° angle of attack this inlet had a critical flow distortion of 16 percent. The pressure contours show that the high-energy flow at the throat had little tendency to expand around the transition section and hence appeared at the duct discharge as a concentrated core directly behind the inlet.

When this inlet was operated at angles of attack up to 12°, there was little change in the magnitude of the flow distortion at the duct discharge. The pattern did change, however. The high-energy core region shifted counterclockwise as the angle of attack increased. Simultaneously, stagnant-flow regions appeared in the duct, as indicated by the shaded regions.

Although the ramp inlet configuration of the X-3 airplane was relatively insensitive to angle of attack in terms of the magnitude of distortion, another inlet configuration investigated for the same airplane had a large variation in distortion with angle of attack. The ramp inlet

DECLASSIFIED

was replaced by an inlet having a wedge-type compression surface normal to the plane of the fuselage. The distortions observed with this inlet are shown in figure 11. At 0° angle of attack the distortion level was quite low compared with the results for the ramp inlet. The distortion increased steadily as angle of attack was increased and reached a magnitude of 16 percent at 12° angle of attack. This increasing distortion level was accompanied by a shift in the contour pattern. At high angles of attack the high-pressure core was concentrated downstream of the lower inlet passage. This section of the inlet has an increased compression strength at angle of attack, whereas the upper passage compression was reduced.

3665

The distortions observed at low angles of attack with the normal wedge inlet were lower than those observed with the other supersonic inlets thus far examined. That this is not a fundamental property of the normal wedge inlet is shown by the data of figure 12. This figure compares the maximum distortions from the inlet of figure 11 at Mach 2.0 with the distortions observed with the same inlet operated at Mach number 1.5 but with the wedge angle reduced from 14° to 8° to improve the match with the engine air-flow requirements. The change in distortion with angle of attack was about the same for the two Mach numbers, but at Mach number 1.5 the distortion at 0° was 7 percent greater than that observed at Mach 2.0.

In contrast to the side inlets previously discussed, which initially turn the air outward during the supersonic compression process, the scoop-type inlet has received considerable attention because it compresses the air inward and thus tends to reduce the cowl drag. To the extent that the internal curvature contributes to the air-flow distortion, it might also be expected that lower distortions might result with scoop inlet installations. In the case of one configuration investigated in model form in the NACA Lewis 8- by 6-foot supersonic tunnel, such expectations did not materialize.

Distortions measured at 0° angle of attack and Mach number 2.0 on a model of the Regulus missile inlet configuration are presented in figure 13. (This inlet is similar in principle, though different in detail, to those proposed for the F-103 and F-105 airplanes.) With critical inlet flow, the total distortion was 13 percent. This value decreased to 9 percent when the mass flow was throttled. The change in distortion level was accompanied by a marked change in distortion pattern, the high-energy core moving to the bottom (outboard) side of the duct. When the terminal shock was allowed to move inside the inlet, the distortion increased rapidly. For the condition shown, the outboard section of the duct maintained a separated flow to the measuring station and the high-energy air was concentrated at the top of the duct.

[redacted]

[redacted]

In several of the side-inlet configurations currently of interest, two inlets are employed to deliver air to a single engine. One such configuration, the F-102, has been evaluated in quarter-scale model tests, and the observed distortions are presented in figures 14 to 16. The inlet configuration presented here was an adjustable inlet designed for an advanced version of the airplane.

The effect of flight Mach number on the distortion levels at maximum engine power conditions is shown in figure 14. At subsonic flight speeds the ramp angle is reduced to 0° in order to give maximum throat area. At supersonic Mach numbers the ramp angle is increased to a maximum of 18° at Mach number 2. The distortions presented are low compared with those observed on most airplanes flying today. At subsonic speeds the maximum distortion was only 6 percent, even though the cowl had sharp supersonic lips. At all speeds a circumferential distortion was present. Each duct discharged a core of high-energy unmixed air.

When the inlet was operated at angles of attack at Mach number 2.0, there was no appreciable change in the distortion level or in the distortion pattern (fig. 15). Yawing the model up to 6° increased the distortion level slightly (fig. 16) and had an appreciable effect on the distortion pattern. At 6° angle of yaw the high-energy air was all concentrated behind the windward duct. For the case illustrated, there was no flow reversal in the leeward duct; however, such reversals were observed at reduced mass-flow ratios and might be anticipated at higher angles of yaw.

CORRELATION OF DISTORTION DATA FOR SUPERSONIC SIDE INLETS

The distortion data thus far examined have yielded wide ranges of distortion at critical flow conditions. In particular, the supersonic-side-inlet configurations have displayed critical flow distortions at 0° angle of attack varying from 4 percent for the X-3 normal wedge configuration at Mach 2 to 16 percent for the X-3 ramp inlet at Mach 2. If the analysis of the supersonic-inlet distortion problem is correct, a large portion of the engine-inlet air-flow distortion is the result of inadequate mixing of the distorted throat flow. The amount of throat distortion should vary with the type of inlet and the location on the fuselage, but the amount of internal mixing-passage length should have some correlating effect.

The maximum distortions measured for a number of supersonic-side-inlet configurations at critical flow conditions and at 0° body angle of attack are plotted as a function of the internal-passage length-diameter ratio in figure 17. The diameter selected is the equivalent hydraulic diameter of the minimum throat passage area. This figure shows that, in general, the distortion is a function of the available mixing length.

[redacted]

DECLASSIFIED

With the exception of the X-3 normal-wedge-inlet data at Mach 2, which appear low, a mean line can be drawn that indicates a definite trend of decreasing distortion as mixing length is increased. This curve does not, of course, predict the distortion magnitude at angle of attack or with noncritical mass flows when the inlet location and inlet geometries become predominant factors.

The powerful influence of mixing length on the reduction of air-flow distortion is further illustrated by the data of figure 18. In this experiment a constant-area straight section was provided downstream of a research side-inlet configuration. By means of a longitudinally traversing total-pressure rake, the duct total-pressure contours could be measured with varying amounts of constant-area section after the diffuser discharge. For the example shown, a total-pressure distortion of 16 percent was measured at the start of the constant-area section. This distortion level decreased steadily until a distortion of only 5 percent was measured $3\frac{1}{2}$ diameters downstream of the diffuser discharge.

METHODS OF REDUCING DISTORTION

The data of figures 17 and 18 show that long subsonic sections can greatly reduce the distortions delivered by supersonic inlets under certain operating conditions. The addition of duct length to improve bad distortions can scarcely be advocated, however, since intolerable weight penalties and losses of useful volume may thereby be incurred. Accordingly, other methods of reducing the delivered distortion magnitude must be considered.

If insufficient mixing takes place to reduce distortions to an acceptable level, it may be necessary to resort to techniques or devices that can force the mixing to take place. Screens have long been known to be beneficial for mixing small-scale velocity distortions, and, accordingly, a preliminary investigation was conducted to determine their effectiveness in reducing major distortions. The results of this investigation are indicated in figures 19 and 20.

The screens were employed in a small-scale duct (3.6 inches in diameter), which received the discharge from a two-dimensional inlet having a ramp compression upper surface. The transition and diffusion section from the inlet to the duct had no offset. When the inlet was operated at 0° angle of attack, the duct distortion was 36 percent (fig. 19). The introduction of a full screen spanning the duct decreased this distortion to 14 percent. This reduction was accompanied by an average total-pressure reduction of about 8 percent, however.

[redacted]

Since the flow contours in the original duct indicated that the high-energy flow was concentrated in the lower half of the duct, additional tests were performed with a half screen covering only this region. With this modification, the distortion was reduced from the original value of 36 percent to only 9 percent. The area-averaged total pressures indicated a negligible total-pressure loss.

When the half screen was replaced by an arrangement of radially mounted round rods having approximately the same area blockage, the distortion was reduced from the original value, but only to 17 percent. As with the half screen, the average pressure losses were negligible with this arrangement.

3665

Although the half-screen arrangement proved very beneficial under the conditions of figure 19, the previously noted shifting pattern of distortion with changes in inlet operating conditions makes it unsatisfactory for general application, as illustrated by figure 20. The characteristics of the supersonic inlet were such that the discharge distortion level for critical operation decreased as angle of attack was increased. Because the high-energy core shifted out of the lower half of the discharge duct in the process, however, the half-screen and rod arrangments became progressively less effective as angle of attack was increased. The full screen maintained its effectiveness over the whole angle-of-attack range, but at the cost of a sizable loss in total-pressure recovery.

Another approach to the reduction of the distortion level that has been little explored lies in modifications to the inlet system to prevent the development of flow distortions. It is not obvious at this time what the nature of these modifications should be for subsonic-inlet systems. For supersonic inlets, it would appear that ways must be found to reduce the nonuniform supersonic compression and to reduce or eliminate separation following shock - boundary-layer interaction. Although this is a formidable problem, there is some information indicating that such efforts may be fruitful.

Figure 21 shows distortion contours for a research side-inlet configuration. The inlet was similar to that of figure 9 and was wrapped around a body of revolution. In the original configuration, the outside re-entrant corners were unfilleted. A distortion level of about 13 percent was measured at a station near the end of the diffuser. Recognizing that the boundary-layer accumulation was probably bad in the outer corners, the inlet and subsonic diffuser were modified by the installation of corner fillets of small radius. The distortion level was reduced to 5 percent as a result of this modification. Corresponding reductions in distortion were observed for all operating conditions of the inlet over a range of Mach numbers from 1.5 to 2.0.

[redacted]

AIRFLOW DISTORTION EFFECTS

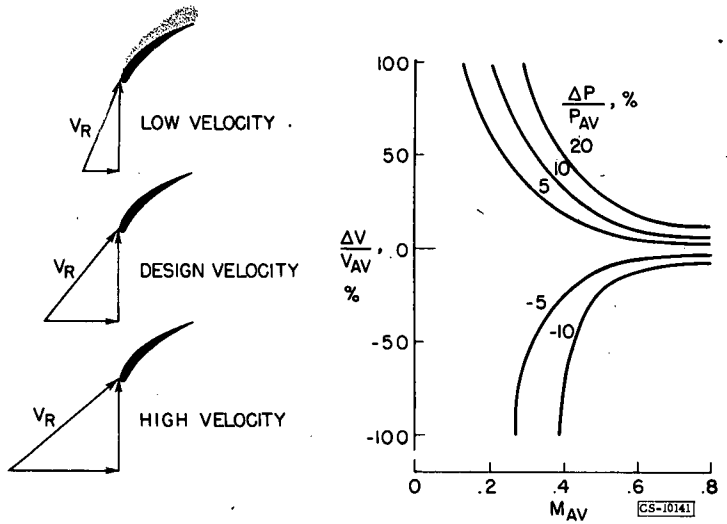

Figure 1.

ENGINE INLET FLOW PROFILE FOR CURRENT AIRPLANES

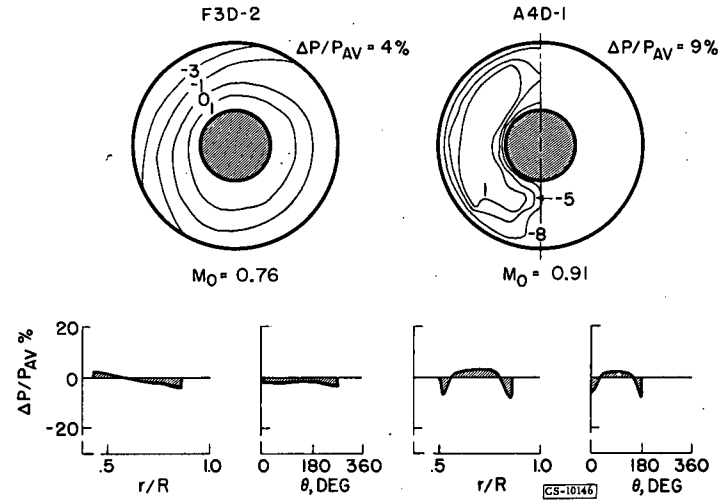

Figure 2.

ENGINE INLET PROFILES FOR CURRENT AIRPLANES

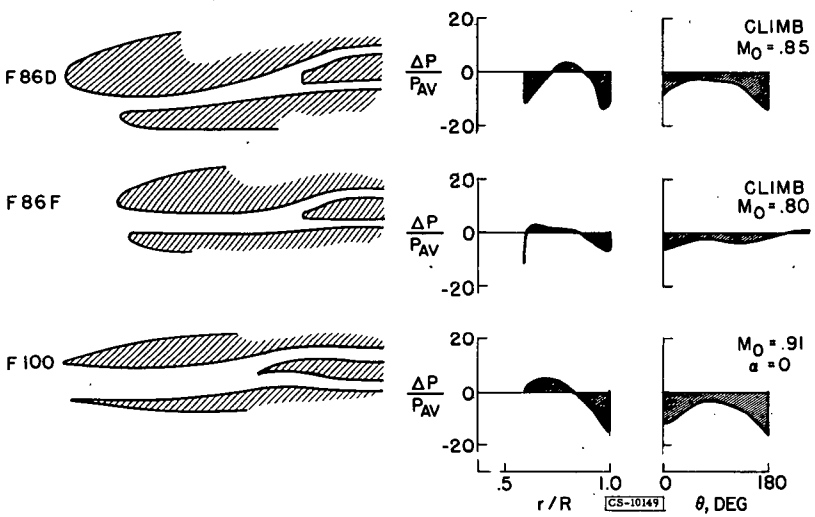

Figure 3.

ENGINE INLET FLOW PROFILES FOR CURRENT AIRPLANES

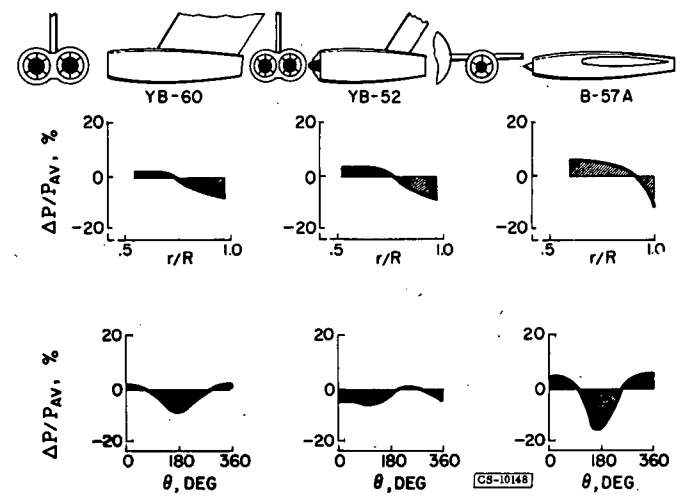

Figure 4.

ORIGIN OF FLOW DISTORTIONS AT SUBSONIC SPEEDS

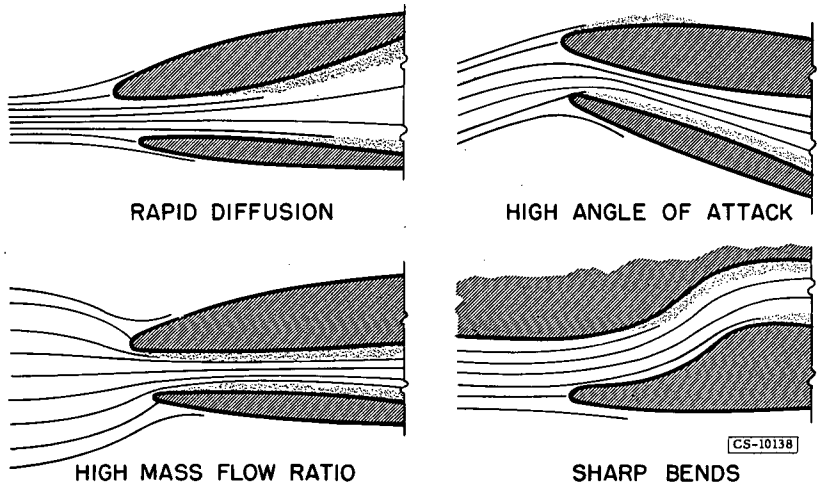

Figure 5.

ORIGIN OF FLOW DISTORTIONS AT SUPERSONIC SPEEDS

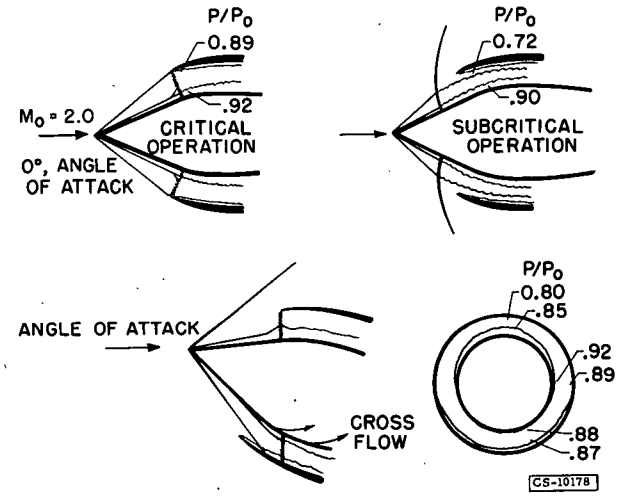

Figure 6.

EFFECT OF MASS FLOW RATIO FOR NOSE INLET
B-58 NACELLE
$M_0 = 2$

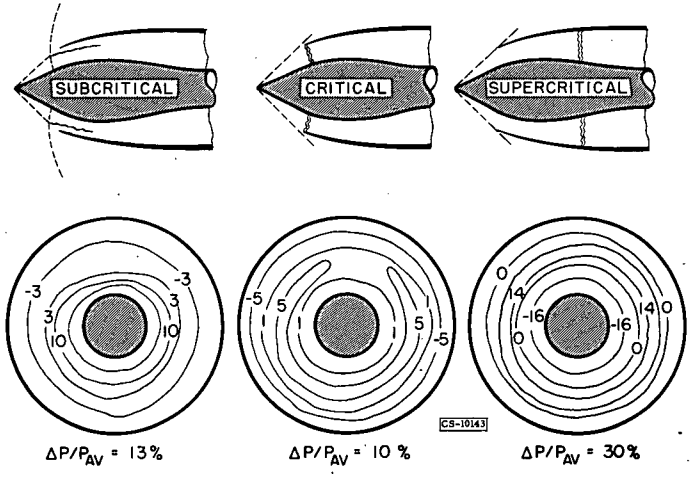

Figure 7.

EFFECT OF ANGLE OF ATTACK FOR NOSE INLET
B-58 NACELLE
$M_0 = 2$

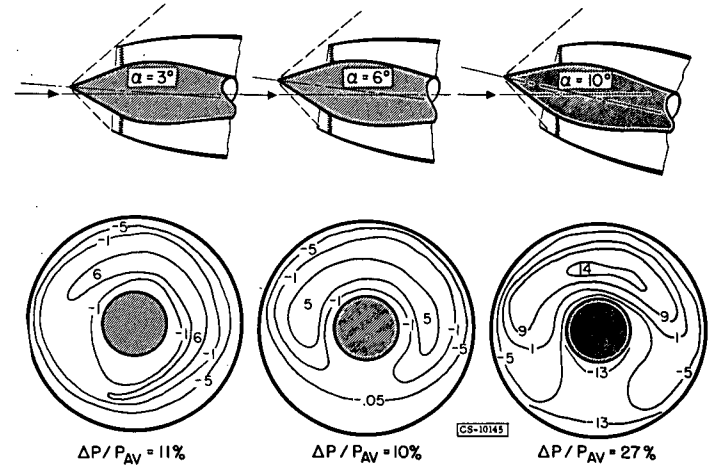

Figure 8.

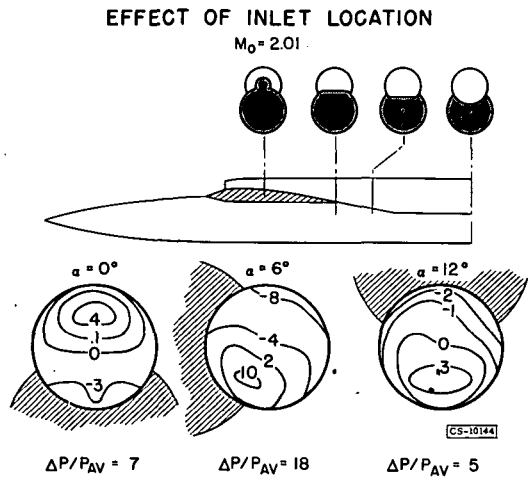

Figure 9.

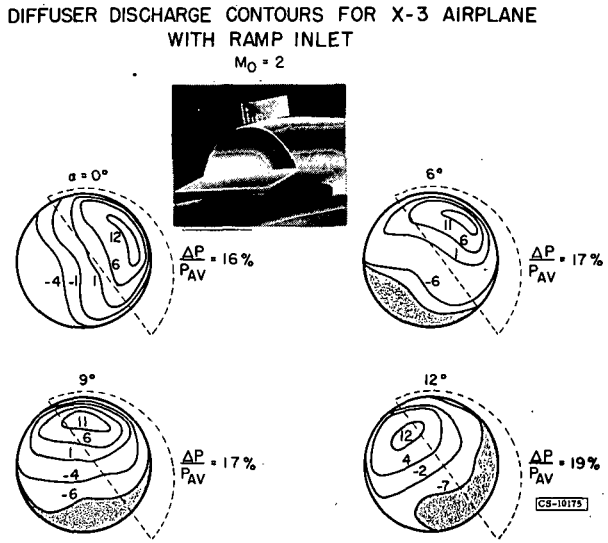

Figure 10.

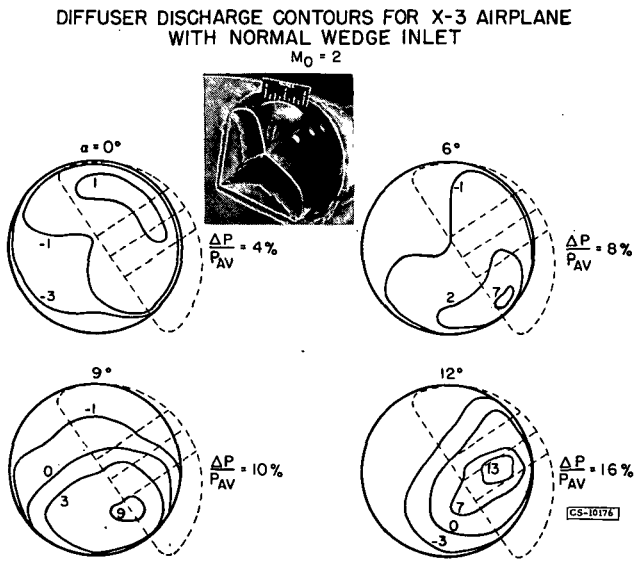

Figure 11.

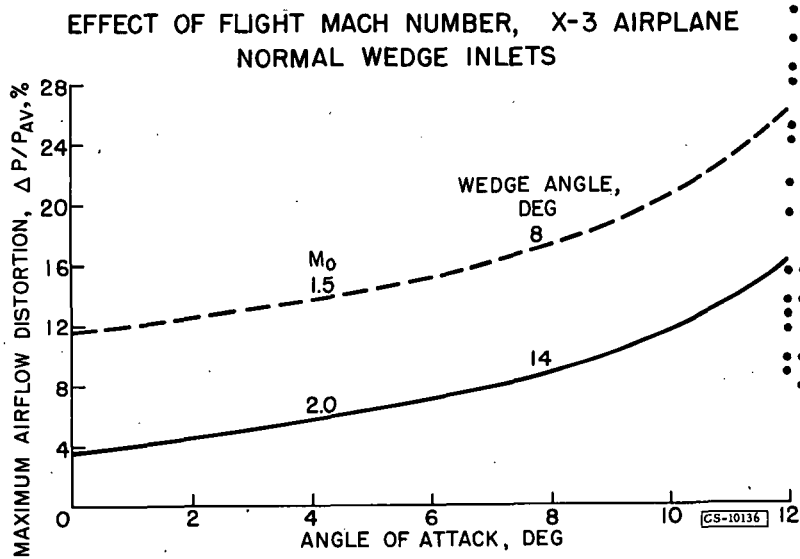

Figure 12.

EFFECT OF MASS FLOW RATIO ON SCOOP TYPE INLET
REGULUS MISSILE
$M_o = 2.0$

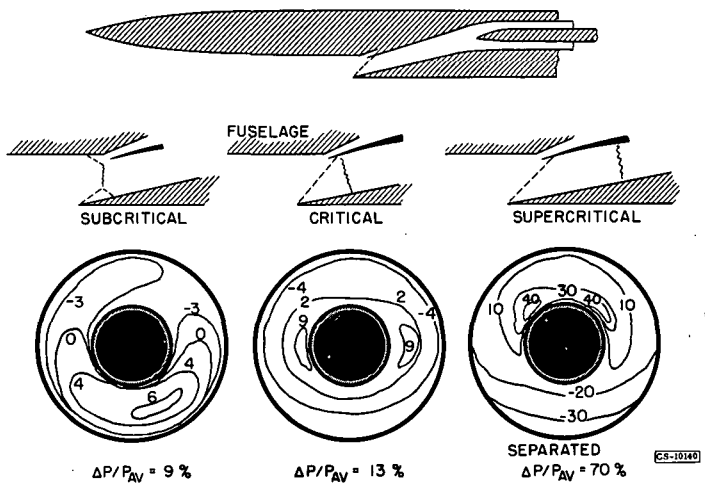

$\Delta P/P_{AV} = 9\%$ $\Delta P/P_{AV} = 13\%$ $\Delta P/P_{AV} = 70\%$

Figure 13.

EFFECT OF FLIGHT MACH NUMBER
F-102

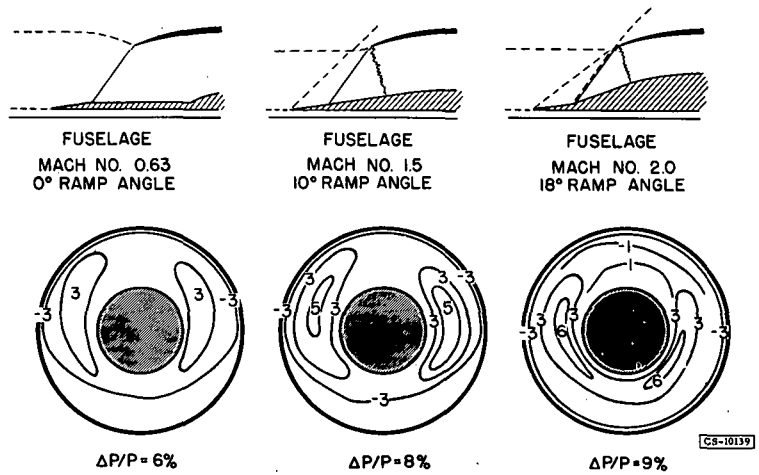

$\Delta P/P = 6\%$ $\Delta P/P = 8\%$ $\Delta P/P = 9\%$

Figure 14.

EFFECT OF ANGLE OF ATTACK
F-102 $M_o = 2.0$

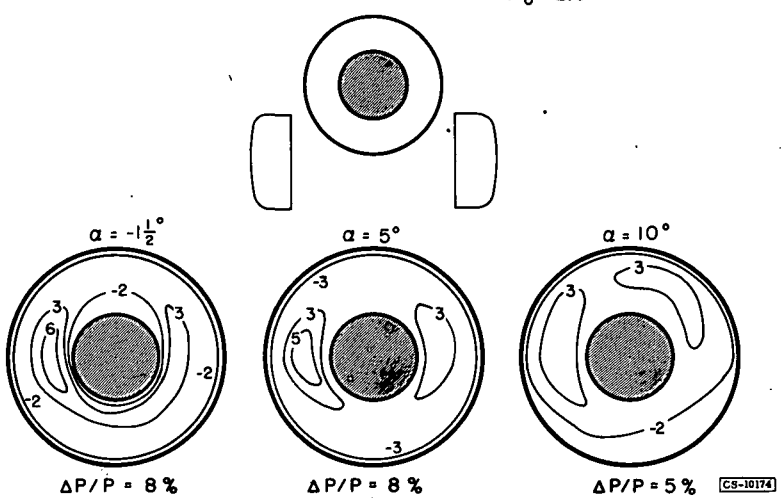

$\Delta P/P = 8\%$ $\Delta P/P = 8\%$ $\Delta P/P = 5\%$

Figure 15.

EFFECT OF ANGLE OF YAW
F-102 $M_o = 1.5$

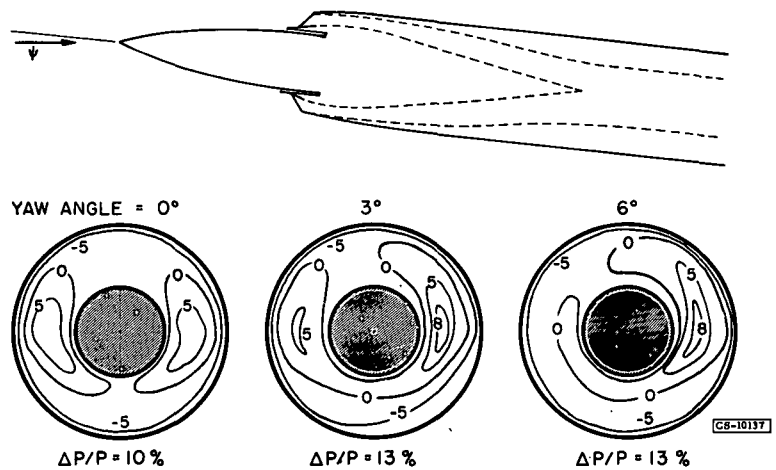

$\Delta P/P = 10\%$ $\Delta P/P = 13\%$ $\Delta P/P = 13\%$

Figure 16.

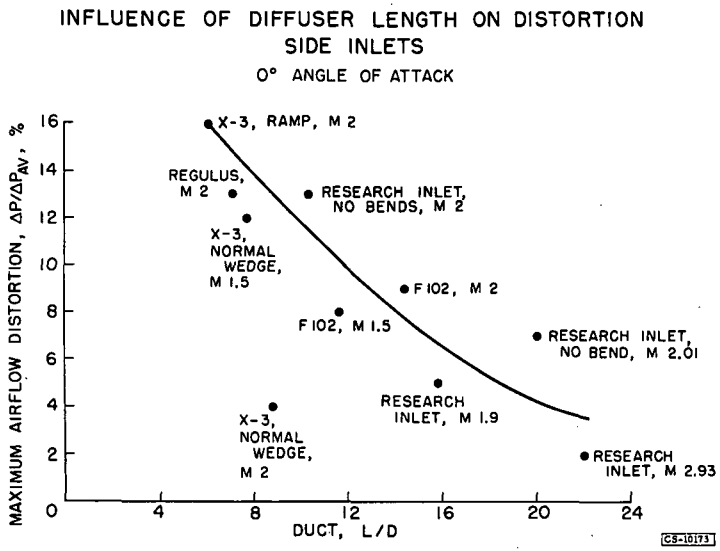

Figure 17.

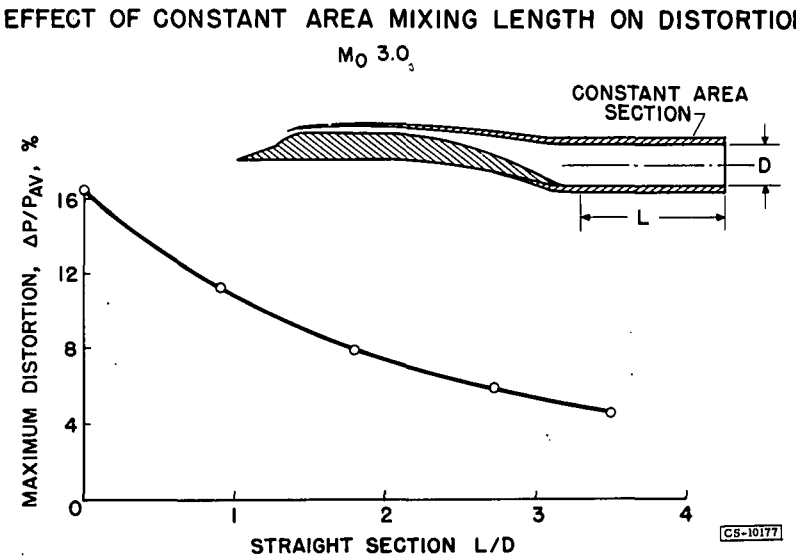

Figure 18.

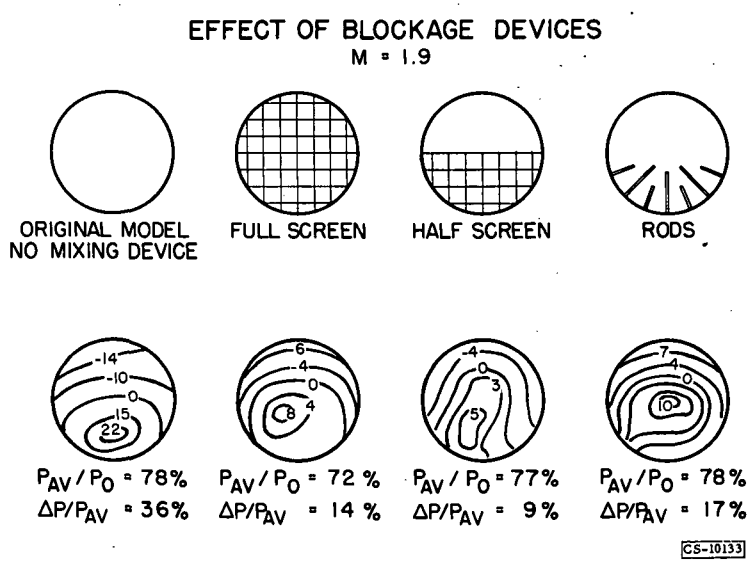

Figure 19.

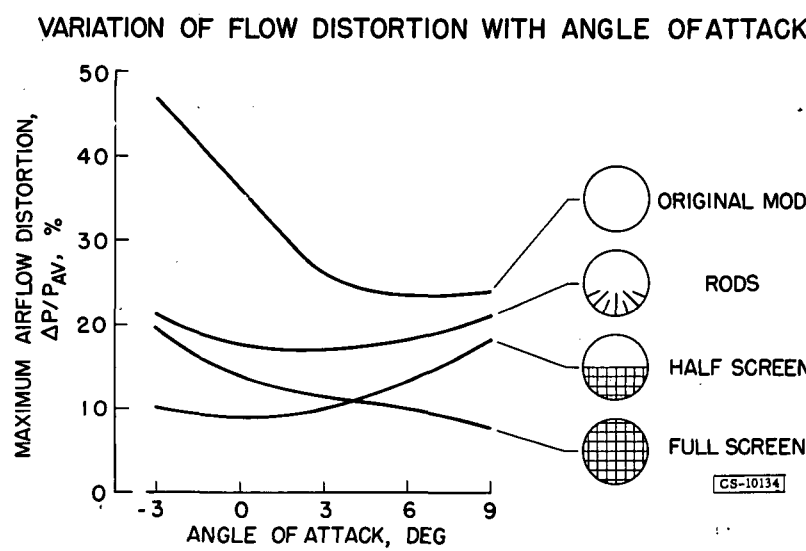

Figure 20.

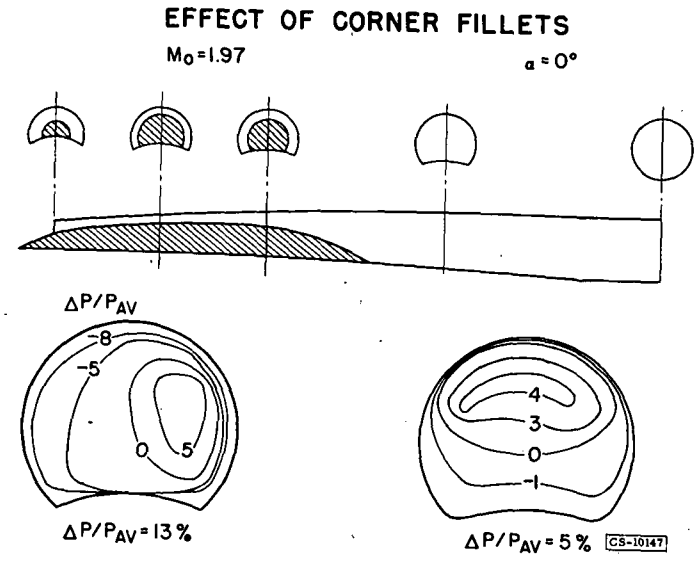
EFFECT OF CORNER FILLETS
M_0=1.97
α=0°
ΔP/P_AV
-8
-5
0
5
4
3
0
-1
ΔP/P_AV=13%
ΔP/P_AV=5%
CS-10147

Figure 21.

DECLASSIFIED

IV - EFFECT OF DISTORTION ON PERFORMANCE

W. A. Fleming, Chairman

R. P. Geye

E. T. Jansen, Jr.

R. R. Miller

DECLASSIFIED

IV - EFFECT OF DISTORTION ON PERFORMANCE

The effects of inlet flow distortion have been investigated on a number of engines during the past $2\frac{1}{2}$ to 3 years. The engines that have been used are listed in figure 1. The J40-WE-8 and J47-GE-25 investigations were relatively brief and simple. The primary purpose of the work on these two engines was to determine the effect of distortion on overall steady-state performance and to learn which portion of the engine was most sensitive to distortions. The J73-GE-3, J65-B-3, and J57-P-1 programs concentrated on those areas that were found to be most important. For example, interstage pressure and temperature surveys and hot-wire anemometers were installed throughout the compressors of these last three engines in order to obtain detailed surveys within the compressor, the component found most sensitive to distortions.

3665

As illustrated in the preceding paper, a wide variety of flow distortions exist at the engine inlet in aircraft ducts. A study of the distortions for a number of inlets revealed a general pattern. Both radial and circumferential distortion components were observed, and the magnitude of these distortions was found to vary from 10 to 20 percent in most inlets. This range of 10 to 20 percent was therefore set as the range of flow distortions to be investigated. It was considered necessary to study the radial and the circumferential distortions separately so as to determine the individual effects of each type of distortion.

After selecting the type and size of distortions to be investigated, it was decided that they could be best simulated by installing screens in the inlet duct. Typical radial and circumferential distortions and the screen arrangements used to obtain these distortions are illustrated in figure 2. The distortions shown here are in general similar to some of the inlet duct profiles shown in the preceding paper. The radial distortions were simulated by installing an annular section of screen in the inlet duct 1 to 3 feet ahead of the compressor. The circumferential distortions were simulated by installing screen segments, varying in density, around the inlet annulus 1 to 3 feet ahead of the compressor.

The magnitude of the inlet pressure distortion increases rapidly as engine speed is increased. This might be expected, since the pressure distortion and the pressure loss across the screens are proportional to the velocity head in the inlet duct. Consequently, the distortion increases approximately as the air flow squared and thus increases rapidly as engine speed is increased (fig. 3). This variation of the distortion with engine speed is similar to that observed in aircraft ducts. It should be noted that the definition of inlet pressure distortion used throughout this paper is the difference between the highest pressure at any point at the compressor inlet minus the lowest pressure at any point divided by the average pressure.

[redacted]

[redacted]

Four aspects of the results of the distortion investigations on the five engines listed in figure 1 are discussed herein:

(1) The extent to which inlet pressure distortions persist through the engines

(2) The effect of distortions on steady-state performance

(3) The manner in which distortions affect the engine stall limits

(4) A summary of the effects of distortion on current engines and the meaning of these effects to operational limits of current aircraft

3665

Extent Distortions Persist through Engine

Circumferential distortion. - The extent of the circumferential distortion existing in an engine is shown in figure 4. For the typical distortion presented, the pressure distribution is about 20 percent at the compressor inlet. At the compressor outlet, this pressure variation is attenuated to about 4 percent. However, temperature variation at the compressor outlet amounts to about 5 percent. This temperature variation is brought about by the fact that the compressor is operating at different values of compressor pressure ratio around the circumference. At the turbine outlet, there is no pressure variation. For the data shown on this figure the average turbine-outlet temperature is the same for both the typical distorted and uniform profiles. With the distortion, a maximum temperature gradient of 300° F results in a peak local temperature 120° above the peak for uniform inlet profile. The large variations in turbine-outlet temperature are brought about by the circumferential variations in compressor-outlet pressure and temperature resulting in an uneven air flow into the combustor. This uneven air flow and a uniform fuel-flow distribution combine to produce the circumferential turbine temperature variation.

The turbine rotor passes through these high peak temperatures much too fast to feel anything but the average temperature. However, the turbine stator does feel these high peak temperatures, and failures can result from just such a condition. In order to avoid these failures, the peak temperature must be reduced, which means that the average turbine-outlet temperature must be reduced. This is a derating effect and will be discussed later. Thus, the effects of the circumferential distortion are felt all the way through the engine.

Radial distortion. - Radial distortions do not extend through the engine to the same extent as circumferential distortions. As can be seen in figure 5, the radial distortions in the pressure profile wash out by the

[redacted]

time the compressor exit is reached. The radial profiles were obtained at the compressor inlet, after the fourth stage, and after the tenth stage of a J73-GE-3 compressor. It is apparent that, with a substantial radial pressure distortion at the compressor inlet, the distortion in the pressure profile practically disappears by the exit of the fourth stage. Thus, radial distortions do not affect the pressure or temperature profiles in the combustor and turbine as was the case with the circumferential distortion.

3665

Effect of Distortions on Steady-State Performance

The performance losses resulting from both radial and circumferential pressure distortions for three current turbojet engines (J47-GE-25, J65-B-3, and J73-GE-3) are shown in figure 6. The losses are presented as a function of percentage pressure distortion, which is the maximum local pressure minus the minimum local pressure divided by the average pressure. The values of efficiency and thrust are the ratio of performance with distortion to performance without distortion at the same engine operating condition; that is, the same corrected engine speed, the same average exhaust-gas temperature, and a flight Mach number of 0.8. There is only a slight decrease in performance as the distortion is increased up to about 20 percent. Although the compressor is subjected to pressure distortions as high as 20 percent, the over-all compressor efficiency does not drop more than 1 to 2 percent. The turbine-efficiency loss was only about 1 percent and then only at the larger pressure distortions. This small loss in turbine efficiency is a result of the circumferential pressure distortions, because the radial distortions wash out before reaching the turbine. These compressor and turbine losses combined to produce only a 1- to 2-percent loss in thrust and a corresponding increase in specific fuel consumption at a flight Mach number of 0.8 and an inlet pressure distortion of 20 percent.

However, with a circumferential distortion there may be an additional thrust loss caused by the turbine temperature profile. Figure 4 showed that operation with circumferential distortion at rated average turbine temperature results in local overheating of the turbine. At an average turbine-outlet temperature of 1300° F without distortion, the peak local temperature is only about 1330° F; while with distortion the peak local temperature is 1450° F, or 120° higher than without distortion. The question is, can the turbine stator stand this local high temperature? That the stator of the J47-GE-25 engine cannot stand this local high temperature is indicated by the fact that precisely at this condition a stator failed (fig. 7). Although the rotor assembly was not affected by the local high temperature directly, the parts of the stator assembly in burning away and passing through the rotor caused it to fail also. Therefore, it is to be expected that the average turbine temperature must be reduced with these circumferential distortions, which amounts to a derating of the engine.

[redacted]

The required reduction in average turbine-outlet temperature and the accompanying thrust loss for the J47-GE-25, J65-B-3, J73-GE-3, and J57-P-1 engines with various circumferential distortions is presented in figure 8. These temperature reductions fall in a band between 50° and 125° for the range of pressure distortions investigated. It might be expected that all the data would not fall on a single line because of differences in engines and differences in the degree of distortions. Reducing the turbine-outlet temperature by these amounts either by reducing engine speed or by increasing the exhaust-nozzle area resulted in thrust losses from 5 to 10 percent at a flight Mach number of 0.8. It should be noted that the temperature data in this figure were measured at the turbine outlet. The temperature gradients would be even greater at the turbine inlet. Consequently, temperature reductions shown in figure 8 are not conservative, and therefore the thrust reductions are slightly optimistic. In summarizing, the effect of distortions on the steady-state performance is not too important unless the engine has to be derated.

3665

Effect of Distortions on Engine Stall Limit

The problems that are often encountered because of the distortion effects on the engine stall limit are as follows: (1) slow acceleration, (2) reduced operable engine speed range, (3) lower maximum altitude limit, and (4) increased compressor blade stresses. These effects differ in magnitude from one engine to another, and all engines do not encounter each problem.

Before discussing the experimental data, it should be pointed out that with uniform inlet flow the acceleration margin and operational limits of turbojet engines are normally reduced as the altitude is increased. Thus, the acceleration margin and operational limits of engines become more and more sensitive to inlet flow distortions as the altitude is increased. The data to be presented are all for an altitude of 35,000 feet and a flight Mach number of 0.8 unless otherwise specified. Consequently, the effects do not represent the sensitivity of the engine to distortions at very low or very high altitudes.

Circumferential distortion. - The effect of circumferential distortion on the stall limit of the J73-GE-3 engine is shown in figure 9. The stall lines with and without distortion, along with the steady-state operating line, are shown as a function of compressor pressure ratio and corrected engine speed.

The circumferential distortion had little effect on the rotating-stall region, as shown by the shaded area. The main effect of circumferential distortion lies above the rotating-stall region. In this high compressor speed region, the acceleration margin is reduced considerably; but the engine may still be operated in steady state, and acceleration is still possible.

[redacted]

The effect of a larger circumferential distortion is presented for the J47-GE-25 engine in figure 10. Acceleration margin is again decreased with a circumferential distortion, and the stall limit actually intersects the steady-state operating line at a corrected speed of 108 percent. This corrected speed corresponds to operation at rated speed with an inlet temperature of -15° F. However, this is an unusually large distortion, amounting to 32 percent.

To explain why the stall line drops when the engine is subjected to a circumferential distortion, the data point at 100-percent corrected speed will be considered. For this particular circumferential distortion at the compressor inlet, a low-pressure area exists around the top portion and a high-pressure area exists around the bottom portion of the compressor. Figure 4 shows that the pressure variation at the compressor outlet is greatly reduced. Thus, the top portion of the compressor is operating at a higher pressure ratio than the bottom portion. The actual variation of compressor pressure ratio around the compressor is shown in figure 11. The top half of the compressor is operating at a pressure ratio of 7, and the bottom half at a pressure ratio of 5, while the average pressure ratio is 6. The stall line with uniform flow, which occurs at a compressor pressure ratio of 7, is represented by the dashed line. The data of this figure indicate that, when the top portion of the compressor reaches a pressure ratio of 7, the whole compressor stalls, even though the bottom portion is operating at a pressure ratio of only 5. This effect of circumferential distortion on the compressor stall limit was found to exist for the range of speeds investigated with the J47-GE-25.

The same concept was also found to hold true for the J73-GE-3 engine (fig. 12). The solid line is the uniform-inlet-flow stall line. The data points for two circumferential distortions represent the maximum local compressor pressure ratio at stall across any circumferential part of the compressor. The two different distortions cover circumferential segments of about 60°. The maximum local pressure ratio at stall and the undistorted stall line show good agreement. A similar agreement has been shown for the J65-B-3 engine.

This simple concept holds for these three engines but may not necessarily hold for all engines or for all circumferential distortions. This relation will have to be checked with a number of other engines to further verify the agreement. The distortions used in these three engines were relatively large circumferential zones, the smallest being 60° in circumference. It might be expected that, for very small segments of circumferential distortion, the concept may no longer hold; but for the time at least this relation does serve as a good rule of thumb.

Radial distortion. - The mechanism by which a radial distortion affects the stall limit is rather complex, and no simple concept exists that might indicate the magnitude of these effects. However, the typical

effect of a radial distortion on the stall limit is presented in figure 13. The data for this figure, obtained from a J65-B-3 engine, are presented in terms of compressor pressure ratio and corrected engine speed. The heavily shaded area is the region in which steady-state rotating stall is encountered with uniform flow. The lightly shaded area represents the extension of this region with a radial distortion. Two effects of the radial distortion are immediately apparent: (1) In the high-speed region, the stall-limit line is encountered at lower pressure ratios; (2) in the intermediate-speed range steady-state rotating stall is extended to higher speeds, and the knee in the stall-limit line is moved nearer the steady-state operating line. The severity of these effects can vary greatly from engine to engine.

Figure 14 illustrates how serious these effects of radial distortions may become. This figure presents the J73-GE-3 performance with open inlet guide vanes; that is, with the guide vanes in their design operating position. With uniform inlet flow, the acceleration margin is very small at the knee of the stall-limit line. With a 6-percent distortion, this acceleration margin decreased to zero, and acceleration to design speed was impossible without first closing the inlet guide vanes.

In the high-speed region, there is no adequate explanation for the effects of radial distortion on the stall limit at the present time. However, the phenomena that cause the rotating-stall region to be extended to higher speeds are reasonably apparent. The first paper pointed out that at these intermediate speeds the first stages are highly loaded, and as a result these stages are forced to operate in a stalled condition. With the radial distortion such as imposed on the J65-B-3 and the J73-GE-3, the loading of the tips of these first stages is increased; hence, these stages are forced to operate in a stalled condition to a higher speed.

Combined distortions. - As pointed out in paper III, in actual practice a combination of the two types of distortion will probably occur, rather than a pure radial or circumferential distortion. One such combination was investigated at the NACA Lewis laboratory in the J73-GE-3 engine. The radial and circumferential components of this combined distortion were also evaluated separately. The results of this investigation are presented in figure 15. The effect of the combined distortion on the stall limit is about the same as the effect of that component of the distortion which by itself had the greatest effect. In the present case the combined distortion stall limit was primarily the result of the radial component of the distortion. However, this is not a general rule. At present, it cannot be predicted which of the two types of distortions is primarily responsible for the losses of the combined distortion. However, each component of the combined distortion will contribute its own predominant characteristics.

UNCLASSIFIED

Effect of Distortions on Engine Operational Characteristics

The high points of the investigations conducted on the engines listed in figure 1 are summarized in this section. Although the compressor and turbine efficiencies of the engines were found to be relatively insensitive to inlet flow distortions, the circumferential distortions imposed on each engine resulted in circumferential temperature gradients at the turbine outlet resulting in local overheating of the turbine-inlet stators. The J73-GE-3 engine was very sensitive to radial distortions; as the engine was accelerated very slowly from low engine speeds with the inlet guide vanes in the open or high speed position compressor stall was encountered well below rated speed due to the intersection of the steady state operating line and the compressor stall line. Imposing the inlet distortions resulted in critical blade vibrations and blade stresses in the J65-B-3 and J73-GE-3 engines.

3665

The distortion effects on the J57-P-1 engine have been more completely evaluated than on any of the other engines, since this investigation was carried to higher altitudes and lower inlet temperatures. Also, not much of the J57-P-1 data have been published, because the investigation has just been concluded; while most of the distortion data obtained on the other engines have been reported (see refs. 1 to 7). For these reasons and because the J57-P-1 engine is the one used in many current aircraft, the J57-P-1 distortion data are summarized in some detail.

The effect of altitude on the J57-P-1 stall limits is presented in figure 16 for operation with the compressor bleeds closed at a flight Mach number of 0.8 and NACA Standard temperatures. In practice the low-speed stall limit is circumvented by opening the compressor bleeds at the scheduled speed. For this reason the curves to the left of the area marked "Bleed Schedule" in figures 16 to 19 are only of design interest and do not apply to the operation of the J57-P-1 engine as installed in the aircraft. The solid line represents the compressor stall limit, the dashed line the maximum permissible turbine-outlet temperature for the engine used in these tests, and the vertical shaded area the region in which the compressor bleeds are normally scheduled to open and close. The variation in engine stall limit with altitude results from the effect of Reynolds number on compressor performance.

The maximum operable altitude shown in this figure is about 62,000 feet. Small oscillations in the fuel flow with the standard or production control resulted in compressor stall at an altitude of 58,000 feet. Installing a special throttle system, which provided very uniform fuel pressures and allowed careful fuel-flow manipulation, permitted attainment of the maximum altitude of 62,000 feet.

[redacted]

Because the compressor stall line is sensitive to inlet-air temperature, the point at which the compressor will stall is a function of corrected instead of actual engine speed. Therefore, for the operating limits shown in figure 16, as the ambient-air temperature is reduced, the stall-limit line will be shifted in the direction of reduced speed. This shift amounts to slightly more than 1 percent in speed for each 10° change in inlet temperature. In addition, the engine manufacturer states that the engine speed at which stall occurs on the J57-P-1 engine may vary as much as 3 percent from engine to engine. Therefore, the operational limits shown in figure 16 with uniform inlet flow and the succeeding figures with distorted inlet flow do not indicate the precise stall limits for all engines at all ambient temperatures, although the trends shown by the data would be similar for all J57-P-1 engines. Furthermore, the particular engine with which the data were obtained had 480 hours of operating time plus about 750 intentional stalls imposed on it.

3665

An interesting observation is that there is an apparent hysteresis effect on the engine stall characteristics. When compressor stall was encountered above an altitude of 50,000 feet, it was impossible to recover from stall even though the fuel flow was reduced and the compressor bleeds open. Recovery was thus possible only by completely shutting down the engine or by reducing the altitude to about 35,000 feet. This compressor stall was accompanied by a very violent surging of the flow within the engine. The engine structure was sufficiently strong to withstand the high surging loads of the hundreds of stalls to which the engine was intentionally subjected during the wind-tunnel investigation at altitudes of 35,000 feet and above.

The effects of a radial distortion on the operating range of the J57-P-1 engine are shown in figure 17. This radial distortion had the low-pressure region in the outer 1-inch region of the annulus. With this distortion the operable speed range of the engine was actually increased slightly over the operable speed range without distortion for the range of altitude conditions investigated. However, the stall-limited maximum speed was only 1 to 2 percent higher than that with uniform inlet flow. Opening the compressor bleeds circumvented the low speed stall limit.

The circumferential distortions, however, had a detrimental effect on the engine operating limits, as shown in figure 18. Not only did the altitude limit decrease sizably, but the operable speed range was also squeezed in from both the high- and low-speed ends. The two different circumferential distortions had about the same magnitude of pressure

[redacted]

deviation but covered considerably different circumferential areas, as shown by the schematics on the figure. The altitude limit was decreased from 62,000 feet for the undistorted condition to about 56,000 feet with the two-spot circumferential distortion. The extended circumferential distortion reduced the altitude limit to 48,000 feet. With these distortions, the stall limit at maximum speed was decreased from 1 to 3 percent below the stall limit without distortion; and with the extended circumferential distortion, the stall limit at maximum speed was encountered below the limiting temperature line. In addition, low-speed stall was encountered at high altitudes for both distortions before the bleeds are scheduled to open. This means that at high altitudes decelerating the engine would result in stall.

The effect of a combined distortion on the altitude operating range of the engine is presented in figure 19. The extent of combined distortion is indicated by the small schematic on the figure. The radial component covered half the annulus, the low-pressure region being the outer portion. The circumferential low-pressure region of the distortion covered a 120° segment. This combined distortion gave inlet pressure variations corresponding to the extended radial and both circumferential distortions previously discussed.

The combined distortions reduced the operable speed range considerably and reduced the altitude limit from 62,000 feet without distortion to about 54,000 feet with distortion. It is also apparent from these data and the preceding data that the circumferential component of the combined distortion has the predominant effect.

To summarize the J57-P-1 data, circumferential distortions extending over reasonably large areas considerably reduced the speed and altitude operating range.

Observations of Stall in Flight

The data presented in figures 16 to 19 indicate the restrictions on engine operating limits that might be expected in aircraft having inlet flow distortions. In order to determine whether these engine operating limits correspond to the operating limits actually observed during flight tests, data obtained during flight tests of current aircraft have been collected from the Air Force, Bureau of Aeronautics, and several airframe contractors. The flight data and NACA data cannot be directly correlated because of differences in the engine models and because of differences between the distortions in the airplanes and the distortions simulated. These data can be used, however, to show the general agreement that exists between the flight and the altitude-wind-tunnel limits.

The F-101A airplane has experienced engine stall at altitude. The effect of distortion on the operating ceiling of this airplane is shown

3665

in figure 20. The shaded area represents the region in which engine stalls have been encountered during flight. The maximum altitude to which the airplane can be flown consistently without encountering stall is about 35,000 feet. The distortion measured in this airplane was of the circumferential type and extended gradually around the circumference The magnitude of the distortion varied from 0.08 to 0.14 over the range of flight conditions represented by the shaded area. On the basis of the altitude-wind-tunnel data, it would be expected that, with a distortion of this type and this magnitude, compressor stall might well be encountered at these altitudes.

The F4D-1 airplane has greater distortions than the F-101A, as indicated in figure 21, but also has higher altitude operating limits. As indicated by the shaded area, the maximum consistent operating altitude without encountering compressor stall is about 45,000 feet. Although the inlet distortion was circumferential and amounted to 16 to 18 percent, the distortions were localized in small areas at the top and bottom of the duct ahead of the compressor. The altitude-wind-tunnel data also showed less severe effects of the local distortions than the extended circumferential distortions. Therefore, it might be concluded that the F4D-1 airplane has higher altitude operating limits than the F-101A airplane because of the difference in the type of distortion.

The F-100A airplane has currently had little trouble with fixed-throttle stalls. The effect of distortion on the operating ceiling of this airplane is indicated in figure 22. The distortions measured amount to about 5 percent in the circumferential direction and about 8 percent in the radial direction. Only a few fixed-throttle stalls have been encountered, these at a flight Mach number of about 0.9 and at altitudes near 50,000 feet. The compressor stalls have not been a limiting factor, however, since the airplane has been flown to altitudes as high as 53,000 feet.

The XB-52 airplane has encountered little trouble with fixed-throttle stalls. The effect of stall on the operating ceiling of this airplane is shown in figure 23. As indicated by the shaded area, a few fixed-throttle stalls have been encountered near an altitude of 50,000 feet, but the airplane has been to altitudes as high as 53,000 feet without encountering stalls. The inlet profiles are very similar to those measured on the F-100A airplane.

A brief comparison of wind-tunnel and flight data shows that a general agreement exists between the engine operating limits experienced in flight tests and those encountered during the distortion investigations in the altitude wind tunnel.

DECLASSIFIED

3665

REFERENCES

1. Wallner, Lewis E., Conrad, E. William, and Prince, William R.: Effect of Uneven Air-Flow Distribution to the Twin Inlets of an Axial-Flow Turbojet Engine. NACA RM E52K06, 1953.

2. Walker, Curtis L., Sivo, Joseph N., and Jansen, Emmert T.: Effect of Unequal Air-Flow Distribution from Twin Inlet Ducts on Performance of an Axial-Flow Turbojet Engine. NACA RM E54E13, 1954.

3. Huntley, S. C., Sivo, Joseph N., and Walker, Curtis L.: Effect of Circumferential Total-Pressure Gradients Typical of Single-Inlet Duct Installations on Performance of an Axial-Flow Turbojet Engine. NACA RM E54K26a, 1954. (To be published.)

4. Conrad, E. William, Hanson, Morgan P., and McAulay, John P.: Effects of Inlet-Air-Flow Distortion on Steady-State Altitude Performance of an Axial-Flow Turbojet Engine. NACA RM E55A04, 1955. (To be published.)

5. Harry, David P., III, and Lubick, Robert J.: Inlet-Air Distortion Effects on Stall, Surge, and Acceleration Margin of a Turbojet Engine Equipped with Variable Compressor Inlet Guide Vanes. NACA RM E54K26, 1954.

6. Wallner, Lewis E., Lubick, Robert J., and Einstein, Thomas H.: Preliminary Data on the Effects of Inlet Pressure Distortions on the J57-P-1 Turbojet Engine. NACA RM SE54K19, 1954.

7. Lubick, Robert J., Meyer, William R., and Wallner, Lewis E.: Preliminary Data on the Effects of Altitude and Inlet-Pressure Distortions on Steady-State and Surge Fuel Flow of the J57-P-1 Turbojet Engine. NACA RM SE55A06, 1955.

ENGINES INVESTIGATED WITH INLET FLOW DISTORTIONS

1.	J40-WE-8	JULY, 1952
2.	J47-GE-25	JUNE, 1953
3.	J73-GE-3	FEB., 1954
4.	J65-B-3	AUG., 1954
5.	J57-P-1	FEB., 1955

CS-10188

Figure 1.

TYPICAL VARIATION OF DISTORTION WITH ENGINE SPEED

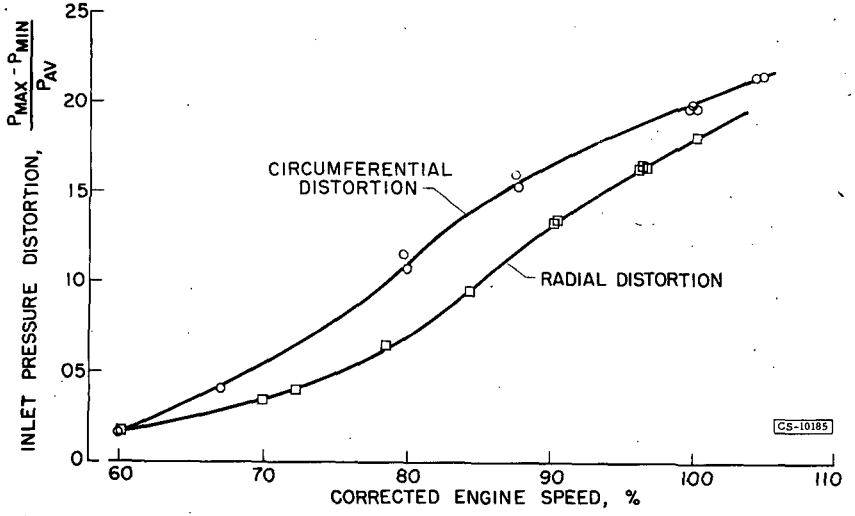

Figure 3.

TYPICAL INLET FLOW DISTORTIONS

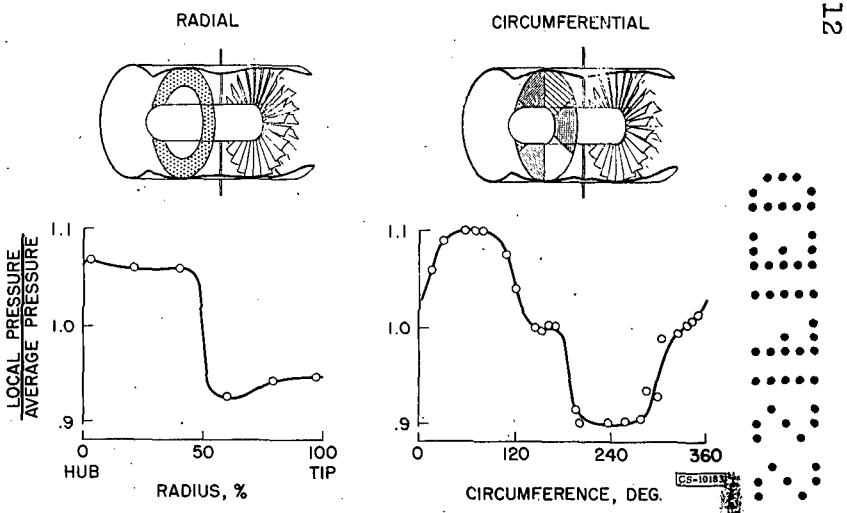

Figure 2.

EXTENT OF CIRCUMFERENTIAL DISTORTION THROUGH ENGINE

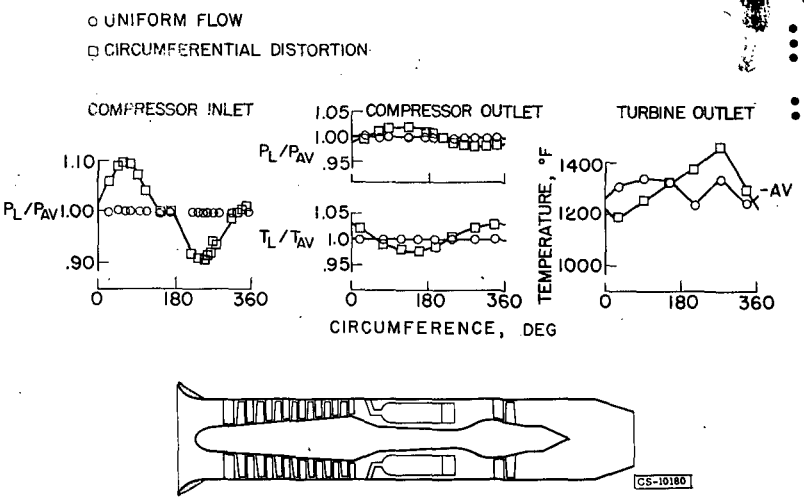

Figure 4.

EXTENT OF RADIAL DISTORTION THROUGH COMPRESSOR

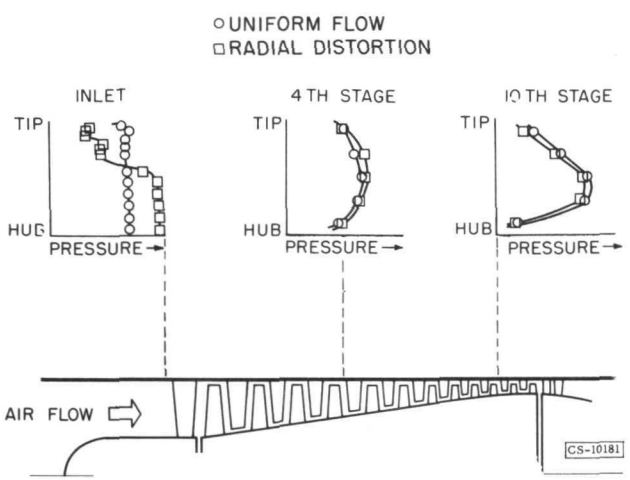

Figure 5.

EFFECT OF DISTORTION ON PERFORMANCE

RATED TURBINE OUTLET TEMPERATURE AND ENGINE SPEED
FLIGHT MACH NUMBER, 0.8

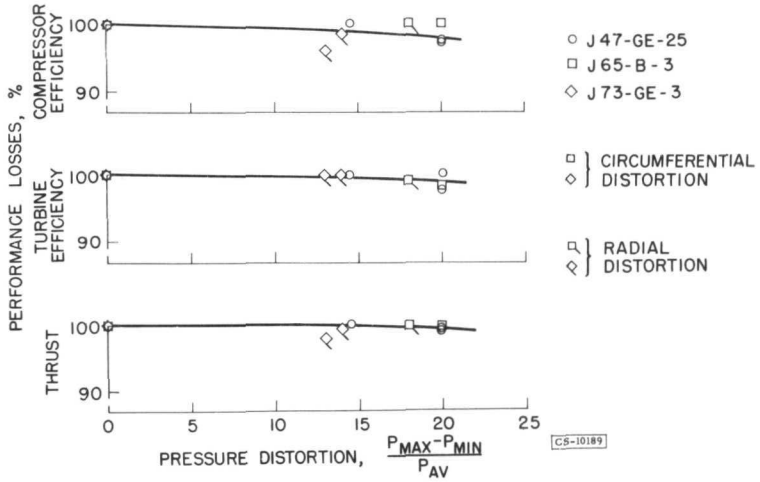

Figure 6.

TURBINE STATOR FAILURE WITH CIRCUMFERENTIAL DISTORTION

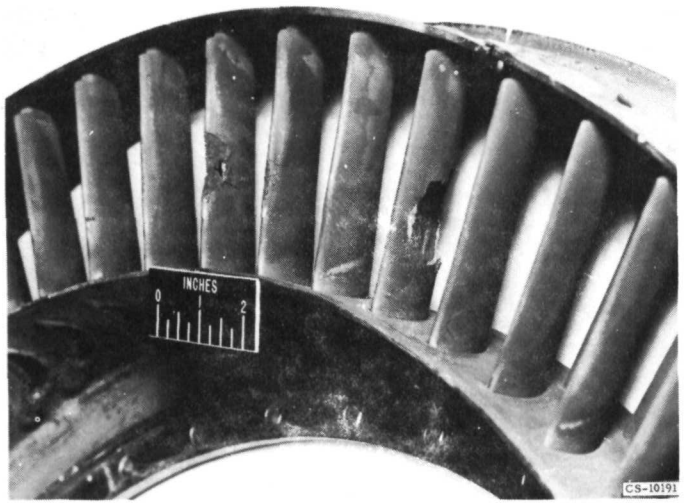

Figure 7.

PERFORMANCE DERATING WITH CIRCUMFERENTIAL DISTORTION

FLIGHT MACH NUMBER, 0.8

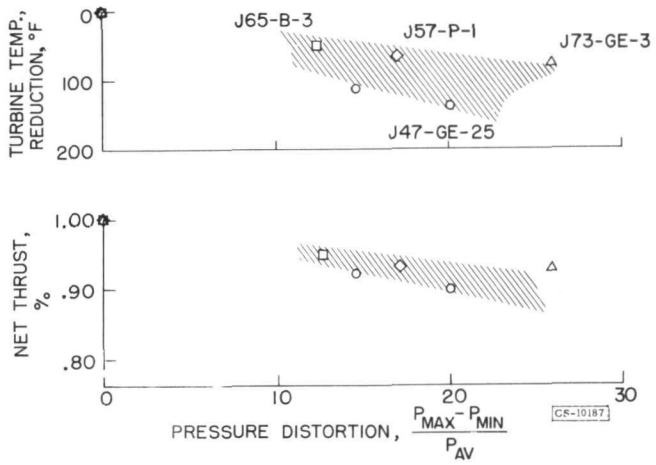

Figure 8.

EFFECT OF CIRCUMFERENTIAL DISTORTION ON STALL LIMIT
J 73 - GE - 3 ENGINE

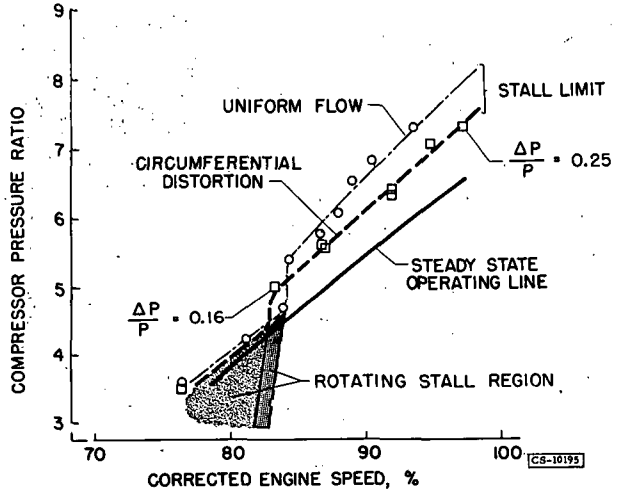

Figure 9.

EFFECT OF CIRCUMFERENTIAL DISTORTION ON STALL LIMIT
J 47 - GE - 25 ENGINE

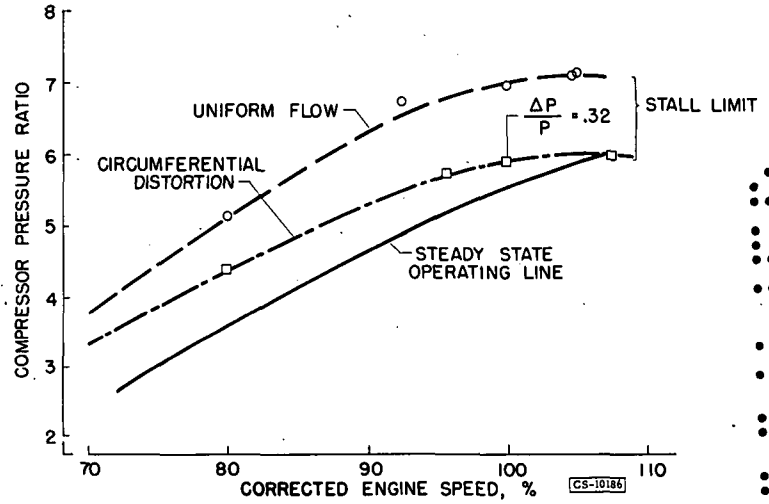

Figure 10.

VARIATION OF LOCAL PRESSURE RATIO AROUND CIRCUMFERENCE
J 47 - GE - 25 ENGINE AT 100% SPEED

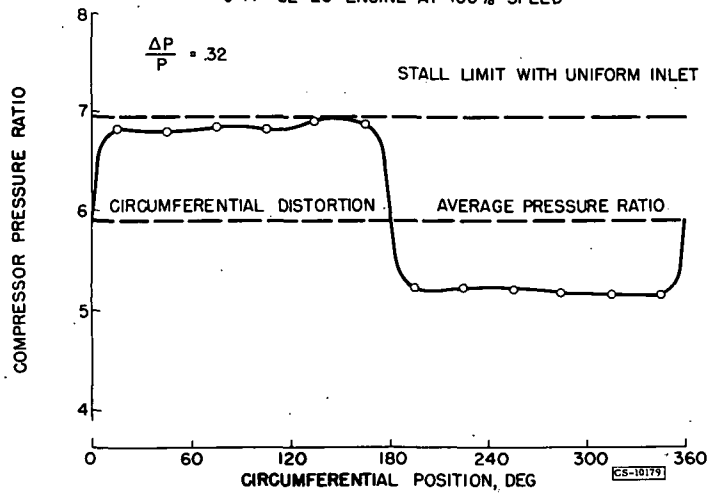

Figure 11.

STALL LIMIT CORRELATION WITH CIRCUMFERENTIAL DISTORTION
J73-GE-3 ENGINE

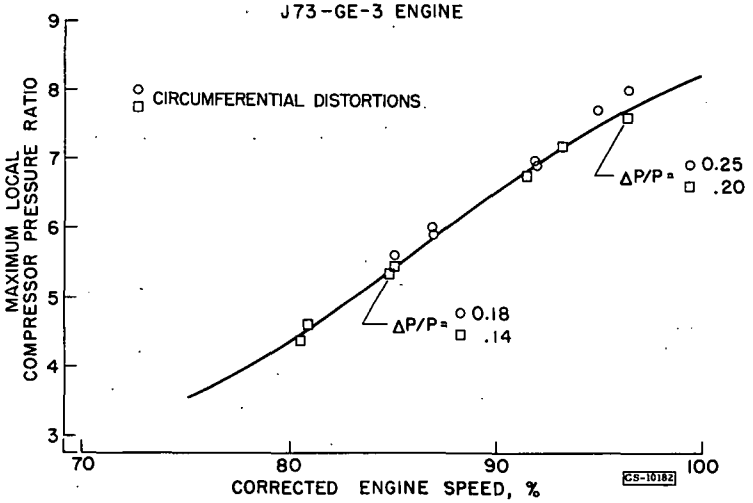

Figure 12.

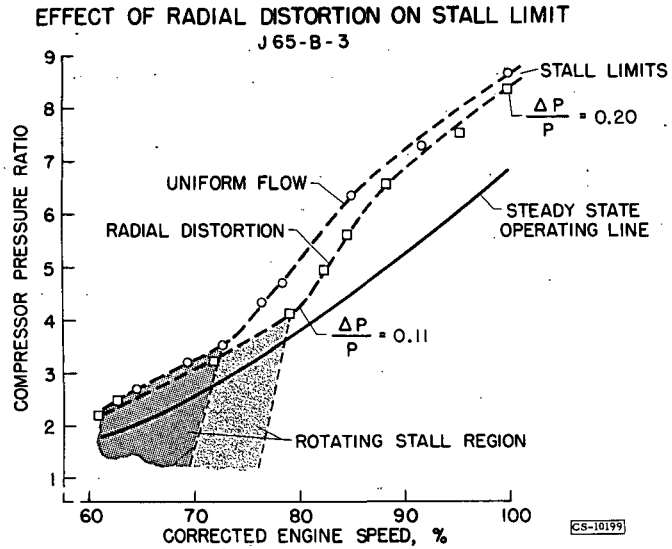

Figure 13.

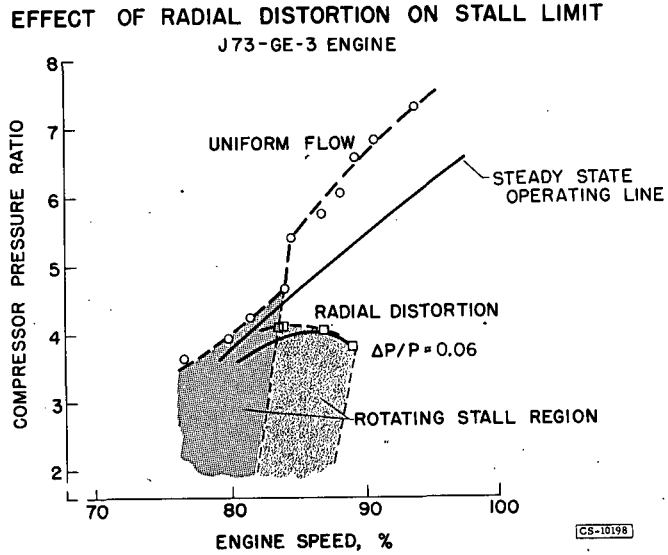

Figure 14.

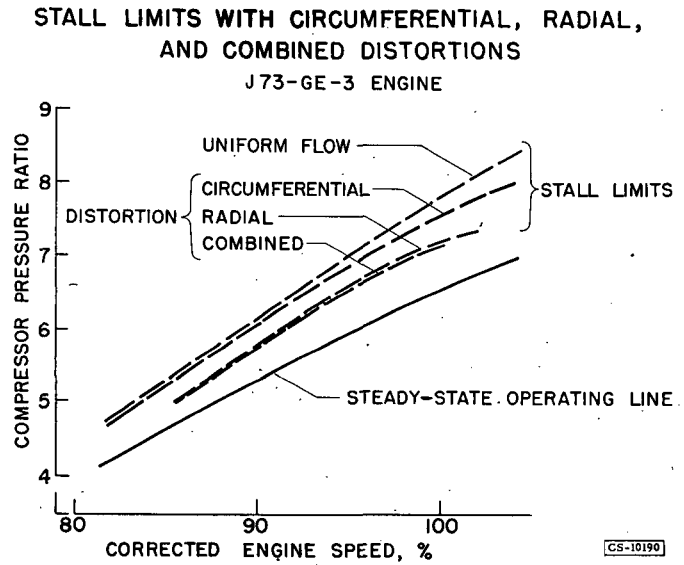

Figure 15.

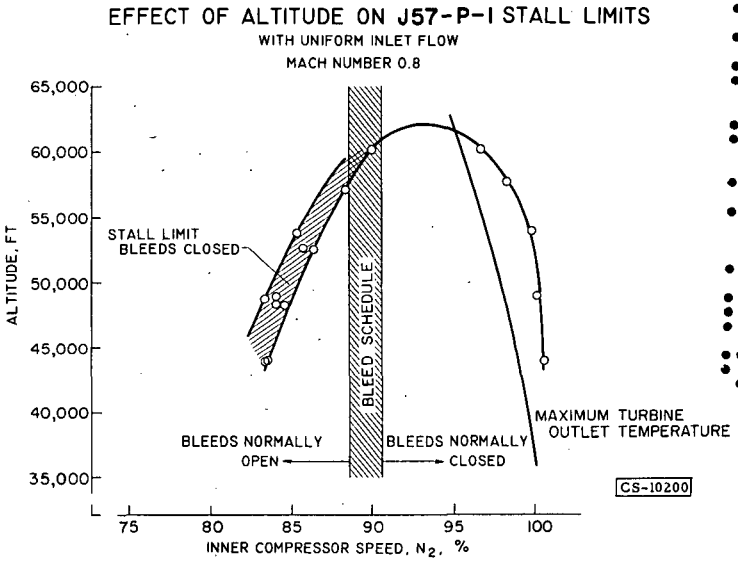

Figure 16.

EFFECT OF RADIAL DISTORTION ON J57-P-1 STALL LIMITS

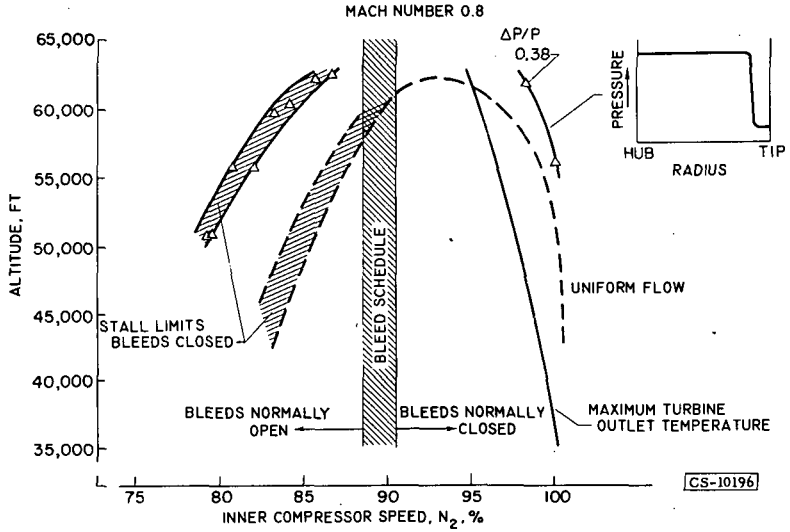

Figure 17.

EFFECT OF CIRCUMFERENTIAL DISTORTIONS ON J57-P-1 STALL LIMITS

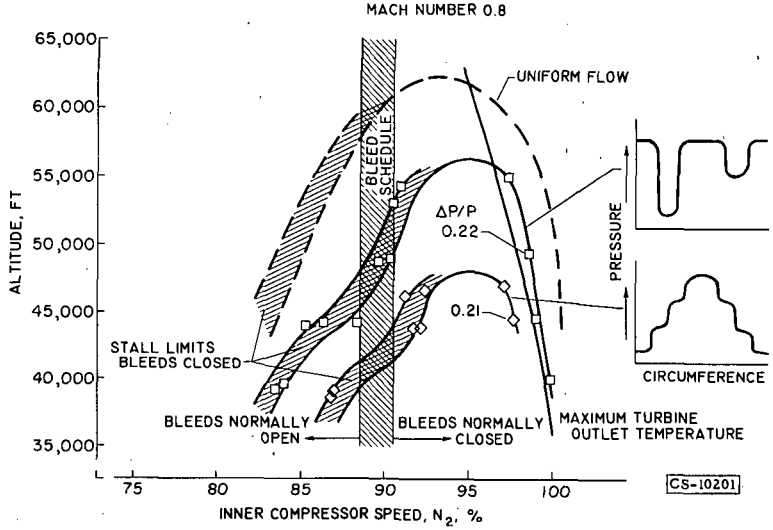

Figure 18.

EFFECT OF COMBINED DISTORTION ON J57-P-1 STALL LIMITS

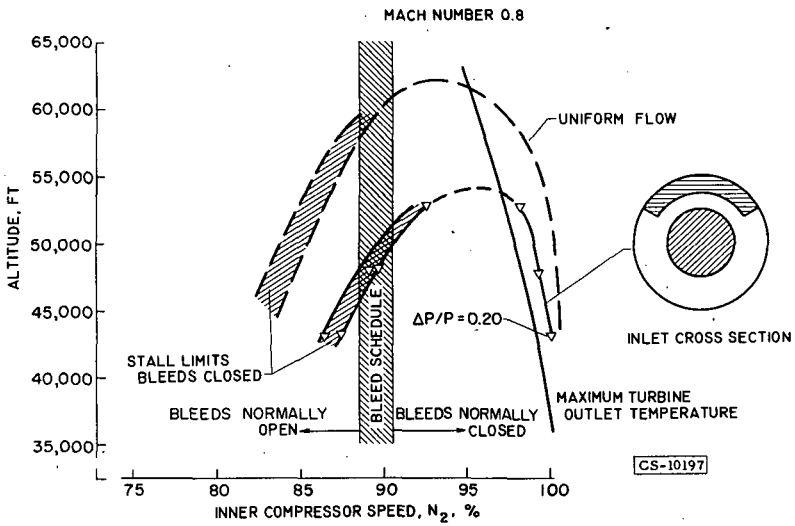

Figure 19.

EFFECT OF DISTORTION ON OPERATING CEILING OF F-101A AIRPLANE

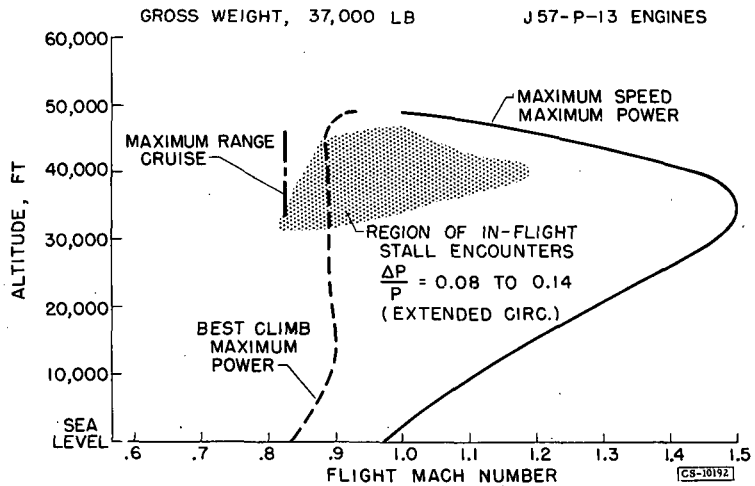

Figure 20.

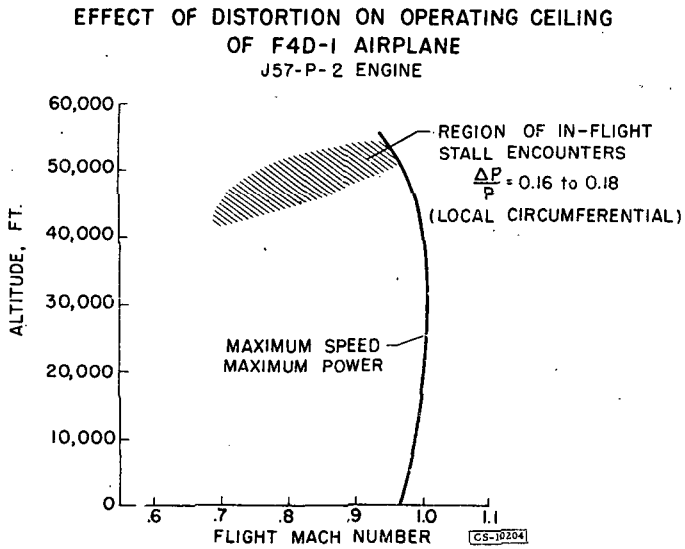

Figure 21.

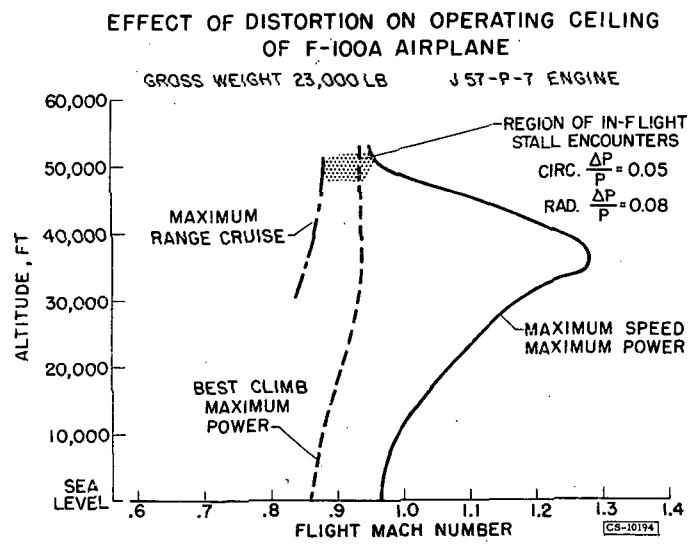

Figure 22.

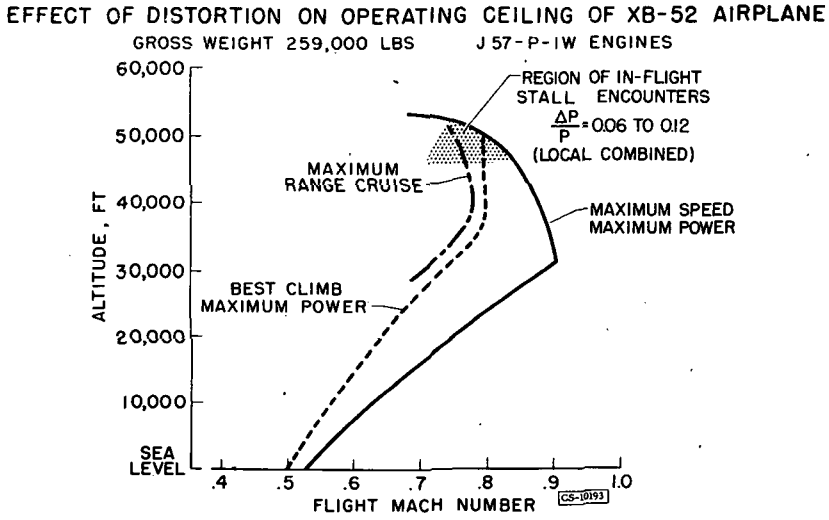

Figure 23.

DECLASSIFIED

3665

V - REMEDIES FOR COMPRESSOR STALL AND BLADE VIBRATION

W. A. Benser, Chairman

M. C. Huppert

L. E. Wallner

H. F. Calvert

CD-4217

DECLASSIFIED

V - REMEDIES FOR COMPRESSOR STALL AND BLADE VIBRATION

INTRODUCTION

In the past few years, the pressure ratio of axial-flow turbojet-engine compressors has been increased appreciably in order to improve altitude performance and engine fuel economy. As a result, compressor stall at low engine speeds has become a serious problem in regard to engine acceleration. Furthermore, rotating stall, which exists in the compressor at these low engine speeds, is a prevalent source of compressor blade vibrations, as discussed in paper II. Recent studies show that inlet airflow distortion has severe adverse effects on the stalling characteristics of axial-flow compressors at all engine speeds (paper IV). As discussed in paper III, some improvement in inlet flow distribution may be achieved by research on inlets and their associated ducting, but variations in flight conditions such as angle of attack and flight Mach number may still result in appreciable flow distortions at the compressor inlet.

In order to obtain satisfactory acceleration, adequate margin between the steady-state operating line and the compressor stall-limit line is required, particularly at low and intermediate values of engine speed. To avoid compressor stall problems resulting from inlet flow distortions, the stall margin at all speeds must be increased from that which is normally considered adequate for operation with uniform flow at the compressor inlet. To eliminate blade vibrations due to rotating stall, resonance between the compressor blading and rotating-stall zones must be eliminated.

This paper considers some of the methods available for alleviating the compressor stall and blade-vibration problems discussed in papers II and IV. The modifications, or remedies, for the compressor stall problem are used to control the location of the compressor stall-limit line with respect to the engine steady-state operating line so as to avoid encountering compressor stall. The remedies for blade-vibration problems are aimed at eliminating rotating stall as a source of blade excitation. The single-spool engine and the two-spool engine are considered separately.

SINGLE-SPOOL ENGINE

The remedies to be considered for the single-spool engine are (1) exhaust-nozzle adjustment, (2) turbine-stator adjustment, (3) compressor-discharge bleed, (4) compressor interstage bleed, (5) inlet-guide-vane adjustment, and (6) inlet baffles. Exhaust-nozzle and turbine-stator adjustments are primarily remedies for compressor stall at high engine speeds. Compressor-discharge bleed, compressor interstage bleed, and adjustable inlet guide vanes are remedies for stall problems at low and intermediate speeds; and the inlet baffle is primarily a remedy for

3665

[redacted]

compressor blade-vibration problems due to rotating stall. Inasmuch as no single engine incorporates all these features, the data presented are for several different engines. In addition to these remedies, compressor design compromises to improve stall margin are discussed briefly.

Definition of Problem

The low-speed stall problem of high-pressure-ratio single-spool turbojet engines is illustrated in figure 1, which shows the variations of stall-limit pressure ratio with speed for the J71-A-2 and J73-GE-3 engines for uniform inlet flow. The steady-state operating line for rated jet nozzle area and no variable-geometry remedies is also shown on these plots. For the J73-GE-3 engine, the compressor stall limit is extremely close to the steady-state operating line at low engine speeds but is appreciably above the operating line at higher speeds. For the J71-A-2 engine, a severe dip or knee occurs in the compressor stall limit between 60 and 80 percent of rated engine speed. In this case, the stall-limit line intersects the operating line at 65- and 75-percent speed. Engine operation in this range of speed is impossible without the use of some stall remedy.

A convenient measure of the margin between the compressor stall limit and the steady-state operating line at a given speed is the ratio of the pressure ratio at stall to the pressure ratio required for steady-state operation at that speed. Figure 2 shows a plot of this stall margin against engine speed for the J73-GE-3 engine. A value of 1 for this stall margin represents an intersection of the operating line and the stall-limit line and is the limit of engine operation. The solid curve in this figure indicates a small stall margin at low engine speeds and a sizable stall margin at high engine speeds for no inlet distortion.

A comparison of the solid and dashed curves in figure 2 shows the effect of a radial distortion of inlet flow on the stall margin of the J73-GE-3 engine. These are the same data presented in paper IV, and, as noted, the magnitude of distortion decreased with engine speed. The value of $\Delta P/P$ at rated speed was 12 percent and decreased to 5 percent at 90-percent speed. As noted in this figure, the effect of distortion is to move the dip or knee in the stall limit to higher speed and to severely decrease the stall margin at high engine speeds. More severe inlet flow distortions would further reduce the stall margin and could conceivably render this engine inoperable both at intermediate and at high engine speeds.

The two ranges of engine speed that are of particular interest are indicated by figure 2. The first is the high-speed range, where inlet distortions may impose severe stall limitations. The second is the low-speed range, where an adequate stall margin is required in order to obtain satisfactory engine acceleration. As pointed out in paper I, compressor stall at high engine speeds is instigated by stall of rear stages, and compressor stall at low speeds is instigated by stall of front stages.

[redacted]

DECLASSIFIED

If a compressor must operate satisfactorily, even when inlet flow distortions are encountered, the stall margin over the entire speed range must be increased above that which is necessary for a uniform inlet flow.

Exhaust-Nozzle Adjustment

3665

Within limits, increasing the exhaust-nozzle area of a single-spool engine increases the stall margin by decreasing the pressure ratio required for steady-state operation at any speed. When the exhaust nozzle is opened, the back pressure on the turbine is decreased. Thus, the work required to drive the compressor can be obtained at lower turbine-inlet pressure and temperature, and the compressor can operate at a reduced pressure ratio.

Effect on stall margin. - The effect of exhaust-nozzle area on the stall margin of the J71-A-2 engine is shown in figure 3, where stall margin is plotted against engine speed. The solid curve is for rated exhaust-nozzle area. As engine speed is increased from 40 to 65 percent, the stall margin decreases to a value of 1.0. Thus, at 65-percent speed, the operating line intersects the stall-limit line, and the engine is not operable in the speed range of 65- to 75-percent speed without the aid of some stall remedies. Above 75-percent speed, the stall margin increases rapidly.

The stall margin obtained for an exhaust-nozzle area that is 60 percent greater than the rated area is shown by the dotted curve in figure 3. This change improves the stall margin somewhat at low engine speeds, but the inoperable region remains essentially the same. At high engine speeds, there is a considerable improvement in stall margin. This increase in stall margin at high speeds is significant with respect to inlet flow distortions.

Effect on engine performance. - At rated speed, the thrust of the J71-A-2 engine decreases rapidly as the exhaust-nozzle area is increased, as shown in figure 4. For a 60-percent increase in area, the thrust is decreased about 30 percent. This thrust loss results from the drop in turbine-inlet temperature. The 60-percent increase in exhaust-nozzle area causes a 450° drop in turbine-inlet temperature (fig. 4). Thus, exhaust-nozzle-area increase may improve stall margin somewhat, but only at the expense of a severe thrust penalty.

Turbine-Stator Adjustment

A combination of turbine-stator-area and exhaust-nozzle-area changes can be used to improve stall margin. As shown previously, increasing the exhaust-nozzle area decreases the compressor pressure ratio and, thus,

[redacted]

[redacted]

improves stall margin. In order to operate with this decreased compressor pressure ratio without reducing the turbine-inlet temperature, the turbine-stator area must be increased. Increases in turbine-stator area can be achieved by simply resetting the angle of the first row of turbine stator blades.

Effect on engine performance. - Thrust and fuel consumption in percent of rated values are plotted in figure 5 against turbine-stator area. These data are the results of an investigation in which a J40-WE-6 engine was operated with increased turbine-stator areas. The J40-WE-6 has a two-stage turbine; however, only the stators for the first stage were reset. As the exhaust-nozzle area was increased to 115 percent of rated area, the turbine-stator area was increased to 110 percent of the rated area to maintain constant turbine-inlet temperature. These changes of area had little effect on engine thrust (fig. 5). The fuel consumption of the engine was increased about $3\frac{1}{2}$ percent when the turbine-stator area was increased 10 percent.

Effect on stall margin. - Stall margin is plotted against engine speed in figure 6. The data in the lower curve give the stall margin for the J40-WE-6 when it was operated with standard exhaust-nozzle and turbine-stator areas. The upper curve presents the stall margin when the engine was operated with 110-percent turbine-stator and 115-percent exhaust-nozzle areas. At rated speed, these area changes increased the stall margin approximately 12 percent. The stall margin was increased over the entire speed range; therefore, these area changes could be considered as permanent changes.

Increasing compressor stall margin by turbine-stator adjustment could be considered as derating the engine in terms of pressure ratio. If the pressure ratio is reduced too much, the compressor efficiency will be lowered appreciably, and a large loss in engine thrust and efficiency will result. The reduced pressure ratio also results in a decreased air density at the compressor discharge and, therefore, increases the combustor-inlet velocities. This velocity increase may adversely affect the altitude performance of the combustor.

Moderate increases of turbine-stator and exhaust-nozzle area can be effectively used to increase stall margin. Extremely large area changes, however, will severely decrease component efficiencies and will decrease thrust as well as increase fuel consumption.

Compressor-Discharge Bleed

Compressor-discharge bleed is a potential method of improving stall margin at low engine speeds. With this remedy, air is bled from the

[redacted]

compressor discharge, and the compressor pressure ratio for steady-state operation is decreased. The turbine-inlet temperature, however, is increased. Calculations of the effect of discharge bleed on the J71 engine indicated that 20-percent bleed was necessary to increase the stall margin sufficiently to permit engine acceleration. Even with this large amount of bleed, engine acceleration was not considered satisfactory. When compressor-discharge bleed is used, the bleed ports must be closed at high engine speeds to avoid severe thrust penalties and to avoid overtemperature of the turbine. Moderate improvements in stall margin at low and intermediate engine speeds can be obtained by use of compressor-discharge bleed. Compressor interstage bleed, however, appears to be a much more effective remedy.

3665

Compressor Interstage Bleed

As pointed out in paper I, stall of the compressor at low engine speeds is a result of insufficient flow through the front stages of the compressor. Interstage bleed is a basic approach to this low-speed stall problem, in that it tends to remove the cause of compressor stall. With interstage bleed, the flow through the front stages of the compressor is increased; midway through the compressor, the excess air is bled off through a system of bleed ports and dumped. This increase of flow through the front stages improves the matching of the front and rear halves of the compressor at low speeds and thus delays compressor stall in this speed range.

Effect on stall margin. - The improvements in stage matching obtained by use of interstage bleed in the J71-A-2 engine resulted in the improvement in stall margin shown in figure 7. The solid line, which shows the stall margin without bleed, is the same plot shown in figure 3. Four-percent interstage bleed resulted in the large improvement in stall margin shown by the dotted curve, in contrast to the 20-percent compressor-discharge bleed that is necessary to obtain any stall margin.

The bleed ports would be closed at about 80-percent speed, because no improvement in margin is obtained beyond that speed. These data show that interstage bleed is a very effective method of improving low-speed stall margin for engines that use high-pressure-ratio single-spool compressors.

Effect on blade vibration. - Interstage bleed should offer some relief for the blade-vibration problem. Although no blade-vibration data were taken on the J71-A-2 compressor, it should be noted that, for the standard compressor, rotating stall existed at all speeds below about 75-percent speed. When interstage bleed is used, stall

[redacted]

of the inlet stages is relieved, and the maximum speed at which rotating stall exists in the compressor is therefore reduced. Thus, interstage bleed may effectively eliminate critical blade vibrations caused by resonance with rotating stall at intermediate engine speeds.

Inlet-Guide-Vane Adjustment

Inlet-guide-vane adjustment is another method of improving compressor stall margin at low engine speeds. Adjustment of the inlet guide vanes alters the performance of the inlet stage of the compressor and, thus, delays stall of the front stages of the compressor at low speed. The effect of guide-vane adjustment on the performance of a typical inlet stage is shown in figure 8, which is a plot of stage pressure ratio against weight flow. The solid curve is for the guide vanes in the open position and the dashed curve is for the guide vanes in the closed position. The orientation of the guide vanes with the inlet flow direction for the opened and closed positions is shown at the right of figure 8. For the open position, the guide vane is set at a small angle with the inlet flow direction, which is indicated by the arrow. In the closed position, the guide vane is rotated about a radial line so as to make a much larger angle with the inlet flow, as shown at the bottom of this figure.

Comparison of the solid and dashed curves in figure 8 shows the effect of guide-vane positions on the stage performance characteristic. With the guide vanes in the closed position, the maximum flow through the stage is decreased, and the stall point of the stage is shifted to a much lower flow. This shift of stall point delays front-stage stall at low engine speeds and thus improves the stall margin in this speed range.

The following discussion is limited to the effects of inlet-guide-vane adjustment. The principle of vane adjustment can be carried further, as is done in the J79 engine, where several of the front stages have adjustable blade rows.

Effect on stall margin. - The effects of guide-vane adjustment have been investigated in several turbojet engines. Results of tests with the J71-A-2 engine are shown in figure 9, where stall margin is plotted as a function of engine speed. Closing the inlet guide vanes 20° increased the stall margin for the entire speed range shown, and made the engine fully operable in the mid-speed region. Although the stall margin is increased at top speed, it would be impractical to use inlet-guide-vane adjustment in this speed region because of the reduction in mass flow and, therefore, engine thrust. Obviously then, the blades must be opened at high engine speeds. Inlet-guide-vane adjustment, however, is an effective means of obtaining additional stall margin in the low-speed region and, thus, would be an aid to acceleration of the engine.

[redacted]

DECLASSIFIED

Effect on blade vibration. - Stall margin is plotted against engine speed for the J65-B-3 in figure 10. This engine has a reasonable stall margin over the entire speed range. The J65, however, has a serious blade-vibration problem, as discussed in paper II. This blade vibration is excited by rotating stall, which exists at speeds below the dip of the stall margin line (75 percent of rated speed). Variable inlet guide vanes were installed on a J65-B-3 to determine the effect of guide-vane positioning on rotating stall and, consequently, rotor blade vibration.

3665

The lower bar graph of figure 11 is a plot of vibratory stress against inlet-guide-vane position for the second stage at approximately 70 percent of rated speed. The 0° position was the standard position for the guide vanes. Opening the guide vanes 7° increased the blade stresses from ±38,000 to ±42,000 psi, because the strength of the rotating stall was increased. These vibrations were excited by a three-zone rotating stall. When the guide vanes were closed to 4°, the stresses were reduced to ±6000 psi. Closing the vanes did not eliminate the rotating stall, but changed the pattern from three zones to four zones. The relative stall frequency of the four-zone pattern was not in resonance with the second-stage rotor blades. Therefore, the stresses were appreciably reduced. Further closing of the guide vanes of this compressor had no effect on the second-stage rotor blade vibration.

The upper bar graph in figure 11 is a plot of the maximum speed for rotating stall against guide-vane position. When the compressor is operated at a speed below that indicated, it will operate with rotating stall. Opening the guide vanes increased this speed, closing 14° decreased the speed, and further closing again increased the maximum speed at which rotating stall was encountered. With the vanes in the open position, the compressor operated with a strong tip stall. As the vanes were closed 4°, the tip stall became less severe. Further closing of the guide vanes resulted in a rotating stall at the hub of the rotor, and this hub stall increased in severity with the degrees of closure.

Variable inlet guide vanes satisfactorily reduced the severe vibratory stresses in the second-stage rotor blade at 70-percent speed for the inlet conditions tested. The rotating stall, however, was not eliminated. Therefore, guide-vane adjustment cannot be considered as a cure for all blade-vibration problems of an engine.

Inlet Baffles

The inlet baffle is primarily a device for eliminating blade vibration excited by rotating stall. The principle of the inlet baffle is illustrated by the sketch in figure 12. This device reduces the compressor-inlet area by use of hinged flaps at the inner diameter of the compressor inlet. These flaps operate in a manner similar to the cowl

[redacted]

flaps on a radial reciprocating engine. When the baffle is extended, a separated-flow region exists behind the baffle. This separated region gradually dissipates back through the compressor, and effectively alters the flow area to more nearly match that required for low-speed operation. In addition, the baffle forces the air out towards the rotor tips and in so doing tends to eliminate the rotating-stall region that normally exists at the blade tips.

Effect on blade vibration. - The baffle was the only one of the remedies considered for the single-spool engine that eliminated the periodic nature of the stall in the front stages of the compressor. When the periodic rotating stall was eliminated, the blade-vibration problem was also eliminated.

Figure 13, a plot of vibratory stress against engine speed, presents the results of an investigation in which a J65-B-3 engine was operated with a baffle at the inner diameter of the compressor inlet. The solid curve presents the maximum vibratory stresses measured in the first and second stages when the engine was operated without the baffle. These stresses were excited by a three-zone stall pattern, as shown by the upper sketch. The dashed curve represents the stresses measured when the engine was operated with the baffle. The stresses were reduced to a minimum, because the periodic nature of the stall had been removed. With baffle, the compressor operated with a continuous stall region around the annulus, as shown by the lower sketch in figure 13.

Thus, the baffle, by eliminating the periodic nature of rotating stall, satisfactorily eliminates blade vibration. This baffle must, of course, be retracted at high engine speeds to avoid severe thrust penalties. Wright Aeronautical Corporation is currently installing an adjustable baffle, or flow modulator, on some of their production J65 engines.

Effect on stall margin. - Inasmuch as the separated-flow region behind the inlet baffle tends to alter the effective area ratio through the compressor to favor low-speed performance, it might be expected that the baffle would improve low-speed stall margin. To date, no stall-limit data have been obtained on an engine incorporating a retractable baffle. Compressor data, however, have been obtained on a version of the J71 compressor. These tests showed that the knee in the stall-limit line was virtually eliminated by use of the baffle, and the engine was made operable at all speeds. The stall margin estimated from the measured compressor stall limit and a computed engine operating line, however, indicated that the stall margin with the baffle was not adequate to permit satisfactory acceleration of this engine.

[redacted]

DECLASSIFIED

3665

Effect of Remedies on Engine Acceleration

The effectiveness of such compressor stall remedies as inlet-guide-vane adjustment and turbine-stator and exhaust-nozzle adjustment depends on the specific engine design. Guide-vane adjustment has proven to be very effective in improving the low-speed stall margins of the J71-A-2 and J73-GE-3 engines. Furthermore, remedies can be combined on a given engine; for example, the J71-A-2 engine that was used to obtain much of the data presented in this paper incorporated both interstage bleed and adjustable inlet guide vanes.

Figure 14 is a plot of time in seconds required for four representative engines to accelerate from 20 to 100 percent of rated thrust. For the J47D(RX3) with fixed nozzle area, the engine accelerated in approximately $6\frac{1}{2}$ seconds. When an adjustable exhaust nozzle was installed, this acceleration time was reduced to $3\frac{1}{4}$ seconds. The J34-36, which like the J47 is a relatively low-pressure-ratio engine, had approximately the same acceleration time as the J47D(RX3) with the adjustable nozzle.

As has been pointed out, the J73 and the J71 are relatively high-pressure-ratio engines and have serious part-speed compressor stall problems. Thus, they require some type of stall remedy to obtain satisfactory acceleration. These data indicate that the J73-GE-3 variable inlet guide vanes and the J71-A-2 with variable inlet guide vanes and interstage bleed have satisfactory acceleration characteristics. It should be noted that these data represent optimum acceleration times and do not include the normal allowance required by conventional control systems to account for such factors as production tolerances and performance deterioration with altitude and service life.

Design Compromises

The items discussed are concerned primarily with remedies for existing compressors. Early low-pressure-ratio compressors were designed to match the individual stages at design or rated rotative speed. As pressure ratio was increased, however, engines became plagued with low-speed stall problems. These stall limitations were in some cases so acute that acceleration of the engine to rated speed was impossible. In order to alleviate this situation, the stages were matched at less than rated speed. This tended to improve the stall problem at low speed at the expense of high-speed stall margin. It has been demonstrated, however, that variable-geometry features that provide adequate stall margin at low engine speeds are available. It has also been shown that, when inlet flow distortions are encountered, large stall margins are required at high engine speeds. Therefore, at this time compressors could be designed for

optimum high-speed operation, and variable-geometry features such as guide-vane adjustment or interstage bleed could be used to facilitate engine acceleration. It should be noted that such stage-matching compromises should be effective for applications up to a flight Mach number of about 1.5. For higher flight Mach numbers, this problem must be re-evaluated.

TWO-SPOOL ENGINES

Experience on the two-spool engine has been limited to tests of the J57 and analyses of similar hypothetical engines. To understand the detailed effects of remedies for the two-spool engine requires a study of the change of performance of each of the individual components. Inasmuch as the interactions between the two compressors and two turbines operating in series are extremely complex, the discussion of this type engine will only consider the present state of knowledge in regard to solution of the compressor stall problems.

Definition of Problem

As shown on the composite compressor performance map (fig. 15), the steady-state operating line for the two-spool engine lies between the inner- and the outer-compressor stall limits (paper I). As indicated here for uniform inlet flow distributions, stall of the outer compressor is expected at low engine speed, and stall of the inner compressor is expected at high engine speeds. This is analogous to the single-spool engine, which exhibits front-stage stall at low speed and rear-stage stall at high engine speeds. It should also be noted that both compressors will move towards their stall limits during rapid accelerations. The variable-geometry features to be considered in the succeeding discussion are indicated in the sketch at the top of figure 15.

The high-speed stall limits of the J57-P-1 can best be illustrated by examining the altitude limits of this engine, which are plotted in figure 16 as altitude against inner-compressor rotative speed. These limits were discussed in paper IV. For uniform or undistorted inlet flow distribution, the upper limit of operational speed of the engine is determined by turbine temperature for altitudes up to about 50,000 feet. Above this altitude, the upper limit of operation is the inner-compressor stall limit. The lower limit of operational speed is the outer-compressor stall limit at all altitudes.

When a circumferential inlet distortion was imposed, where $\Delta P/P$ was about 22 percent, the limits of operational speed were reduced as shown in figure 16. For operations with inlet flow distortion, both the upper and lower limits of operable speed were a result of compressor stall.

It may be surmised that the inner-compressor stall limit has been shifted to a lower speed and the outer-compressor stall limit shifted to a higher speed as a result of flow distortion. If, however, the outer compressor is more susceptible to flow distortions than the inner compressor, the high-speed limit may be due to outer-compressor stall. Inasmuch as the effects of stall are measured simultaneously throughout the entire engine, it is impossible to determine which compressor instigated stall on the basis of the transient measurements that were taken. Therefore, in the discussion of high-speed stall problems for the two-spool engine, both inner- and outer-compressor stall are considered.

3665

Outer-Compressor Stall at Low Engine Speeds

Interspool bleed on the two-spool engine, which is analogous to interstage bleed on the single-spool engine, is an effective means of avoiding outer-compressor stall at low engine speeds. The J57-P-1 engine incorporates interspool bleed, and the effect on outer- and inner-compressor stall margin is shown in figure 17, where compressor pressure ratio is plotted against percent rotative speed for the two compressors. The solid lines represent the compressor stall limits; and the dotted lines, the steady-state operating lines for operation with the bleed ports closed. For operation with about 10-percent interspool bleed, the operating line is indicated by the dot-dashed line. As can be seen from figure 17, interspool bleed shifts the operating line of the outer compressor downward and, thus, appreciably improves the stall margin of the outer compressor. The stall margin of the inner compressor is only slightly altered. These data show that interspool bleed is an effective method of improving the stall margin of the outer compressor to aid engine acceleration.

Inner-Compressor Stall at High Engine Speeds

It has been shown that high-speed or rear-stage stall of the single-spool engine can be alleviated by a combination of turbine-stator and exhaust-nozzle-area changes. Analysis has indicated that inner-compressor stall of the two-spool engine can be effectively handled by these same geometry changes. In this analysis, the outer-compressor operating condition was held constant and the pressure ratio of the inner compressor reduced to increase the stall margin of the inner compressor. In order to maintain turbine-inlet temperature when the pressure ratio was reduced, it was necessary to reset the stators of both turbines and to adjust the exhaust-nozzle area. These changes have the same effect on the performance of the two-spool engine as on the single-spool engine. The specific fuel consumption is increased, but the thrust is not appreciably reduced. Of course, as in the single-spool engine, the allowable magnitude of such changes will be limited, because radical changes will result in large losses in component efficiency and will adversely affect combustor performance.

[redacted]

Outer-Compressor Stall at High Engine Speeds Due to Inlet Distortions

As discussed previously, outer-compressor stall may occur at high engine speeds as a result of inlet flow distortions. Although this problem is not completely understood, analysis to date has indicated that any attempt to increase the stall margin of the outer compressor without compressor design changes will result in an appreciable reduction in engine thrust.

When the inner compressor of a two-spool engine is operated at a constant speed, the inlet volume flow to this compressor must remain essentially constant. The flow capacity of the inner compressor might be increased by overspeeding of this unit, but this may result in a serious turbine stress problem. Therefore, if the pressure ratio of the outer compressor is reduced to improve stall margin, the weight flow through the engine must also be reduced in order to maintain constant volume flow at the inlet of the inner compressor. A reduction in weight flow, of course, results in a thrust penalty. In order to reduce both the flow and pressure ratio of the outer compressor, the speed of this unit must be reduced. As the speed of a compressor is reduced, the pressure ratio obtainable before stall occurs is also reduced. Therefore, the benefits obtained in stall margin, as a result of turbine and exhaust-nozzle-area changes, will depend on the shape of the stall-limit line of the outer compressor. Very large changes of speed and thrust may be required to avoid outer-compressor stall when serious inlet flow distortions are encountered. Thus, it appears that increases in stall margin of the outer compressor without sacrifices in engine thrust will require compressor design modifications.

CONCLUDING REMARKS

The study of stall remedies for single-spool engines indicated that the stall margin on this type engine can be improved and blade vibration due to rotating stall can be virtually eliminated. A combination of turbine-stator and exhaust-nozzle-area changes can be used to alleviate compressor stall problems at high engine speeds. These can be fixed changes and need not be adjustable features. Within limits, this remedy has little effect on engine thrust, but it does increase fuel consumption somewhat. Interstage bleed and adjustable inlet guide vanes have proven to be effective remedies for compressor stall problems at low engine speeds. A retractable inlet baffle is an effective means of eliminating compressor blade vibrations induced by rotating stall.

For the two-spool engine, intercompressor bleed appears to be an effective means of avoiding low-speed stall of the outer compressor during engine acceleration. Remedies for a high-speed stall of the inner compressor have not been proved by

[redacted]

test, but calculations indicate that this problem can be solved by the use of turbine-stator and exhaust-nozzle changes. These changes should have little effect on thrust but probably will increase fuel consumption. Analysis to date has shown no effective remedy for an outer-compressor stall problem at high engine speeds without a severe thrust derating of the engine. At present, the only satisfactory solution to this problem appears to be a modification of the compressor to provide sufficient stall margin to cope with inlet distortions.

[redacted]

OPERATING AND STALL LINES FOR TWO HIGH-PRESSURE-RATIO TURBOJET ENGINES

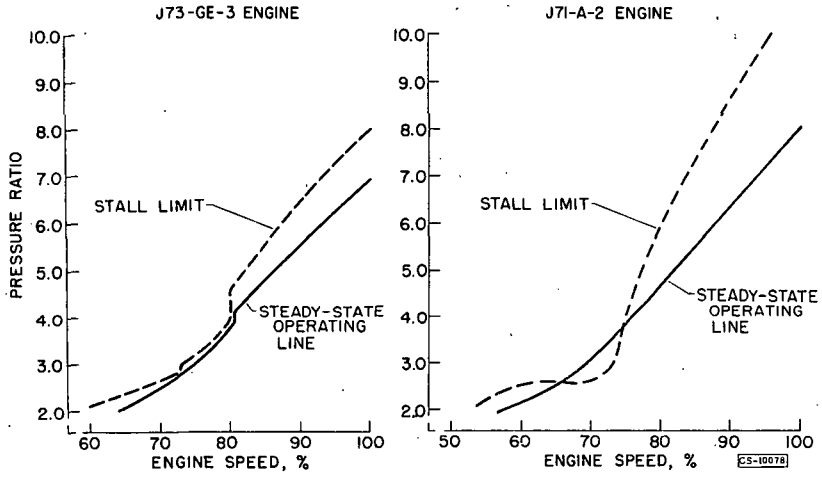

Figure 1.

EFFECT OF INLET FLOW DISTORTION ON STALL MARGIN

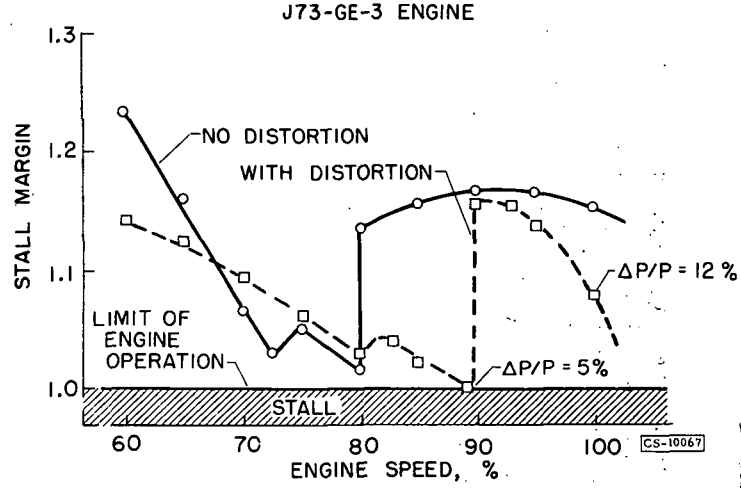

Figure 2.

EFFECT OF EXHAUST-NOZZLE-AREA CHANGES ON COMPRESSOR STALL MARGIN

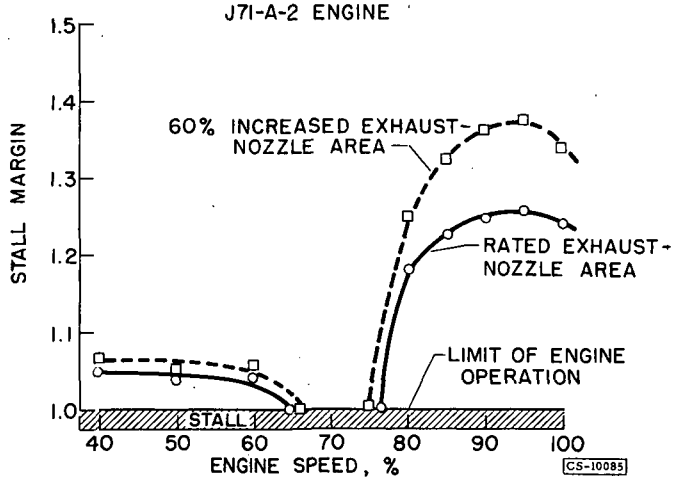

Figure 3.

EFFECT OF EXHAUST-NOZZLE AREA ON TURBINE-INLET TEMPERATURE AND THRUST

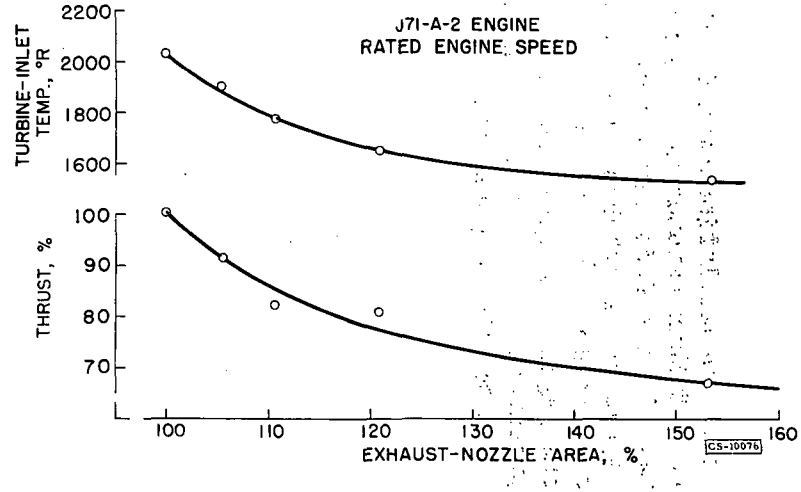

Figure 4.

EFFECT OF TURBINE NOZZLE AREA ON THRUST AND FUEL CONSUMPTION

J40-WE-6 ENGINE
RATED TURBINE-INLET TEMPERATURE
RATED ENGINE SPEED

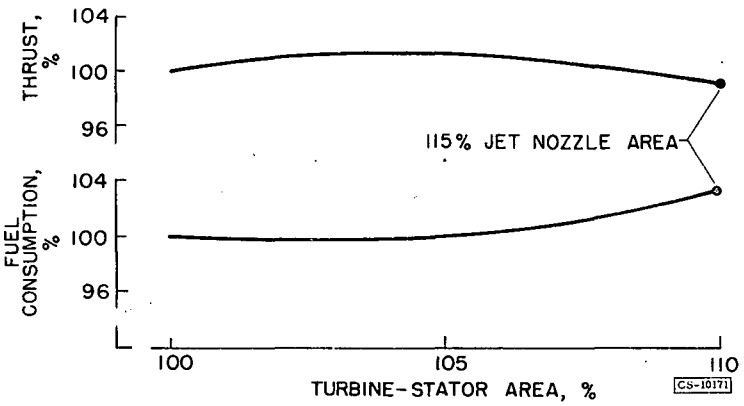

Figure 5.

EFFECT OF INCREASING TURBINE-STATOR AREA ON STALL MARGIN

J40-WE-6 ENGINE

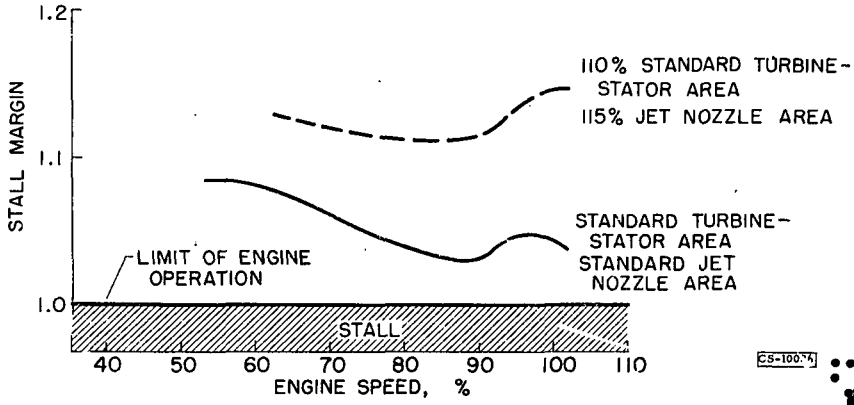

Figure 6.

EFFECT OF COMPRESSOR INTERSTAGE BLEED ON STALL MARGIN

J71-A-2 ENGINE

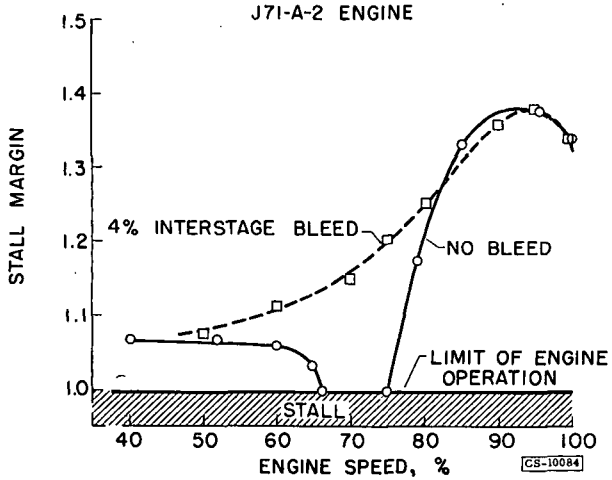

Figure 7.

EFFECT OF GUIDE VANE POSITION ON FIRST STAGE PERFORMANCE

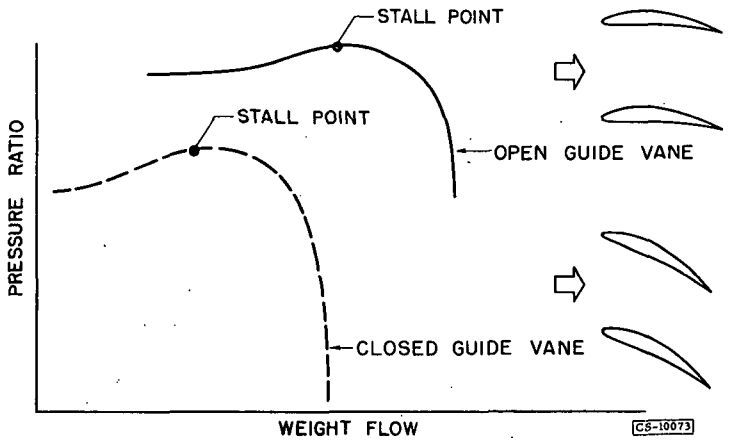

Figure 8.

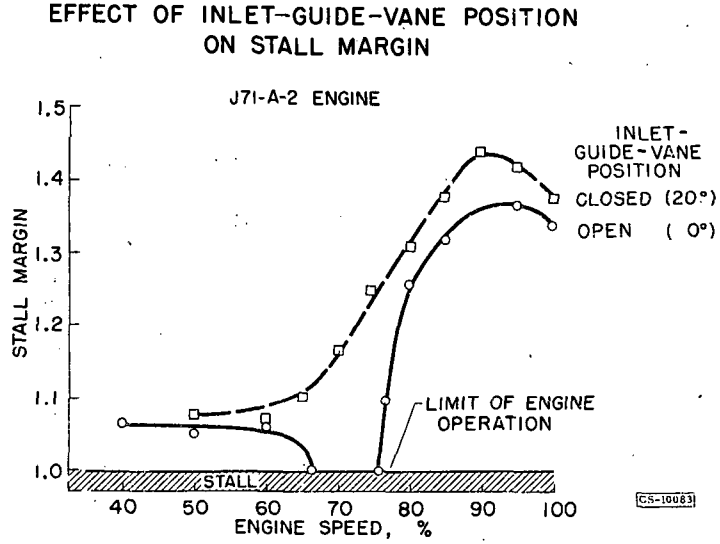

Figure 9.

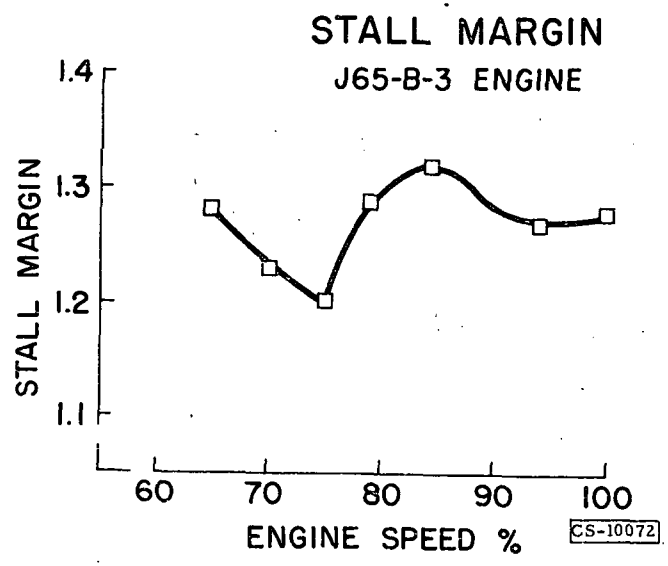

Figure 10.

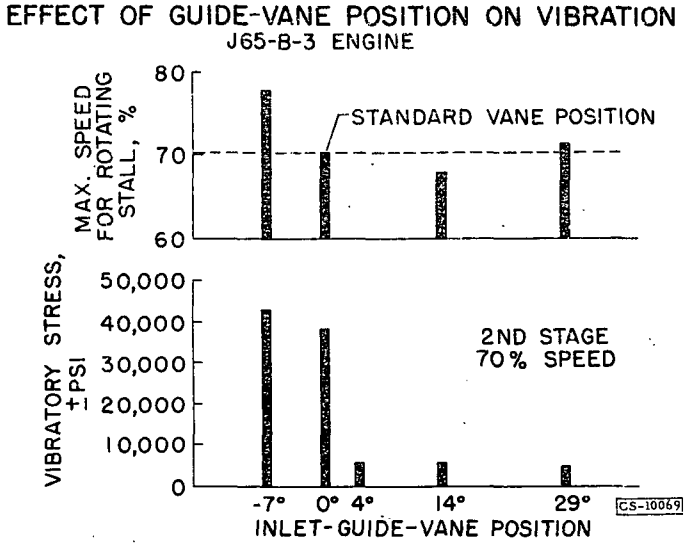

Figure 11.

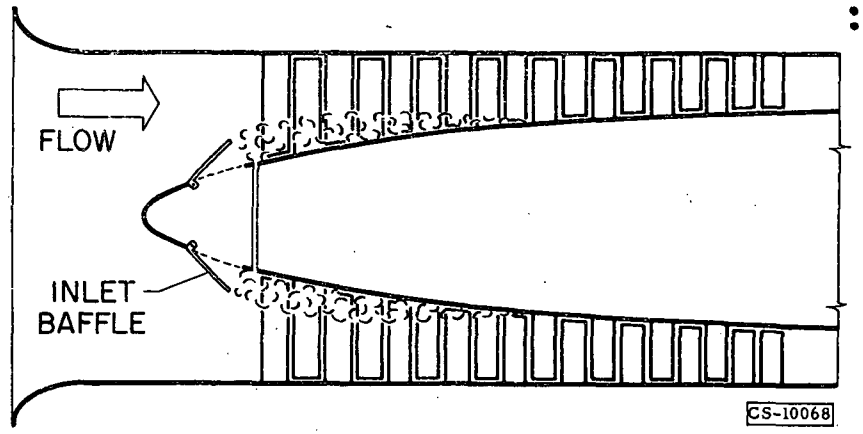

Figure 12.

EFFECT OF INLET-AIR BAFFLE ON BLADE VIBRATORY STRESS
J65-B-3 ENGINE

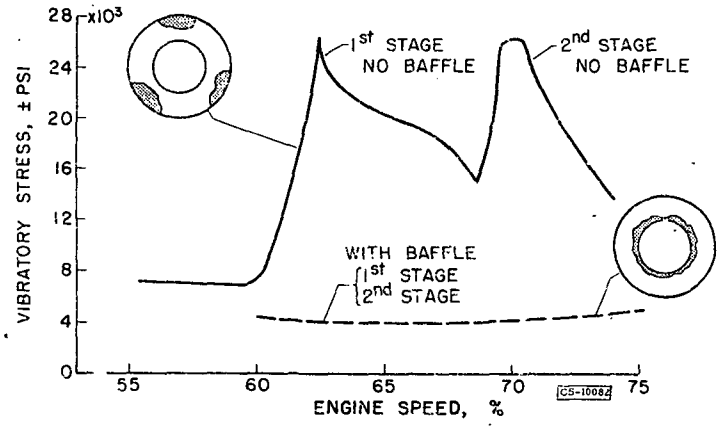

Figure 13.

REPRESENTATIVE ACCELERATION TIMES FOR VARIOUS ENGINES

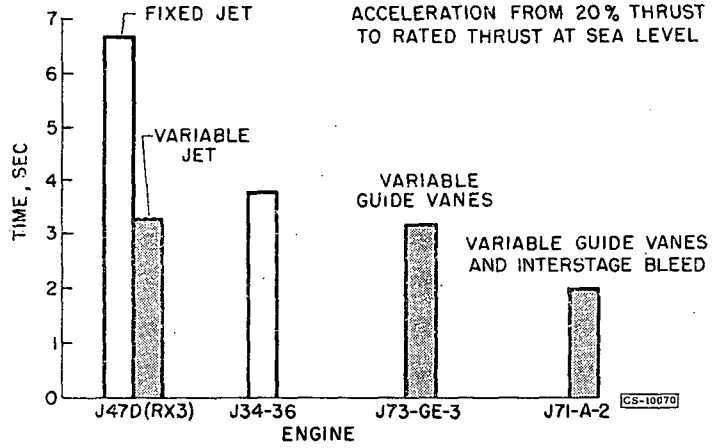

Figure 14.

TWO SPOOL ENGINE MODIFICATIONS

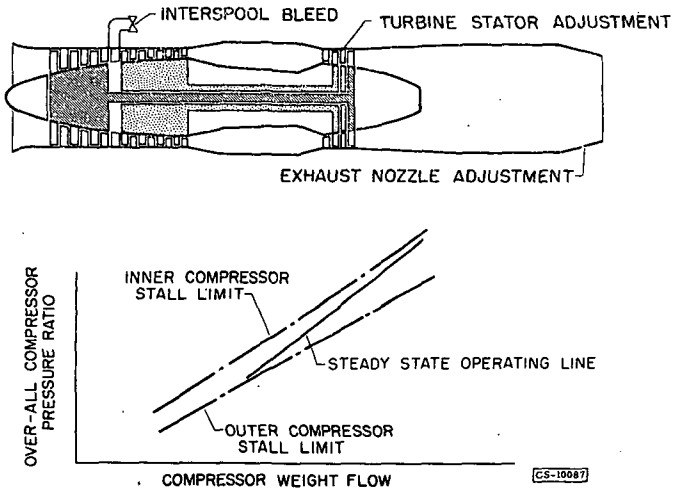

Figure 15.

EFFECT OF DISTORTION ON ALTITUDE OPERATING LIMITS
J57-P-1 ENGINE

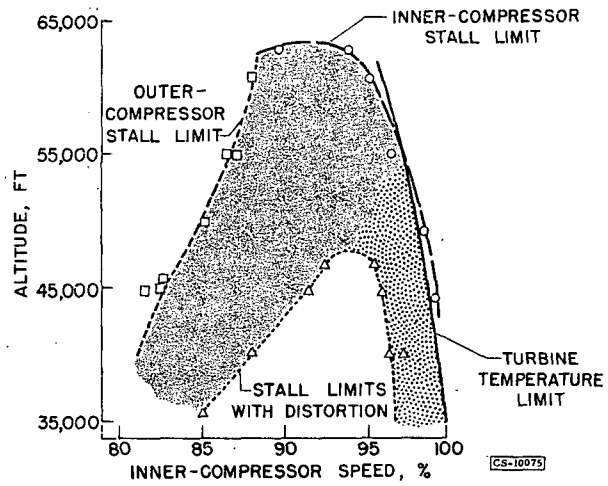

Figure 16.

EFFECT OF INTERSPOOL BLEED ON STALL MARGIN
FOR TWO-SPOOL J57-P-1 ENGINE

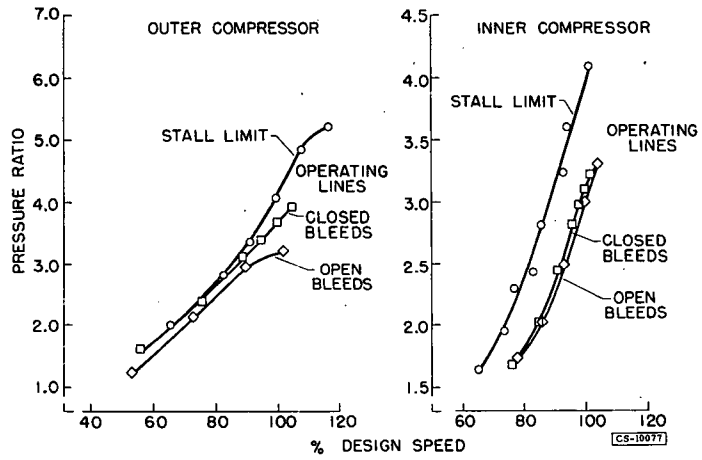

Figure 17.

DECLASSIFIED

3665

VI - STALL AND FLAME-OUT RESULTING FROM FIRING OF ARMAMENT

J. H. Childs, Chairman

F. D. Kochendorfer

R. J. Lubick

R. Friedman

DECLASSIFIED

VI - STALL AND FLAME-OUT RESULTING FROM FIRING OF ARMAMENT

INTRODUCTION

Compressor stall and flame-out in turbojet engines have occurred on numerous occasions when rocket missiles and cannon were fired at high altitudes. The U.S. Air Force has reported stall and flame-out in the F-86 and the F-94C, and the U.S. Navy in the Cutlass and the Fury. In addition, the British have encountered this problem in their Swift and Hunter airplanes. Obviously, then, the problem is rather general in nature and is not one that is peculiar to any one aircraft or to any one engine.

3665

One factor that obviously contributes to these engine difficulties is the ingestion of rocket and cannon shell exhaust gases into the engines. The extent to which rocket exhaust can enter the engine air intakes is illustrated in figure 1, which shows a photograph of an F-94C aircraft approximately 0.7 second after firing rockets. The exhaust smoke and vapor trails from the rockets envelop a large part of the airplane. Appreciable quantities of rocket exhaust can enter the air intakes.

The following things happen at the engine inlet during the firing of armament:

(1) Increased inlet temperature

(2) Changed inlet pressure

(3) Distortions in inlet pressure and temperature profiles

(4) Entry of combustibles into engine

(5) Reduced oxygen content in gases entering engine

The object of this paper is to examine each of these things that occur when armament is fired and to show by analysis and by experimental data which of these items are important and how each affects engine performance. An attempt is made to deduce the causes of the compressor stall and flame-out that have been encountered in flight. Finally, some remedial measures are suggested.

EFFECTS AT ENGINE INLET

Rocket Firing

Analysis. - The magnitude of the temperature and pressure effects at the engine inlet cannot be obtained directly from existing data. Several sets of data on jet spreading and mixing must be considered together.

[redacted]

For the case of the 2.75-inch air-to-air rocket (fig. 2), the combustion-chamber pressure is 1100 pounds per square inch and the temperature is 4500° R. The design exit Mach number is 2.7 and the exit static pressure is 42 pounds per square inch. Since this pressure is considerably above ambient pressure at altitude, the jet will expand greatly upon leaving the nozzle. The amount of initial expansion can be obtained directly from existing data (ref. 1), but the amount of mixing farther downstream cannot. Experimental data on jet mixing are presented in reference 2. These mixing data were obtained with low velocities for both the jet and the stream; in addition, the two streams had equal temperatures and static pressures. These conditions are in marked contrast to the high velocities and the temperature and pressure differences noted for the rocket. Nevertheless, an estimate of rocket jet spreading can be obtained by adding the results of reference 2 to the supersonic expansion, as indicated by the diagram in figure 2.

Results of a typical calculation are shown in figure 3. The stream Mach number relative to the launching station is taken to be 0.9 and the altitude 45,000 feet. The coordinates are distance from launching station and distance from rocket center line. At the time shown (about 0.3 sec after firing), the rocket is 60 feet from the launcher and is moving away at a speed of 400 feet per second. Contours of temperature are shown for the exhaust from a single rocket; these temperatures are expressed as the difference between the temperature at various locations and the ambient temperature.

If the position of the inlet relative to the launcher is known, temperature increments at the engine inlet can be estimated. For example, consider an inlet 1 foot in diameter whose center line is spaced 1.5 feet from that of the rocket. If the inlet is in the plane of the launcher, the average temperature of the entering stream would be about 200° F above ambient. The temperature increment will vary from 260° F at the inner face to 140° F at the outer, as indicated by the inset in figure 3.

If the calculations represented in figure 3 are repeated for other times after firing, the temperature profiles at any station can be obtained as a function of time. Temperature variations at the launcher station are shown in figure 4. Variations in total pressure are also shown in figure 4, and these pressures are expressed as the difference between the local pressure and the free-stream total pressure divided by the free-stream total pressure. For the example cited of an inlet 1 foot in diameter and located 1.5 feet from the rocket center line, a maximum temperature increase of 400° F is reached at the inner face of the inlet 0.15 second after firing. At this time, there is a variation in temperature across the inlet of 400°. A maximum total-pressure increase of 25 percent above free-stream pressure is experienced at a slightly later time after firing, 0.22 second. At this time, the total-pressure variation across the inlet is 25 percent. Figure 4 also shows the duration

of these increases. A temperature increase of 200° at the inner face, for example, will be reached at 0.09 second and will persist until 0.32 second after firing.

Experiment. - The only available experimental data showing the magnitude of increase in inlet temperature when firing rockets were obtained by Lockheed for the F-94C fighter firing a charge of 24 rockets during a 0.15-second time interval. Figure 5 shows the relative position of the rockets and the engine-inlet ducts in the F-94C. The rocket cluster is located in the nose section, while the fuselage scoop-type air inlets are located just rearward. Because of this positioning, it can be expected that more rocket exhaust will be diverted into the inlet duct and higher temperatures will result than for the sample inlet indicated in figures 3 and 4.

The actual temperature rise measured by Lockheed (ref. 3) is presented in figure 6, which shows the variation in temperature measured at the engine inlet as a function of time elapsed after firing the rockets. Three curves represent the minimum, average, and maximum temperature rise where peak temperatures are approximately 300°, 600°, and 900° F, respectively. One reason for the wide variation in temperature rise lies in the large difference in burning characteristics of the individual rockets. Ignition lag may vary from 0.025 to 0.035 second and total burning time from 1.4 to 2.0 seconds. For a burst of 24 rockets, these variations can result in a large range of possible temperatures in the wake of the rockets.

The approximate time during which these hot gases pass into the engine (fig. 6) agrees quite well with the calculations presented earlier. The hot gases start to pass into the engine about 0.1 second after the beginning of rocket firing and continue to enter the engine until about 0.4 second after the beginning of firing. The values of temperature increase are higher than would be predicted from figure 4, because a large number of rockets were fired and because the nose section tends to divert the exhaust gases into the inlets.

Cannon Firing

The effects of cannon fire are different in certain respects from those for rockets. Figure 7 shows an aircraft in the process of firing cannon. As the muzzle gases move out ahead of the inlet, they mix with the incoming air and the inlet temperature is increased. In certain cases, the gun chambers are vented into the inlet; this permits a considerable blast of hot gases directly into the engine. An additional factor is muzzle flash, a sudden burning or explosion of the gases ahead of the guns. If this occurs, the hot gases can expand ahead of the aircraft and enter the engine at greater than normal rates.

[redacted]

In addition to the temperature effects, cannon firing can alter inlet pressures. Pressure effects should be in a direction opposite to those noted for rockets, because the momentum of the muzzle gases opposes that of the incoming air. Mixing effects are even more difficult to evaluate than those for the rocket. However, it has been estimated that, at a Mach number of 0.9 and an altitude of 45,000 feet, firing four 20-millimeter guns at the rate of 1500 rounds per minute could reduce inlet pressures by as much as 9 percent if the guns were located close beside the inlet.

EFFECTS ON COMPRESSOR

Analysis

Increased inlet temperature. - Figure 8 is a compressor operating map for the J47D(RX1) single-spool axial-flow turbojet engine. The map shows the variation of compressor pressure ratio with corrected air flow for lines of constant corrected engine speed. Also shown are the steady-state operating line and the stall line for no inlet flow distortion. Calculations of the point of compressor operation have been made for an increase in inlet temperature. The initial point of operation (point A) was taken at rated mechanical engine speed at an altitude of 45,000 feet and a flight Mach number of 0.9. For these calculations, fuel flow and engine speed were assumed to remain constant while the inlet temperature increased. This is a valid assumption, since, during the short time (approximately 0.3 sec for an actual rocket-firing case), the engine control would not have time to adjust fuel flow nor would engine speed have time to change.

To completely analyze compressor operation during an inlet-temperature increase would necessitate calculating the history of the compressor operating point as the armament gases pass through the engine. However, with only the operating map for the complete compressor, this calculation is not possible. The discussion must therefore be limited to the operating point that is reached after the armament gases reach the turbine station (point B, fig. 8). The location of point B depends on two factors: (1) The compressor equivalent speed $N/\sqrt{\theta}$ must be corrected for the increased value of θ; and (2) the reduced equivalent speed produces a reduced air-flow rate, and, since fuel flow remains constant during the short time involved, the turbine-inlet temperature rises. Point B is therefore located on a line of lower equivalent speed and is shifted upward from the steady-state operating line.

Since the path followed in the transient from points A to B cannot be calculated, the dashed curve in figure 8 serves only as an indication of one possible path. The obvious question as to what happens if the path enters the stall region cannot be answered at present. Since time

is required for stall to set in, it is possible that some stages of the compressor could momentarily operate above their steady-state stall limit. On the other hand, if the path crosses the stall-limit line and stall does occur, then operation at point B will not be realized.

Compressor operating points calculated by this procedure for several values of inlet-temperature increase for the J47D(RX1) engine are presented in figure 9. A 300° increase results in an operating point just at the stall line. For this particular compressor, an inlet-temperature increase of slightly over 300° F would certainly cause compressor stall.

Changed inlet pressure. - If a pressure change accompanies the temperature change, the stall tendency can be affected. Three paths between points A and B are shown in figure 10. Assume that the center path would be followed for a temperature change alone. Now, if the inlet pressure is reduced as a result of cannon fire, the reduction in compressor-inlet pressure effectively increases the compressor pressure ratio. The path will therefore be shifted upward toward the stall limit. The amount of shift will, of course, depend on the magnitude and duration of both the temperature and pressure change. The pressure effects of cannon fire should, in general, increase the probability of stall.

For rockets, the inlet pressure is increased and the compressor pressure ratio is momentarily decreased. This moves the path downward away from stall.

Inlet flow distortions. - As shown in the jet-spreading analysis, both temperature gradients and pressure distortions may be expected after armament firing. Pressure distortions effectively lower the stall limit, as was discussed in the fourth paper. Temperature distortions may also have a similar effect. The reduction in stall margin due to these changes is indicated in figure 11. In many instances, armament firing takes place while the aircraft is at high angle of attack. The inlet flow distortions caused by angle of attack also affect the stall margin as indicated in figure 11.

Combustibles in compressor. - Numerous instances of afterburning from rockets and muzzle flash from guns serve to show that the armament gases can undergo further burning. If burning occurs while these gases are in the compressor, then the pressure will rise where the burning takes place. This means that the pressure ratio across the compressor stages upstream of this location will be greatly increased. The resultant effect cannot be shown on the compressor map, but the probability of encountering stall is increased.

Experiment

Lockheed (ref. 3) reports that a 300° increase in inlet temperature is the critical value in the F-94C, which uses a J48 engine. They state

that a temperature increase of less than 300° can be tolerated, while a temperature increase in excess of this value causes engine difficulties. These temperature effects were probably accompanied by inlet flow distortion and pressure changes; consequently, the 300° value is probably unique for the F-94C configuration.

Experimental data showing the effect of an increase in inlet temperature on the J57-P-1 engine are presented in figure 12. Conditions for which surge did not occur are denoted by open circles, and surge conditions are indicated by solid points. These data were obtained in the NACA Lewis altitude wind tunnel by deflecting hot air into the engine inlet. A time interval of 1 to 2 seconds was required for the complete temperature rise to be felt at the compressor inlet during these tests; consequently, these data are not strictly analogous to the more rapid temperature increase accompanying armament firing.

3665

Figure 12 shows that, for engine speeds above 5000 rpm, surge was produced by inlet temperature increases of 70° F or more. At engine speeds below 5000 rpm, where the intercompressor bleeds are opened to improve the stall margin, surge was not encountered with temperature increases as high as 230°.

EFFECTS ON COMBUSTOR

Before considering the effects of armament on the combustor, the factors that affect combustor performance will be reviewed briefly. A combustor performance map is shown in figure 13. Combustion efficiency is plotted as a function of the combustion parameter $\alpha \frac{P_3 T_3}{V_r} \Phi(\alpha)$, where α is the oxygen concentration in the inlet gases, P_3 and T_3 are the total pressure and temperature at the combustor inlet, V_r is the combustor reference velocity and is equal to the inlet volume flow rate divided by the maximum cross-sectional area of the combustor, and $\Phi(\alpha)$ is an exponential function that depends primarily on the oxygen concentration. The combustion parameter was derived from theory by assuming that chemical reaction kinetics control the rate of burning in the combustor (refs. 4 and 5). For most combustors, a reasonable correlation of data can be obtained with the parameter.

A typical family of experimental curves is shown in figure 13 for several fuel-air ratios. For lower values of the combustion parameter,

efficiency decreases sharply. The solid points at the ends of the curves denote flame-out. The value of the combustion parameter at which flame-out occurs is a function of fuel-air ratio, as shown in figure 14. Each of the solid points indicates an experimental flame-out for the J47-GE-25 combustor. Since flame-outs are not exactly reproducible, a shaded band is used to indicate the flame-out region. Above this band, combustion is stable; below, no burning is possible.

To facilitate estimation of flame-out margin for the J47-GE-25 combustor, operating points are indicated at several altitudes. These points correspond to rated engine speed and a flight Mach number of 0.9. This combustor obviously has ample steady-state flame-out limits.

The J47-GE-25 combustor operating may can now be used to analyze the effect of armament firing on combustor performance in a hypothetical turbojet engine that uses the J47-GE-25 combustor and the J47D(RX1) compressor. Consider an initial operating point at an altitude of 45,000 feet, rated mechanical speed, and a flight Mach number of 0.9; this is point A on the J47-GE-25 combustor map (fig. 15). If the armament firing causes a 300° F increase in compressor-inlet temperature, then the combustor operating conditions become those of point B (fig. 15). The location of point B depends on both the change in inlet temperature and gas composition and the change in compressor operating point. On the compressor map (fig. 9), it was shown that a 300° F increase in compressor-inlet temperature causes a marked decrease in both compressor pressure ratio and mass-flow rate. The decreases in oxygen content and in combustor-inlet pressure adversely affect the combustor; however, these effects are largely offset by the increase in inlet temperature and the decrease in air-flow rate. Thus, the change in the combustion parameter between points A and B is slight. However, the fuel-air ratio increases considerably from point A to point B, since fuel flow remains constant and air flow decreases. For the J47 combustor map illustrated in figure 15, point B lies in the stable burning region, and flame-out does not occur.

As indicated by figure 9, the operating point corresponding to a 300° F increase in inlet temperature lies just underneath the J47D(RX1) compressor stall line. If the compressor stalls at this condition, then the combustor operating point changes to the values indicated by the two points labeled C in figure 15. The upper point corresponds to the highest and the lower point to the lowest of the oscillating pressure that have been measured in a J47 engine operating in a stalled condition at this particular value of equivalent speed (ref. 6). Since these operating points for the combustor during stall lie outside the stable burning region, combustor flame-out will follow the occurrence of compressor stall.

The foregoing discussion does not mean that in all engines compressor stall must precede combustor flame-out. Obviously, if this same sequence of events took place in some engine for which the combustor did

not have as wide a fuel-air ratio range for stable operation as does the J47 combustor, then combustor flame-out could occur at point B, because the fuel-air ratio would be too high even though the compressor did not stall.

The possibility of the entry of some combustible material into the engine due to incomplete combustion in the armament exhaust gases has been mentioned. If these materials pass through the compressor without burning and then burn in the combustor, their effect is shown in figure 16.

For a combustion efficiency in the armament gases of 85 percent, and the remaining 15 percent of their chemical heat release assumed to occur in the combustor, point B would be moved over to the location indicated by point D. The effect is quite small.

EFFECT ON SUPERSONIC AIRCRAFT

At supersonic speeds, an additional component, the air inlet, must be considered. If reduced air flow accompanies the temperature increase, a supersonic inlet can be forced into its subcritical operating range, and the inlet then becomes an additional source for pressure and flow pulsations. The effects of firing rocket exhaust into an inlet-engine combination operating at a Mach number of 1.9 have been briefly investigated in the NACA Lewis 8- by 6-foot supersonic wind tunnel. Although quantitative data are not as yet available, it is known that large pressure fluctuations existed at both the compressor inlet and outlet stations. Because of compressor surge or inlet instability, a quasi-steady operating condition was never reached.

REMEDIAL MEASURES

Possible remedial measures are as follows:

Transient adjustments	Close inlet guide vanes Open compressor bleeds Reduce fuel flow Inject water at compressor inlet Open engine exhaust nozzle
Avoid intake of exhaust gases	Move armament away from inlet Vent gun chambers away from inlet Deflect muzzle gas away from inlet

The first course of action is the use of transient adjustments, such as closing the inlet guide vanes, opening the compressor bleeds, reducing fuel flow, and injecting water at the compressor inlet. These are all

measures that can be put into action an instant before armament is fired and maintained during the critical period. It should be remembered that the length of time the hot gases are passing into the engine is approximately 0.3 second, so that the use of these adjustments may be limited by the speed of actuation. Unfortunately, all these items (except water injection) also appreciably decrease the engine thrust level, and this effect on performance must be considered. Lockheed has had success with reducing fuel flow during rocket firing on the F-94C.

The compressor operating margin between the steady-state line and the stall limit decreases as altitude is increased. The gains resulting from design changes to increase this stall margin will be largely taken up by future increases in flight altitude. In addition, angle-of-attack operation decreases the stall margin, and the size and firing rate of armament are being steadily increased. From these considerations it would appear that the use of transient adjustments to increase the stall margin may prove to be only a temporary solution to the problem of armament firing.

The best course of action, and the most obvious, is to completely avoid the intake of exhaust gases. Moving the armament, venting the gun chambers, and deflecting muzzle gas away from the inlet are all possible solutions. North American has greatly alleviated their problem for the F-86F by installing blast deflectors on the nose-mounted cannon. It is noteworthy that the Northrup F-89, which has wing-tip mounted rocket pods, has encountered no engine problems due to rocket firing.

CONCLUSIONS

The increased compressor-inlet temperature during armament firing is probably the most important single factor affecting engine performance. This increased temperature is sufficient by itself to account for the observed occurrences of compressor stall and flame-out.

The effects of the changed compressor-inlet pressure, the inlet flow distortions, and the combustibles in the compressor are, for the most part, of such nature as to increase the likelihood of compressor stall beyond that for an inlet-temperature increase alone.

If the combustible materials entering the engine inlet do not burn until they reach the combustor, then their effect will be very small. Also, the reduction in oxygen concentration is not sufficient to affect combustor performance appreciably.

The principal change that the combustor feels during armament firing is the greatly increased fuel-air ratio due to the reduced compressor air flow. In some engines, this increase in fuel-air ratio may be enough to cause a flame-out before compressor stall occurs. However, for the particular engine analyzed here, the J47, it appears that compressor stall precedes flame-out.

[redacted]

Measures to help alleviate these engine difficulties during armament firing include all the features of variable engine geometry that increase the margin between the compressor operating point and the stall limit. A reduction in fuel flow during armament firing will decrease the likelihood of compressor stall and should also prevent combustor flame-out as long as stall does not occur. However, the best solution to the problem is to move the armament away from the engine inlets so that the hot gases never enter the engine.

REFERENCES

1. Love, Eugene S., and Grigsby, Carl E.: Some Studies of Axisymmetric Free Jets Exhausting from Sonic and Supersonic Nozzles into Still Air and into Supersonic Streams. NACA RM

2. Forstall, Walton, Jr., and Shapiro, Ascher H.: Momentum and Mass Transfer in Coaxial Gas Jets. Meteor Rep. No. 39, Dept. Mech. Eng., M.I.T., July 1949. (Bur. Ord. Contract NOrd 9661.)

3. Anon.: Engine Performance During Rocket Firing at High Altitude with the F-94C Starfire. Rep. PN/459808, Lockheed Aircraft Corp.

4. Childs, J. Howard: Preliminary Correlation of Efficiency of Aircraft Gas-Turbine Combustors for Different Operating Conditions. NACA RM E50F15, 1950.

5. Graves, Charles C.: Effect of Oxygen Concentration of the Inlet Oxygen-Nitrogen Mixture on the Combustion Efficiency of a Single J33 Turbojet Combustor. NACA RM E52F13, 1952.

6. Delio, G. J., and Stiglic, P. M.: Experimental Investigation of Control Signals and the Nature of Stall and Surge Behavior in a Turbojet Engine. NACA RM E54I15, 1954.

[redacted]

Figure 1.

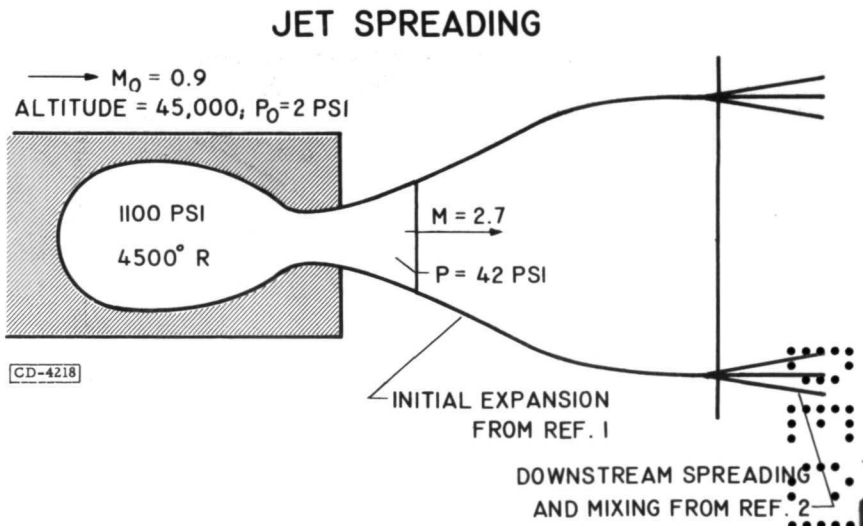

Figure 2.

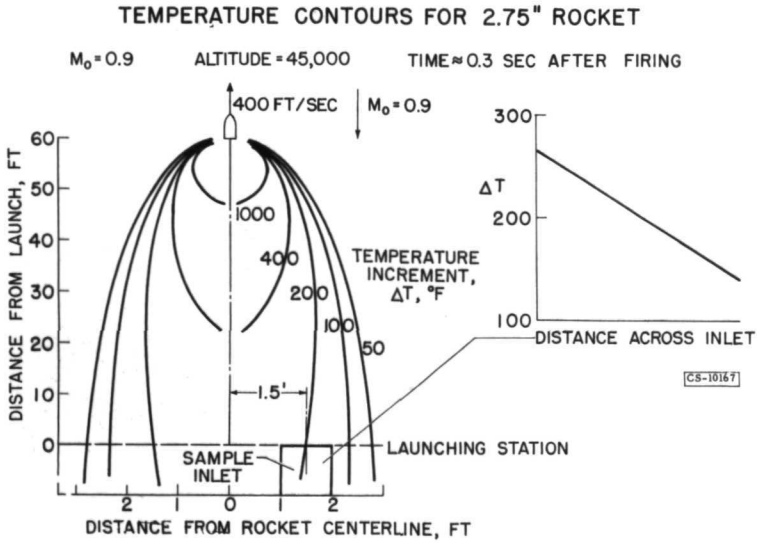

Figure 3.

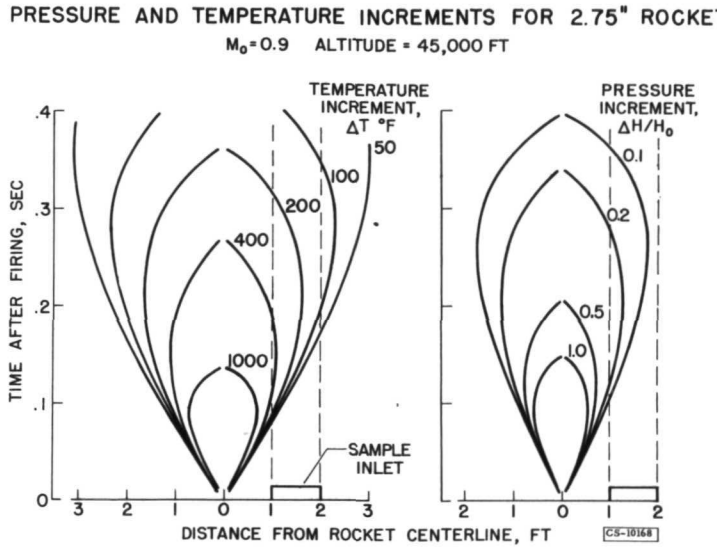

Figure 4.

ROCKET INSTALLATION FOR F-94C

Figure 5.

INLET TEMPERATURES FOR F-94C AFTER FIRING ROCKETS
(LOCKHEED DATA)

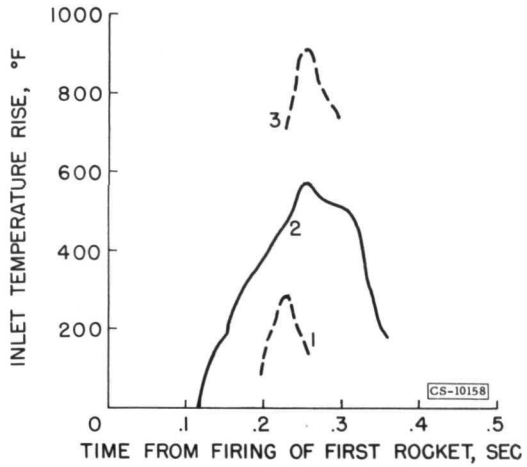

Figure 6.

CANNON BLAST EFFECT

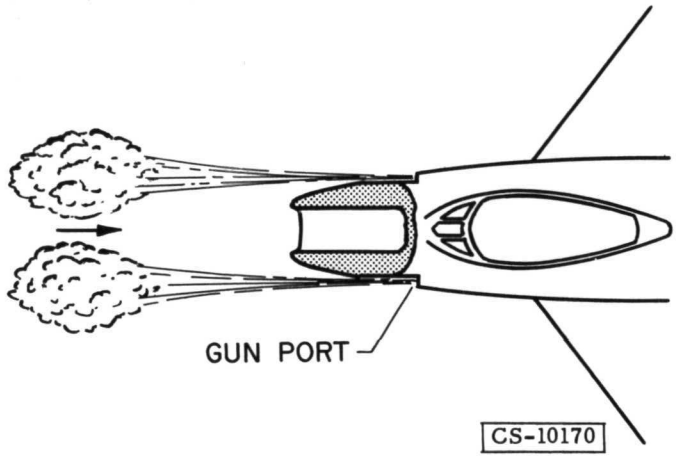

Figure 7.

THEORETICAL COMPRESSOR OPERATION FOR INSTANTANEOUS INLET TEMPERATURE INCREASE

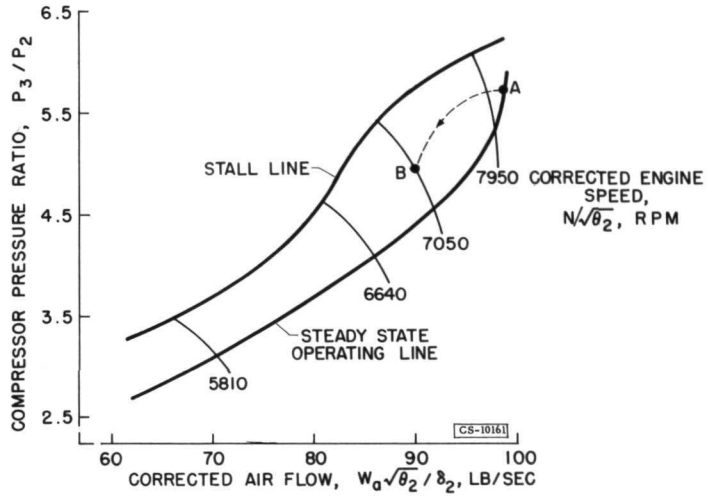

Figure 8.

EFFECT OF VARIOUS INLET-TEMPERATURE INCREASES

J47D(RX1)

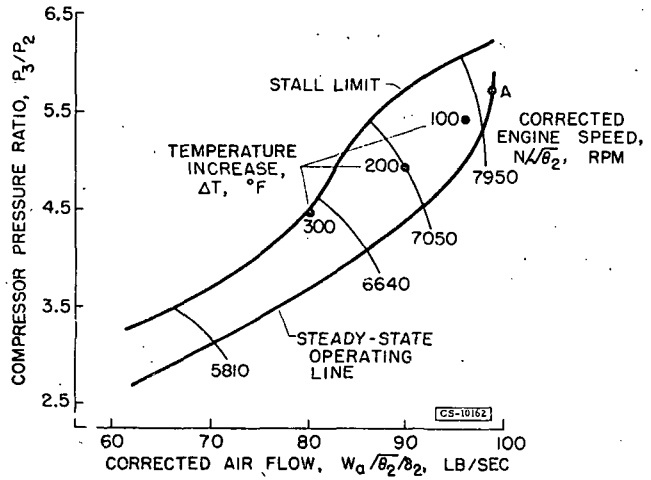

Figure 9.

EFFECT OF INLET DISTORTIONS

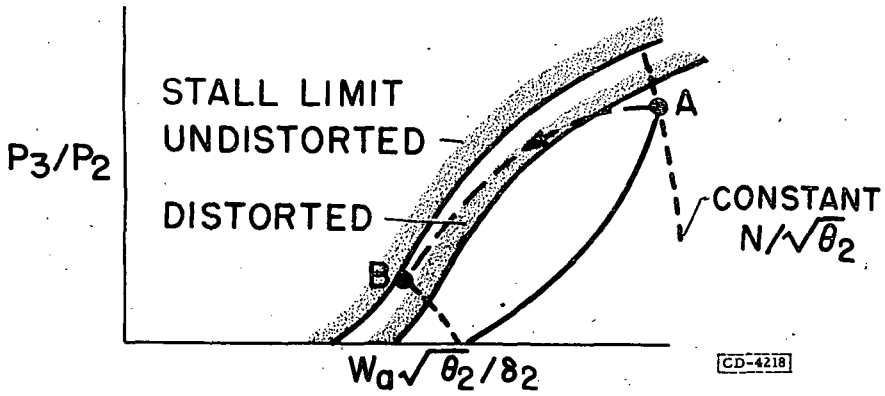

Figure 11.

EFFECT OF CHANGED INLET PRESSURE

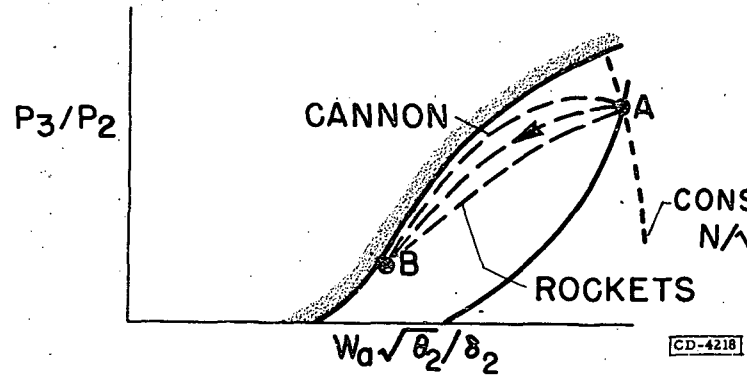

Figure 10.

EFFECT OF VARIOUS INLET-TEMPERATURE INCREASES

J57-P-1

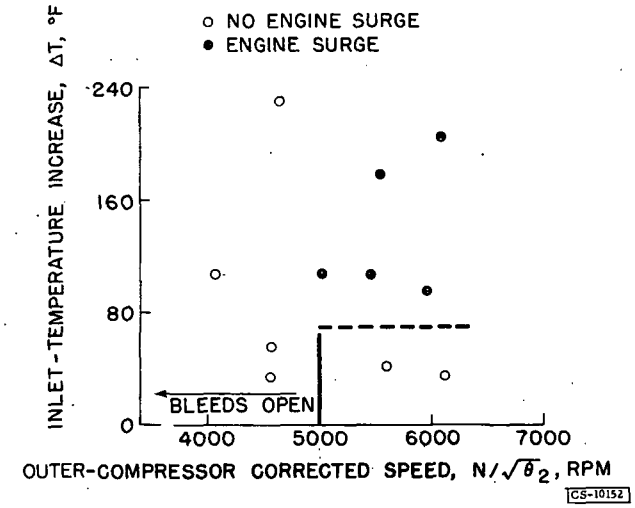

Figure 12.

COMBUSTOR OPERATING LINES FOR SEVERAL FUEL-AIR RATIOS

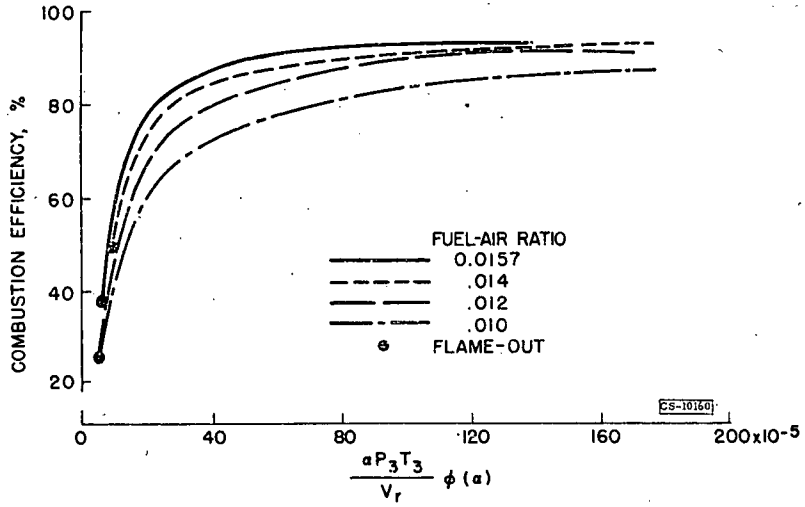

Figure 13.

J47-GE-25 FLAME-OUTS

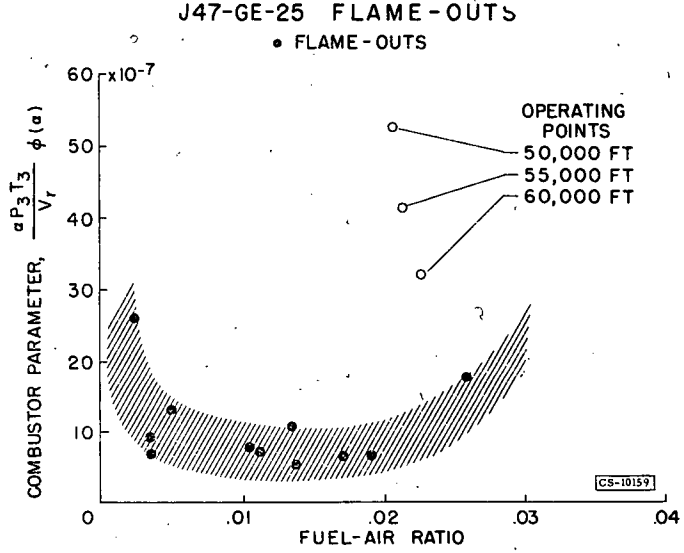

Figure 14.

COMBUSTOR CONDITIONS DURING ROCKET FIRING

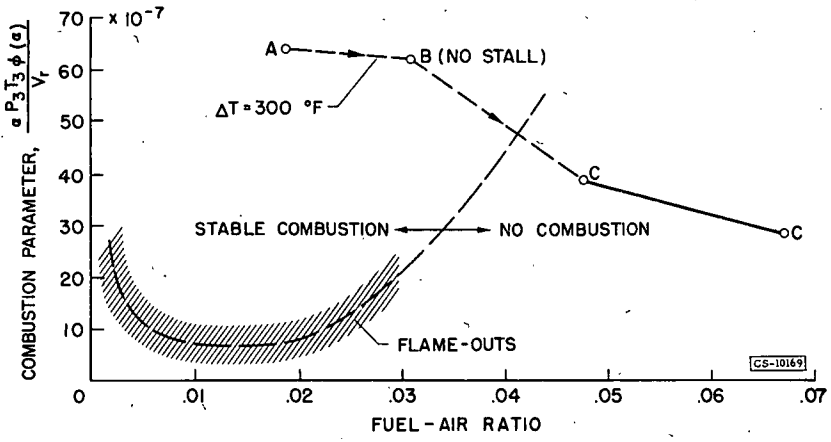

Figure 15.

COMBUSTOR CONDITIONS DURING ROCKET FIRING

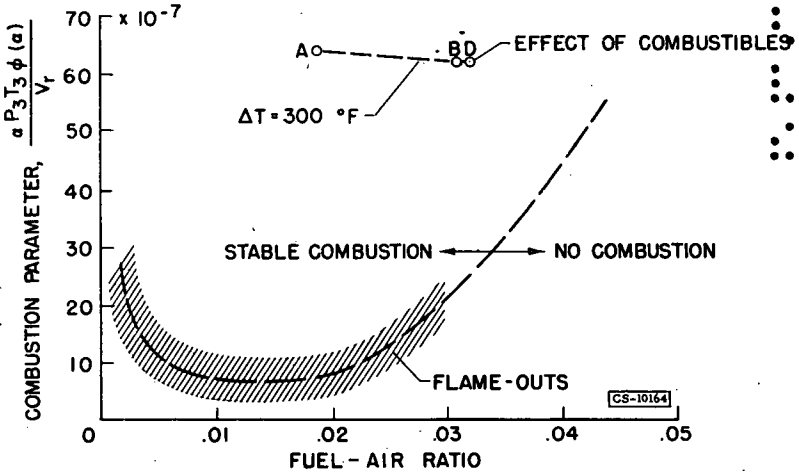

Figure 16.

NACA-CLEVELAND